11

Biological Membranes and Transport

The first cell probably came into being when a membrane formed, enclosing a small volume of aqueous solution and separating it from the rest of the universe. Membranes define the external boundaries of cells and control the molecular traffic across that boundary **(Fig. 11–1)**; in eukaryotic cells, they divide the internal space into discrete compartments to segregate processes and components. They organize complex reaction sequences and are central to both biological energy conservation and cell-to-cell communication. The biological activities of membranes flow from their remarkable physical properties. Membranes are flexible, self-sealing, and selectively permeable to polar solutes. Their flexibility permits the shape changes that accompany cell growth and movement (such as amoeboid movement). With their ability to break and reseal, two membranes can fuse, as in exocytosis, or a single membrane-enclosed compartment can undergo fission to yield two sealed compartments, as in endocytosis or cell division, without creating gross leaks through cellular surfaces. Because membranes are selectively permeable, they retain certain compounds and ions within cells and within specific cellular compartments while excluding others.

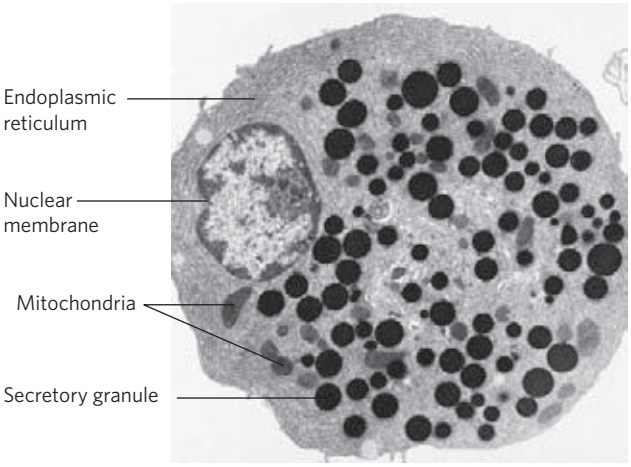

FIGURE 11–1 Biological membranes. This electron micrograph of a thin-sectioned exocrine pancreas cell shows several compartments made of or bounded by membranes: the endoplasmic reticulum, mitochondria, secretory granules, and the nuclear membrane.

Membranes are not merely passive barriers. They include an array of proteins specialized for promoting or catalyzing various cellular processes. At the cell surface, transporters move specific organic solutes and inorganic ions across the membrane; receptors sense extracellular signals and trigger molecular changes in the cell; adhesion molecules hold neighboring cells together. Within the cell, membranes organize cellular processes such as the synthesis of lipids and certain proteins, and the energy transductions in mitochondria and chloroplasts. Because membranes consist of just two layers of molecules, they are very thin—essentially two-dimensional. Intermolecular collisions are far more probable in this two-dimensional space than in three-dimensional space, so the efficiency of enzyme-catalyzed processes organized within membranes is vastly increased.

In this chapter we first describe the composition of cellular membranes and their chemical architecture—the molecular structures that underlie their biological functions. Next, we consider the remarkable dynamic features of membranes, in which lipids and proteins move relative to each other. Cell adhesion, endocytosis, and the membrane fusion accompanying neurotransmitter secretion illustrate the dynamic roles of membrane proteins. We then turn to the protein-mediated passage of solutes across membranes via transporters and ion channels. In later chapters we discuss the roles of membranes in signal transduction (Chapters 12 and 23), energy transduction (Chapter 19), lipid synthesis (Chapter 21), and protein synthesis (Chapter 27).

11.1 The Composition and Architecture of Membranes

One approach to understanding membrane function is to study membrane composition—to determine, for example, which components are common to all membranes and which are unique to membranes with specific functions. So before describing membrane structure and function, we consider the molecular components of membranes: proteins and polar lipids, which account for almost all the mass of biological membranes, and carbohydrates, present as part of glycoproteins and glycolipids.

Each Type of Membrane Has Characteristic Lipids and Proteins

The relative proportions of protein and lipid vary with the type of membrane (Table 11–1), reflecting the diversity of biological roles. For example, certain neurons have a myelin sheath—an extended plasma membrane that wraps around the cell many times and acts as a passive electrical insulator. The myelin sheath consists primarily of lipids, whereas the plasma membranes of bacteria and the membranes of mitochondria and chloroplasts, the sites of many enzyme-catalyzed processes, contain more protein than lipid (in mass per total mass).

For studies of membrane composition, the first task is to isolate a selected membrane. When eukaryotic cells are subjected to mechanical shear, their plasma membranes are torn and fragmented, releasing cytoplasmic components and membrane-bounded organelles such as mitochondria, chloroplasts, lysosomes, and nuclei. Plasma membrane fragments and intact organelles can be isolated by techniques described in Chapter 1 (see Fig. 1–8) and in Worked Example 2–1 (p. 57).

Cells clearly have mechanisms to control the kinds and amounts of membrane lipid they synthesize and to target specific lipids to particular organelles. Each kingdom, each species, each tissue or cell type, and the organelles of each cell type have a characteristic set of membrane lipids. Plasma membranes, for example, are enriched in cholesterol and contain no detectable cardiolipin **(Fig. 11–2)**; mitochondrial membranes are very low in cholesterol and sphingolipids, but they contain phosphatidylglycerol and cardiolipin, which are synthesized within the mitochondria. In all but a few cases, the functional significance of these combinations is not yet known.

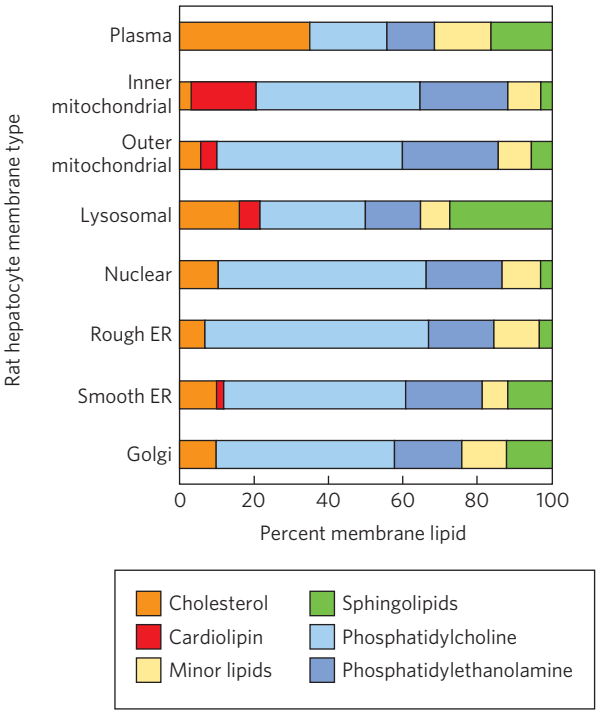

FIGURE 11–2 Lipid composition of the plasma membrane and organelle membranes of a rat hepatocyte. The functional specialization of each membrane type is reflected in its unique lipid composition. Cholesterol is prominent in plasma membranes but barely detectable in mitochondrial membranes. Cardiolipin is a major component of the inner mitochondrial membrane but not of the plasma membrane. Phosphatidylserine, phosphatidylinositol, and phosphatidylglycerol are relatively minor components of most membranes but serve critical functions; phosphatidylinositol and its derivatives, for example, are important in signal transductions triggered by hormones. Sphingolipids, phosphatidylcholine, and phosphatidylethanolamine are present in most membranes but in varying proportions. Glycolipids, which are major components of the chloroplast membranes of plants, are virtually absent from animal cells.

TABLE 11–1 Major Components of Plasma Membranes in Various Organisms

	Components (% by weight)				
	Protein	Phospholipid	Sterol	Sterol type	Other lipids
Human myelin sheath	30	30	19	Cholesterol	Galactolipids, plasmalogens
Mouse liver	45	27	25	Cholesterol	—
Maize leaf	47	26	7	Sitosterol	Galactolipids
Yeast	52	7	4	Ergosterol	Triacylglycerols, steryl esters
Paramecium (ciliated protist)	56	40	4	Stigmasterol	—
E. coli	75	25	0	—	—

Note: Values do not add up to 100% in every case because there are components other than protein, phospholipids, and sterol; plants, for example, have high levels of glycolipids.

The protein composition of membranes from different sources varies even more widely than their lipid composition, reflecting functional specialization. In addition, some membrane proteins are covalently linked to oligosaccharides. For example, in glycophorin, a glycoprotein of the erythrocyte plasma membrane, 60% of the mass consists of complex oligosaccharides covalently attached to specific amino acid residues. Ser, Thr, and Asn residues are the most common points of attachment (see Fig. 7–30). The sugar moieties of surface glycoproteins influence the folding of the proteins as well as their stability and intracellular destination, and they play a significant role in the specific binding of ligands to glycoprotein surface receptors (see Fig. 7–37).

Some membrane proteins are covalently attached to one or more lipids, which serve as hydrophobic anchors that hold the proteins to the membrane, as we shall see.

All Biological Membranes Share Some Fundamental Properties

Membranes are impermeable to most polar or charged solutes, but permeable to nonpolar compounds. They are 5 to 8 nm (50 to 80 Å) thick when proteins protruding on both sides are included and appear trilaminar when viewed in cross section with the electron microscope. The combined evidence from electron microscopy and studies of chemical composition, as well as physical studies of permeability and the motion of individual protein and lipid molecules within membranes, led to the development of the **fluid mosaic model** for the structure of biological membranes **(Fig. 11–3)**. Phospholipids form a bilayer in which the nonpolar regions of the lipid molecules in each layer face the core of the bilayer and their polar head groups face outward, interacting with the aqueous phase on either side. Proteins are embedded in this bilayer sheet, held by hydrophobic interactions between the membrane lipids and hydrophobic domains in the proteins. Some proteins protrude from only one side of the membrane; others have domains exposed on both sides. The orientation of proteins in the bilayer is asymmetric, giving the membrane "sidedness": the protein domains exposed on one side of the bilayer are different from those exposed on the other side, reflecting functional asymmetry. The individual lipid and protein units in a membrane form a fluid mosaic with a pattern that, unlike a mosaic of ceramic tile and mortar, is free to change constantly. The membrane mosaic is fluid because most of the interactions among its components are noncovalent, leaving individual lipid and protein molecules free to move laterally in the plane of the membrane.

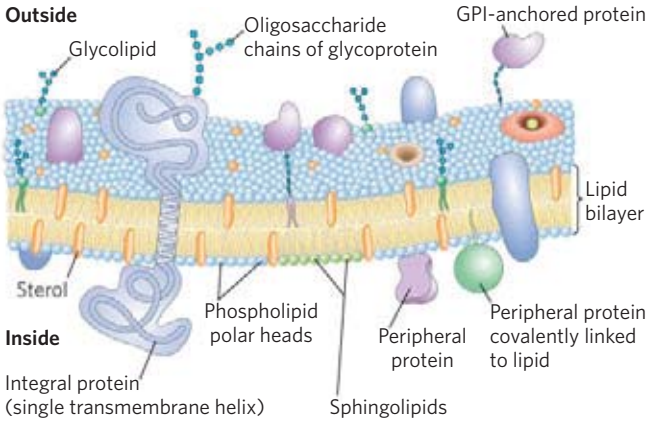

FIGURE 11–3 Fluid mosaic model for plasma membrane structure. The fatty acyl chains in the interior of the membrane form a fluid, hydrophobic region. Integral proteins float in this sea of lipid, held by hydrophobic interactions with their nonpolar amino acid side chains. Both proteins and lipids are free to move laterally in the plane of the bilayer, but movement of either from one leaflet of the bilayer to the other is restricted. The carbohydrate moieties attached to some proteins and lipids of the plasma membrane are exposed on the extracellular surface.

We now look at some of these features of the fluid mosaic model in more detail and consider the experimental evidence that supports the basic model but has necessitated its refinement in several ways.

A Lipid Bilayer Is the Basic Structural Element of Membranes

Glycerophospholipids, sphingolipids, and sterols are virtually insoluble in water. When mixed with water, they spontaneously form microscopic lipid aggregates, clustering together, with their hydrophobic moieties in contact with each other and their hydrophilic groups interacting with the surrounding water. This clustering reduces the amount of hydrophobic surface exposed to water and thus minimizes the number of molecules in the shell of ordered water at the lipid-water interface (see Fig. 2–7), resulting in an increase in entropy. Hydrophobic interactions among lipid molecules provide the thermodynamic driving force for the formation and maintenance of these clusters.

Depending on the precise conditions and the nature of the lipids, three types of lipid aggregate can form when amphipathic lipids are mixed with water **(Fig. 11–4)**. **Micelles** are spherical structures that contain anywhere from a few dozen to a few thousand amphipathic molecules. These molecules are arranged with their hydrophobic regions aggregated in the interior, where water is excluded, and their hydrophilic head groups at the surface, in contact with water. Micelle formation is favored when the cross-sectional area of the head group is greater than that of the acyl side chain(s), as in free fatty acids, lysophospholipids (phospholipids lacking one fatty acid), and detergents such as sodium dodecyl sulfate (SDS; p. 94).

A second type of lipid aggregate in water is the **bilayer**, in which two lipid monolayers (leaflets) form a two-dimensional sheet. Bilayer formation is favored if the cross-sectional areas of the head group and acyl side chain(s) are similar, as in glycerophospholipids and

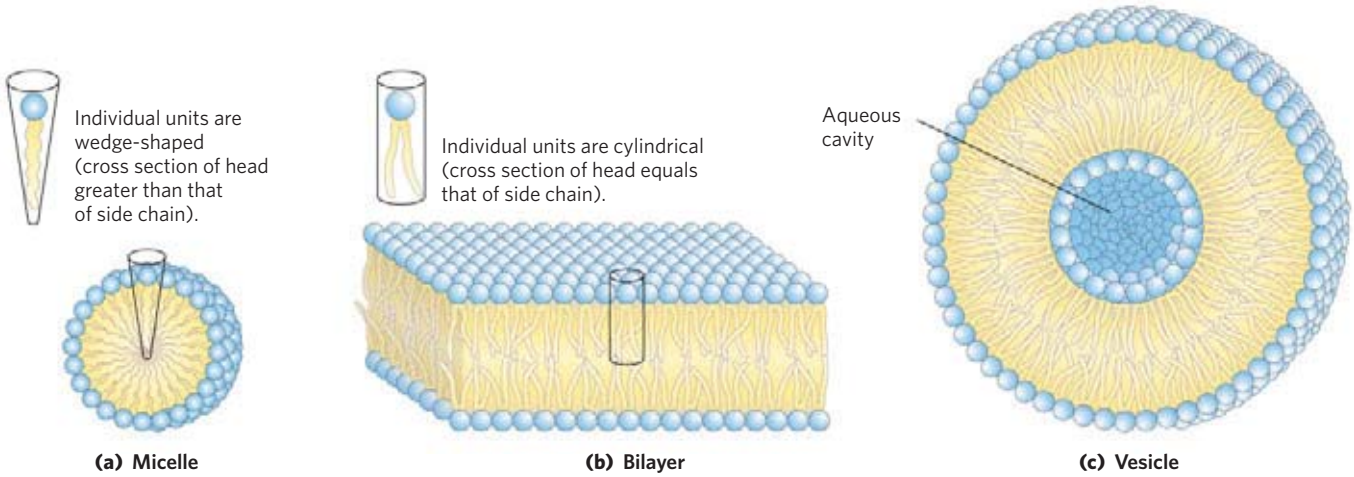

FIGURE 11–4 Amphipathic lipid aggregates that form in water. (a) In micelles, the hydrophobic chains of the fatty acids are sequestered at the core of the sphere. There is virtually no water in the hydrophobic interior. **(b)** In an open bilayer, all acyl side chains except those at the edges of the sheet are protected from interaction with water. **(c)** When a two-dimensional bilayer folds on itself, it forms a closed bilayer, a three-dimensional hollow vesicle (liposome) enclosing an aqueous cavity.

sphingolipids. The hydrophobic portions in each monolayer, excluded from water, interact with each other. The hydrophilic head groups interact with water at each surface of the bilayer. Because the hydrophobic regions at its edges (Fig. 11–4b) are in contact with water, the bilayer sheet is relatively unstable and spontaneously folds back on itself to form a hollow sphere, a **vesicle** (Fig. 11–4c). The continuous surface of vesicles eliminates exposed hydrophobic regions, allowing bilayers to achieve maximal stability in their aqueous environment. Vesicle formation also creates a separate aqueous compartment. It is likely that the precursors to the first living cells resembled lipid vesicles, their aqueous contents segregated from their surroundings by a hydrophobic shell.

The lipid bilayer is 3 nm (30 Å) thick. The hydrocarbon core, made up of the —CH_2— and —CH_3 of the fatty acyl groups, is about as nonpolar as decane, and vesicles formed in the laboratory from pure lipids (liposomes) are essentially impermeable to polar solutes, as is the lipid bilayer of biological membranes (although biological membranes, as we shall see, are permeable to solutes for which they have specific transporters).

Plasma membrane lipids are asymmetrically distributed between the two monolayers of the bilayer, although the asymmetry, unlike that of membrane proteins, is not absolute. In the plasma membrane of the erythrocyte, for example, choline-containing lipids (phosphatidylcholine and sphingomyelin) are typically found in the outer (extracellular, or exoplasmic) leaflet **(Fig. 11–5)**, whereas phosphatidylserine, phosphatidylethanolamine, and the phosphatidylinositols are much more common in the inner (cytoplasmic) leaflet. The flow of membrane components from the endoplasmic reticulum through the Golgi apparatus and to the plasma membrane via transport vesicles is accompanied by changes in lipid composition and disposition across the bilayer **(Fig. 11–6)**. Phosphatidylcholine is the principal phospholipid in the lumenal monolayer of the Golgi membrane, but in transport vesicles phosphatidylcholine has been largely replaced by sphingolipids and cholesterol, which, on fusion of transport vesicles with the plasma membrane, make up the majority of the lipids in the outer monolayer of the plasma membrane.

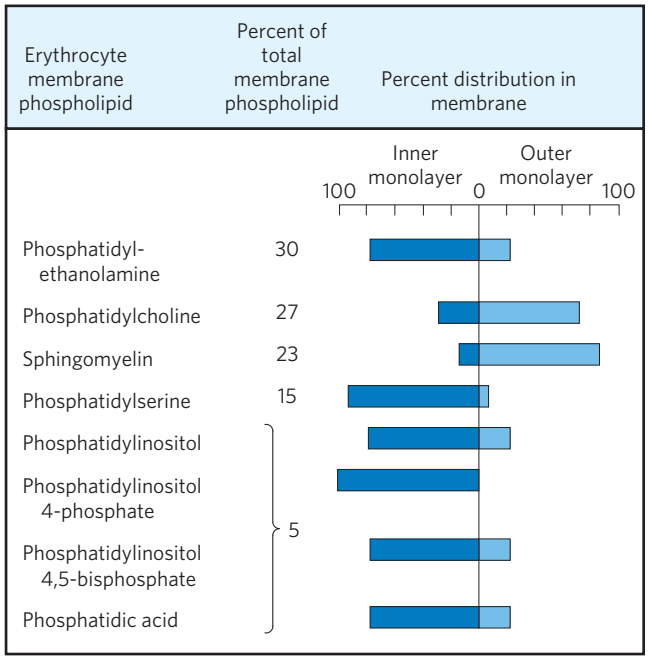

FIGURE 11–5 Asymmetric distribution of phospholipids between the inner and outer monolayers of the erythrocyte plasma membrane. The distribution of a specific phospholipid is determined by treating the intact cell with phospholipase C, which cannot reach lipids in the inner monolayer (leaflet) but removes the head groups of lipids in the outer monolayer. The proportion of each head group released provides an estimate of the fraction of each lipid in the outer monolayer.

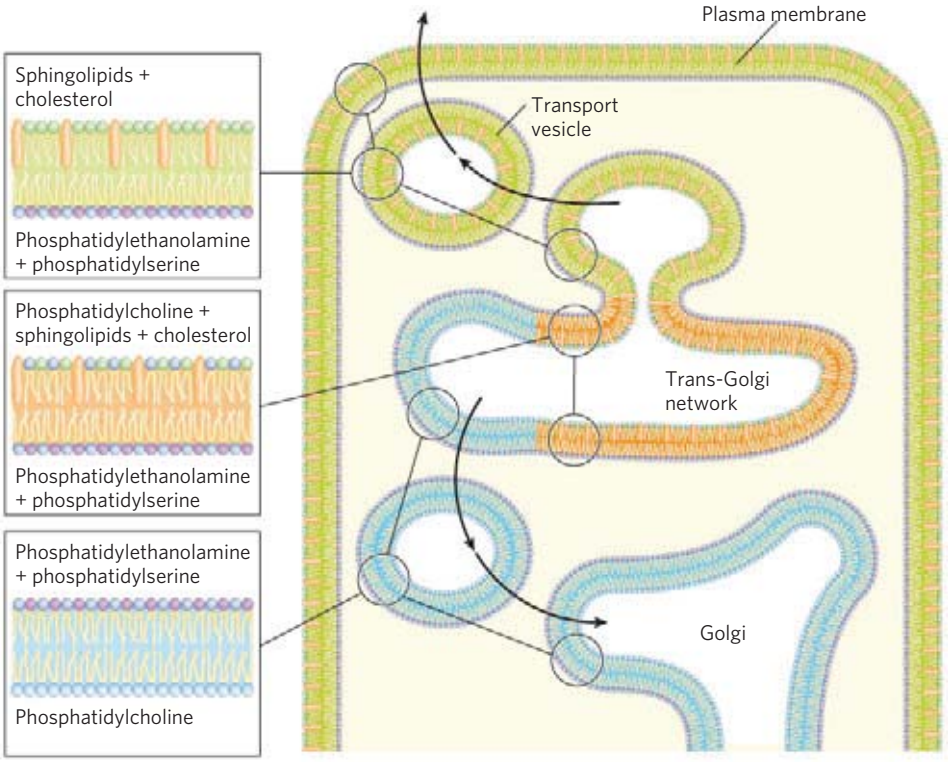

FIGURE 11–6 The distribution of lipids in the membranes of a typical cell. Each membrane has its own characteristic composition, and the two monolayers of a given membrane may differ in composition as well.

Changes in the distribution of lipids between plasma membrane leaflets have biological consequences. For example, only when the phosphatidylserine in the plasma membrane moves into the outer leaflet is a platelet able to play its role in formation of a blood clot. For many other cell types, phosphatidylserine exposure on the outer surface marks a cell for destruction by programmed cell death. The transbilayer movement of phospholipid molecules is catalyzed and regulated by specific proteins (see Fig. 11–17).

Three Types of Membrane Proteins Differ in Their Association with the Membrane

Integral membrane proteins are very firmly associated with the lipid bilayer and are removable only by agents that interfere with hydrophobic interactions, such as detergents, organic solvents, or denaturants **(Fig. 11–7)**. **Peripheral membrane proteins** associate with the membrane through electrostatic interactions and hydrogen bonding with the hydrophilic domains of integral proteins and with the polar head

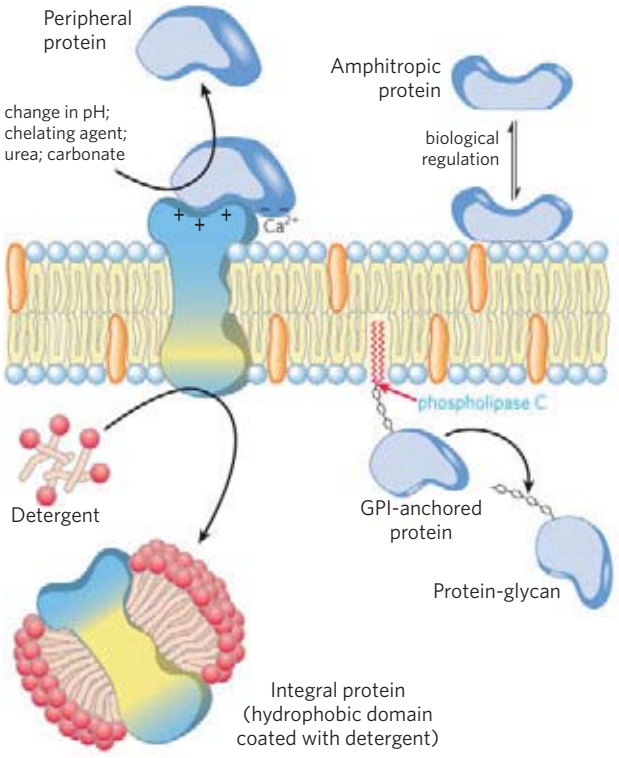

FIGURE 11–7 Peripheral, integral, and amphitropic proteins. Membrane proteins can be operationally distinguished by the conditions required to release them from the membrane. Most peripheral proteins are released by changes in pH or ionic strength, removal of Ca^{2+} by a chelating agent, or addition of urea or carbonate. Integral proteins are extractable with detergents, which disrupt the hydrophobic interactions with the lipid bilayer and form micelle-like clusters around individual protein molecules. Integral proteins covalently attached to a membrane lipid, such as a glycosyl phosphatidylinositol (GPI; see Fig. 11–15), can be released by treatment with phospholipase C. Amphitropic proteins are sometimes associated with membranes and sometimes not, depending on some type of regulatory process such as reversible palmitoylation.

groups of membrane lipids. They can be released by relatively mild treatments that interfere with electrostatic interactions or break hydrogen bonds; a commonly used agent is carbonate at high pH. **Amphitropic proteins** are found both in the cytosol and in association with membranes. Their affinity for membranes results in some cases from the protein's noncovalent interaction with a membrane protein or lipid, and in other cases from the presence of one or more lipids covalently attached to the amphitropic protein (see Fig. 11–15). Generally, the reversible association of amphitropic proteins with the membrane is regulated; for example, phosphorylation or ligand binding can force a conformational change in the protein, exposing a membrane-binding site that was previously inaccessible.

Many Membrane Proteins Span the Lipid Bilayer

Membrane protein topology (the localization of protein domains relative to the lipid bilayer) can be determined with reagents that react with protein side chains but cannot cross membranes—polar chemical reagents that react with primary amines of Lys residues, for example, or enzymes such as trypsin that cleave proteins but cannot cross the membrane. The human erythrocyte is convenient for such studies because it has no membrane-bounded organelles; the plasma membrane is the only membrane present. If a membrane protein in an intact erythrocyte reacts with a membrane-impermeant reagent, that protein must have at least one domain exposed on the outer (extracellular) face of the membrane. Trypsin cleaves extracellular domains but does not affect domains buried within the bilayer or exposed on the inner surface only, unless the plasma membrane is broken to make these domains accessible to the enzyme.

Experiments with such topology-specific reagents show that the erythrocyte glycoprotein **glycophorin** spans the plasma membrane. Its amino-terminal domain (bearing the carbohydrate chains) is on the outer surface and is cleaved by trypsin. The carboxyl terminus protrudes on the inside of the cell, where it cannot react with impermeant reagents. Both the amino-terminal and carboxyl-terminal domains contain many polar or charged amino acid residues and are therefore hydrophilic. However, a segment in the center of the protein (residues 75 to 93) contains mainly hydrophobic amino acid residues, suggesting that glycophorin has a transmembrane segment arranged as shown in **Figure 11–8**.

These noncrystallographic experiments also revealed that the orientation of glycophorin in the membrane is asymmetric: its amino-terminal segment is always on the outside. Similar studies of other membrane proteins show that each has a specific orientation in the bilayer, giving the membrane a distinct sidedness. For glycophorin, and for all other glycoproteins of the plasma membrane, the glycosylated domains

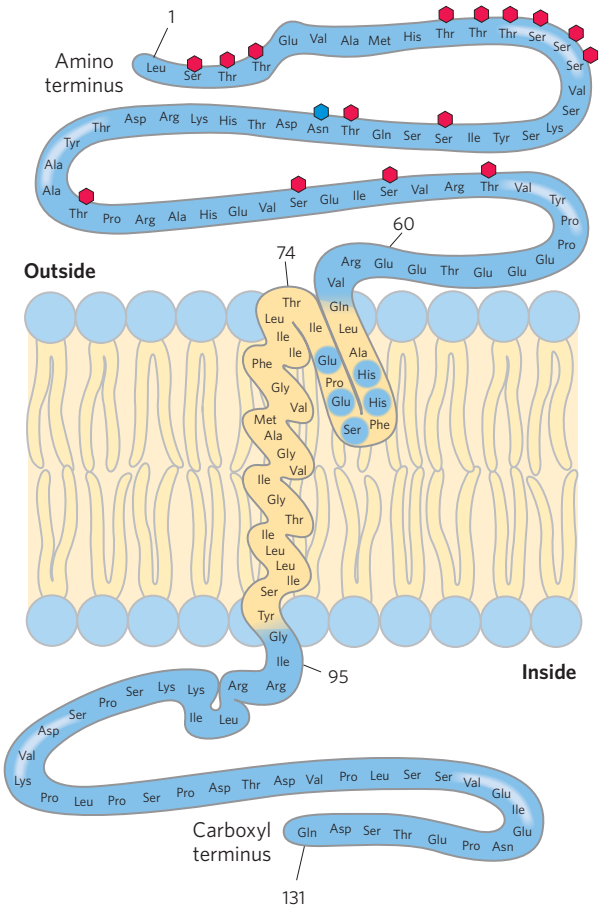

FIGURE 11–8 Transbilayer disposition of glycophorin in an erythrocyte. One hydrophilic domain, containing all the sugar residues, is on the outer surface, and another hydrophilic domain protrudes from the inner face of the membrane. Each red hexagon represents a tetrasaccharide (containing two Neu5Ac (sialic acid), Gal, and GalNAc) *O*-linked to a Ser or Thr residue; the blue hexagon represents an oligosaccharide *N*-linked to an Asn residue. The relative size of the oligosaccharide units is larger than shown here. A segment of 19 hydrophobic residues (residues 75 to 93) forms an α helix that traverses the membrane bilayer (see Fig. 11–12a). The segment from residues 64 to 74 has some hydrophobic residues and probably penetrates the outer face of the lipid bilayer, as shown.

are invariably found on the extracellular face of the bilayer. As we shall see, the asymmetric arrangement of membrane proteins results in functional asymmetry. All the molecules of a given ion pump, for example, have the same orientation in the membrane and pump ions in the same direction.

Integral Proteins Are Held in the Membrane by Hydrophobic Interactions with Lipids

The firm attachment of integral proteins to membranes is the result of hydrophobic interactions between membrane lipids and hydrophobic domains of the protein. Some proteins have a single hydrophobic sequence in the middle (as in glycophorin) or at the amino or carboxyl terminus. Others have multiple hydrophobic sequences,

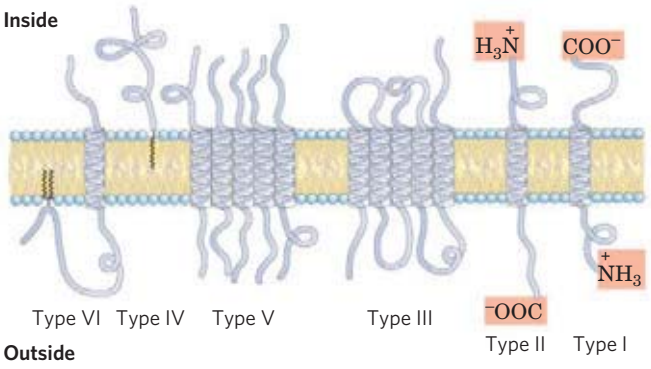

FIGURE 11–9 Integral membrane proteins. For known proteins of the plasma membrane, the spatial relationships of protein domains to the lipid bilayer fall into six categories. Types I and II have a single transmembrane helix; the amino-terminal domain is outside the cell in type I proteins and inside in type II. Type III proteins have multiple transmembrane helices in a single polypeptide. In type IV proteins, transmembrane domains of several different polypeptides assemble to form a channel through the membrane. Type V proteins are held to the bilayer primarily by covalently linked lipids (see Fig. 11–15), and type VI proteins have both transmembrane helices and lipid anchors.

In this figure, and in figures throughout the book, we represent transmembrane protein segments in their most likely conformations: as α helices of six to seven turns. Sometimes these helices are shown simply as cylinders. As relatively few membrane protein structures have been deduced by x-ray crystallography, our representation of the extramembrane domains is arbitrary and not necessarily to scale.

each of which, when in the α-helical conformation, is long enough to span the lipid bilayer **(Fig. 11–9)**.

One of the best-studied membrane-spanning proteins, bacteriorhodopsin, has seven very hydrophobic internal sequences and crosses the lipid bilayer seven times. Bacteriorhodopsin is a light-driven proton pump densely packed in regular arrays in the purple membrane of the bacterium *Halobacterium salinarum*. X-ray crystallography reveals a structure with seven α-helical segments, each traversing the lipid bilayer, connected by nonhelical loops at the inner and outer face of the membrane **(Fig. 11–10)**. In the amino acid sequence of bacteriorhodopsin, seven segments of about 20 hydrophobic residues can be identified, each forming an α helix that spans the bilayer. The seven helices are clustered together and oriented not quite perpendicular to the bilayer plane, a pattern that (as we shall see in Chapter 12) is a common motif in membrane proteins involved in signal reception. Hydrophobic interactions between the nonpolar amino acids and the fatty acyl groups of the membrane lipids firmly anchor the protein in the membrane.

Crystallized membrane proteins solved (i.e., their molecular structure deduced) by crystallography often include molecules of phospholipids, which are presumed to be positioned in the crystals as they are in the native membranes. Many of these phospholipid molecules lie on the protein surface, their head groups interacting with polar amino acid residues at the inner

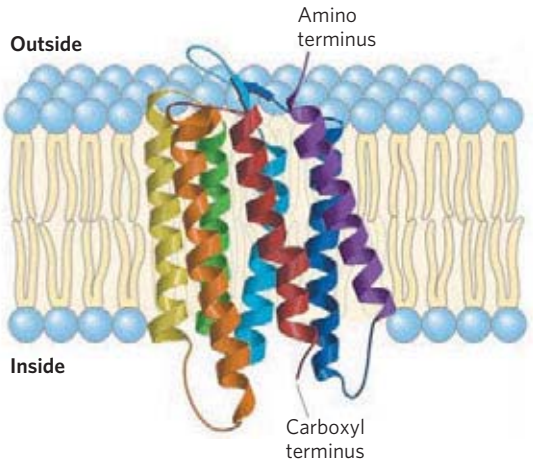

FIGURE 11–10 Bacteriorhodopsin, a membrane-spanning protein. (PDB ID 2AT9) The single polypeptide chain folds into seven hydrophobic α helices, each of which traverses the lipid bilayer roughly perpendicular to the plane of the membrane. The seven transmembrane helices are clustered, and the space around and between them is filled with the acyl chains of membrane lipids. The light-absorbing pigment retinal (see Fig. 10–21) is buried deep in the membrane in contact with several of the helical segments (not shown). The helices are colored to correspond with the hydropathy plot in Figure 11–12b.

and outer membrane–water interfaces and their side chains associated with nonpolar residues. These **annular lipids** form a bilayer shell (annulus) around the protein, oriented roughly as expected for phospholipids in a bilayer **(Fig. 11–11)**. Other phospholipids are found at the interfaces between monomers of multisubunit membrane proteins, where they form a "grease seal." Yet others are embedded deep within a membrane protein, often with their head groups well below the plane of the bilayer. For example, succinate dehydrogenase (Complex II, found in mitochondria; see Fig. 19–10) has several deeply embedded phospholipid molecules.

The Topology of an Integral Membrane Protein Can Sometimes Be Predicted from Its Sequence

Determination of the three-dimensional structure of a membrane protein—that is, its topology—is generally much more difficult than determining its amino acid sequence, either directly or by gene sequencing. The amino acid sequences are known for thousands of membrane proteins, but relatively few three-dimensional structures have been established by crystallography or NMR spectroscopy. The presence of unbroken sequences of more than 20 hydrophobic residues in a membrane protein is commonly taken as evidence that these sequences traverse the lipid bilayer, acting as hydrophobic anchors or forming transmembrane channels. Virtually all integral proteins have at least one such sequence. Application of this logic to entire genomic sequences leads to the conclusion that in many species, 20% to 30% of all proteins are integral membrane proteins.

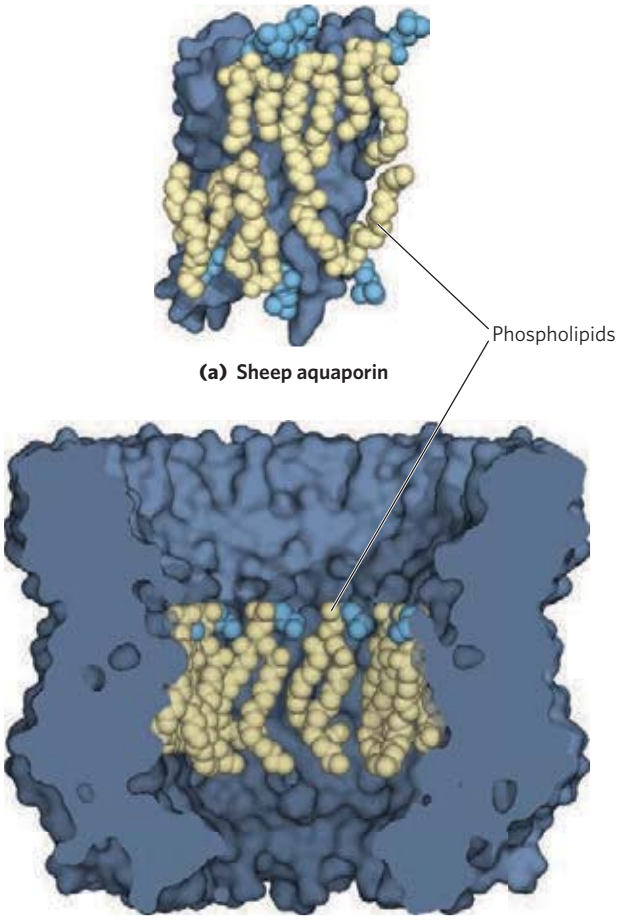

(a) Sheep aquaporin

(b) V_o from V-type ATPase

FIGURE 11–11 Lipid annuli associated with two integral membrane proteins. (a) The crystal structure of sheep aquaporin (PDB ID 2B6O), a transmembrane water channel, includes a shell of phospholipids positioned with their head groups (blue) at the expected positions on the inner and outer membrane surfaces and their hydrophobic acyl chains (gold) intimately associated with the surface of the protein exposed to the bilayer. The lipid forms a "grease seal" around the protein, which is depicted as a dark blue surface representation. **(b)** The crystal structure of the V_o integral protein complex of the V-type Na^+ ATPase from *Enterococcus hirae* (PDB ID 2BL2) has 10 identical subunits, each with four transmembrane helices, surrounding a central cavity filled with phosphatidylglycerol (PG). Here five of the subunits have been cut away to reveal the PG molecules associated with each subunit around the interior of this structure.

What can we predict about the secondary structure of the membrane-spanning portions of integral proteins? An α-helical sequence of 20 to 25 residues is just long enough to span the thickness (30 Å) of the lipid bilayer (recall that the length of an α helix is 1.5 Å (0.15 nm) per amino acid residue). A polypeptide chain surrounded by lipids, having no water molecules with which to hydrogen-bond, will tend to form α helices or β sheets, in which intrachain hydrogen bonding is maximized. If the side chains of all amino acids in a helix are nonpolar, hydrophobic interactions with the surrounding lipids further stabilize the helix.

Several simple methods of analyzing amino acid sequences yield reasonably accurate predictions of secondary structure for transmembrane proteins. The relative polarity of each amino acid has been determined experimentally by measuring the free-energy change accompanying the movement of that amino acid side chain from a hydrophobic solvent into water. This free energy of transfer, which can be expressed as a **hydropathy index** (see Table 3–1), ranges from very exergonic for charged or polar residues to very endergonic for amino acids with aromatic or aliphatic hydrocarbon side chains. The overall hydropathy index (hydrophobicity) of a sequence of amino acids is estimated by summing the free energies of transfer for the residues in the sequence. To scan a polypeptide sequence for potential membrane-spanning segments, an investigator calculates the hydropathy index for successive segments (called windows) of a given size, from 7 to 20 residues. For a window of seven residues, for example, the average indices for residues 1 to 7, 2 to 8, 3 to 9, and so on are plotted as in **Figure 11–12** (plotted for the

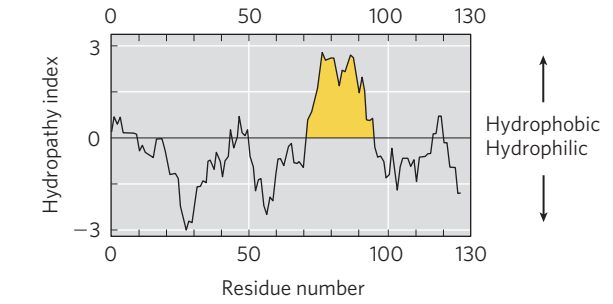

(a) Glycophorin

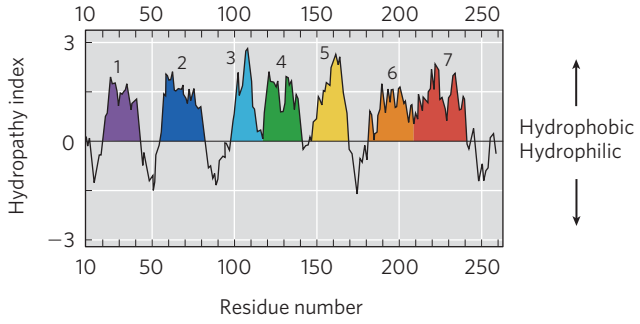

(b) Bacteriorhodopsin

FIGURE 11–12 Hydropathy plots. Average hydropathy index (see Table 3–1) is plotted against residue number for two integral membrane proteins. The hydropathy index for each amino acid residue in a sequence of defined length, or "window," is used to calculate the average hydropathy for that window. The horizontal axis shows the residue number in the middle of the window. **(a)** Glycophorin from human erythrocytes has a single hydrophobic sequence between residues 75 and 93 (yellow); compare this with Figure 11–8. **(b)** Bacteriorhodopsin, known from independent physical studies to have seven transmembrane helices (see Fig. 11–10), has seven hydrophobic regions. Note, however, that the hydropathy plot is ambiguous in the region of segments 6 and 7. X-ray crystallography has confirmed that this region has two transmembrane segments.

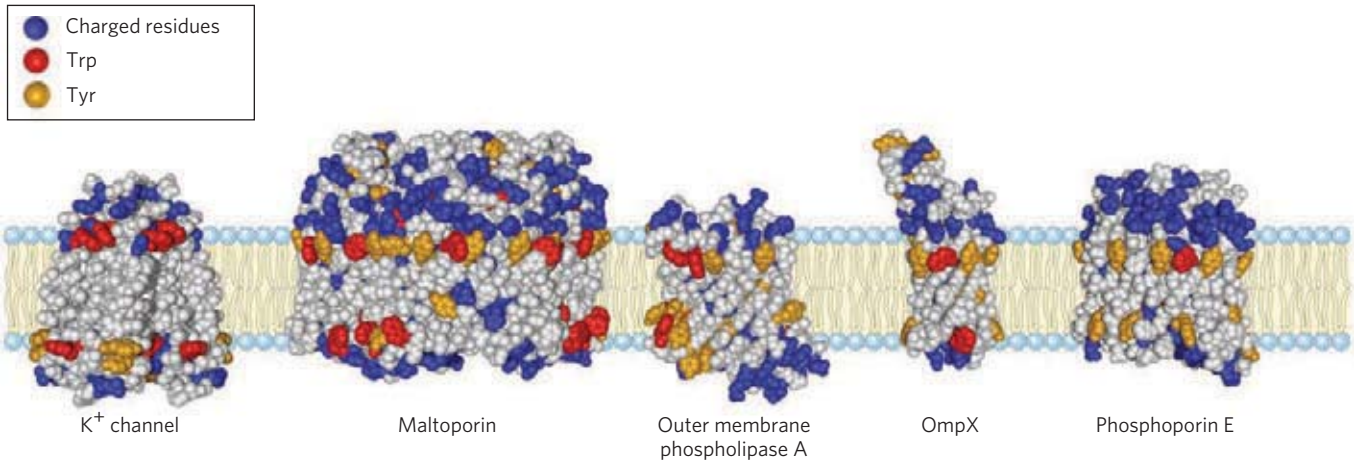

FIGURE 11–13 Tyr and Trp residues of membrane proteins clustering at the water-lipid interface. The detailed structures of these five integral membrane proteins are known from crystallographic studies. The K^+ channel (PDB ID 1BL8) is from the bacterium *Streptomyces lividans* (see Fig. 11-47); maltoporin (PDB ID 1AF6), outer membrane phospholipase A (OmpLA, PDB ID 1QD5), OmpX (PDB ID 1QJ9), and phosphoporin E (PDB ID 1PHO) are proteins of the outer membrane of *E. coli*. Residues of Tyr and Trp are found predominantly where the nonpolar region of acyl chains meets the polar head group region. Charged residues (Lys, Arg, Glu, Asp) are found almost exclusively in the aqueous phases.

middle residue in each window—residue 4 for residues 1 to 7, for example). A region with more than 20 residues of high hydropathy index is presumed to be a transmembrane segment. When the sequences of membrane proteins of known three-dimensional structure are scanned in this way, we find a reasonably good correspondence between predicted and known membrane-spanning segments. Hydropathy analysis predicts a single hydrophobic helix for glycophorin (Fig. 11–12a) and seven transmembrane segments for bacteriorhodopsin (Fig. 11–12b)—in agreement with experimental studies.

On the basis of their amino acid sequences and hydropathy plots, many of the transport proteins described in this chapter are believed to have multiple membrane-spanning helical regions—that is, they are type III or type IV integral proteins (Fig. 11–9). When predictions are consistent with chemical studies of protein localization (such as those described above for glycophorin and bacteriorhodopsin), the assumption that hydrophobic regions correspond to membrane-spanning domains is much better justified.

A further remarkable feature of many transmembrane proteins of known structure is the presence of Tyr and Trp residues at the interface between lipid and water **(Fig. 11–13)**. The side chains of these residues apparently serve as membrane interface anchors, able to interact simultaneously with the central lipid phase and the aqueous phases on either side of the membrane. Another generalization about amino acid location relative to the bilayer is described by the **positive-inside rule**: the positively charged Lys, His, and Arg residues of membrane proteins occur more commonly on the cytoplasmic face of membranes.

Not all integral membrane proteins are composed of transmembrane α helices. Another structural motif common in bacterial membrane proteins is the **β barrel** (see Fig. 4–18b), in which 20 or more transmembrane segments form β sheets that line a cylinder **(Fig. 11–14)**. The same factors that favor α-helix formation in the hydrophobic interior of a lipid bilayer also stabilize β barrels: when no water molecules are available to hydrogen-bond with the carbonyl oxygen and nitrogen of the peptide bond, maximal intrachain hydrogen bonding gives the most stable conformation. Planar β sheets do not maximize these interactions and are generally not found in the membrane interior; β barrels allow all possible hydrogen bonds and are apparently common among membrane proteins. **Porins**, proteins that allow certain polar solutes to cross the outer membrane of gram-negative bacteria such as *E. coli*, have many-stranded β barrels lining the polar transmembrane passage. The outer membranes of mitochondria and chloroplasts also contain a variety of β barrels.

A polypeptide is more extended in the β conformation than in an α helix; just seven to nine residues of β conformation are needed to span a membrane.

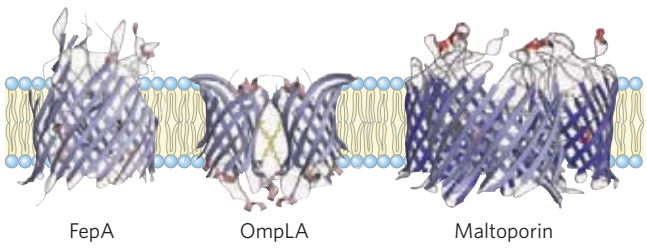

FIGURE 11–14 Membrane proteins with β-barrel structure. Three proteins of the *E. coli* outer membrane are shown, viewed in the plane of the membrane. FepA (PDB ID 1FEP), involved in iron uptake, has 22 membrane-spanning β strands. OmpLA (derived from PDB ID 1QD5), a phospholipase, is a 12-stranded β barrel that exists as a dimer in the membrane. Maltoporin (derived from PDB ID 1MAL), a maltose transporter, is a trimer; each monomer consists of 16 β strands.

Recall that in the β conformation, alternating side chains project above and below the sheet (see Fig. 4–6). In β strands of membrane proteins, every second residue in the membrane-spanning segment is hydrophobic and interacts with the lipid bilayer; aromatic side chains are commonly found at the lipid-protein interface. The other residues may or may not be hydrophilic. The hydropathy plot is not useful in predicting transmembrane segments for proteins with β barrel motifs, but as the database of known β-barrel motifs increases, sequence-based predictions of transmembrane β conformations have become feasible. For example, sequence analysis has correctly predicted that some outer membrane proteins of gram-negative bacteria (Fig. 11–14) contain β barrels.

Covalently Attached Lipids Anchor Some Membrane Proteins

Some membrane proteins contain one or more covalently linked lipids, which may be of several types: long-chain fatty acids, isoprenoids, sterols, or *g*lycosylated derivatives of *p*hosphatidyl*i*nositol (GPIs; **Fig. 11–15**). The attached lipid provides a hydrophobic anchor that inserts into the lipid bilayer and holds the protein at the membrane surface. The strength of the hydrophobic interaction between a bilayer and a single hydrocarbon chain linked to a protein is barely enough to anchor the protein securely, but many proteins have more than one attached lipid moiety. Other interactions, such as ionic attractions between positively charged Lys residues in the protein and negatively charged lipid head groups, probably contribute to the stability of the attachment. The association of these lipid-linked proteins with the membrane is certainly weaker than that for integral membrane proteins and is, at least in the case of cysteine palmitoylation, reversible.

Beyond merely anchoring a protein to the membrane, the attached lipid may have a more specific role. In the plasma membrane, proteins with GPI anchors are exclusively on the outer face and are clustered in certain regions, as discussed later in the chapter (p. 399), whereas other types of lipid-linked proteins (with farnesyl or geranylgeranyl groups attached; Fig. 11–15) are exclusively on the inner face. In polarized epithelial cells (such as intestinal epithelial cells; see Fig. 11–43), in which apical and basal surfaces have different roles, GPI-anchored proteins are directed specifically to the apical surface. Attachment of a specific lipid to a newly synthesized membrane protein therefore has a targeting function, directing the protein to its correct membrane location.

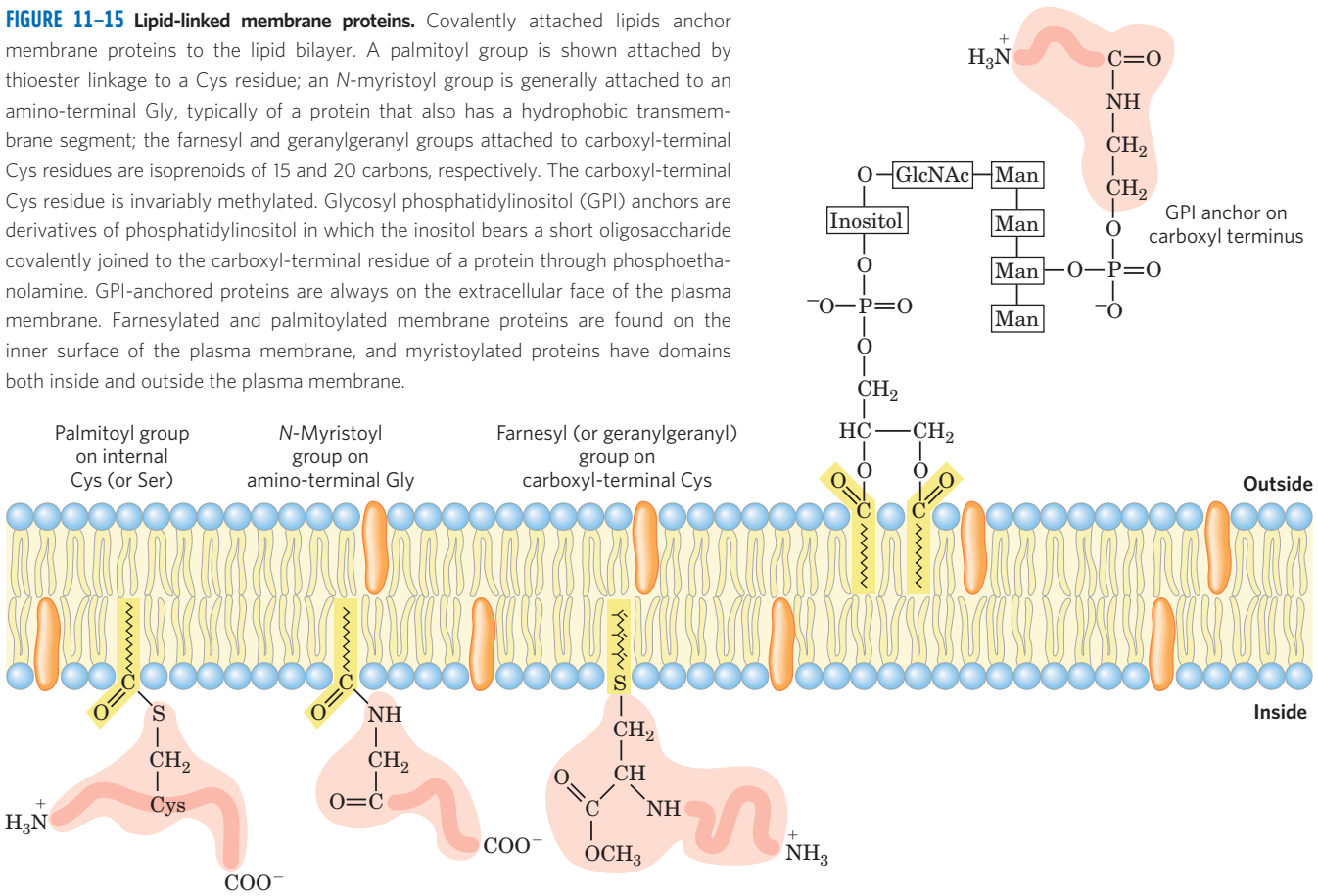

FIGURE 11–15 Lipid-linked membrane proteins. Covalently attached lipids anchor membrane proteins to the lipid bilayer. A palmitoyl group is shown attached by thioester linkage to a Cys residue; an *N*-myristoyl group is generally attached to an amino-terminal Gly, typically of a protein that also has a hydrophobic transmembrane segment; the farnesyl and geranylgeranyl groups attached to carboxyl-terminal Cys residues are isoprenoids of 15 and 20 carbons, respectively. The carboxyl-terminal Cys residue is invariably methylated. Glycosyl phosphatidylinositol (GPI) anchors are derivatives of phosphatidylinositol in which the inositol bears a short oligosaccharide covalently joined to the carboxyl-terminal residue of a protein through phosphoethanolamine. GPI-anchored proteins are always on the extracellular face of the plasma membrane. Farnesylated and palmitoylated membrane proteins are found on the inner surface of the plasma membrane, and myristoylated proteins have domains both inside and outside the plasma membrane.

SUMMARY 11.1 The Composition and Architecture of Membranes

- Biological membranes define cellular boundaries, divide cells into discrete compartments, organize complex reaction sequences, and act in signal reception and energy transformations.
- Membranes are composed of lipids and proteins in varying combinations particular to each species, cell type, and organelle. The lipid bilayer is the basic structural unit.
- Peripheral membrane proteins are loosely associated with the membrane through electrostatic interactions and hydrogen bonds or by covalently attached lipid anchors. Integral proteins associate firmly with membranes by hydrophobic interactions between the lipid bilayer and their nonpolar amino acid side chains, which are oriented toward the outside of the protein molecule. Amphitropic proteins associate reversibly with membranes.
- Many membrane proteins span the lipid bilayer several times, with hydrophobic sequences of about 20 amino acid residues forming transmembrane α helices. Multistranded β barrels are also common in integral proteins in bacterial membranes. Tyr and Trp residues of transmembrane proteins are commonly found at the lipid-water interface.
- The lipids and proteins of membranes are inserted into the bilayer with specific sidedness; thus membranes are structurally and functionally asymmetric. Plasma membrane glycoproteins are always oriented with the oligosaccharide-bearing domain on the extracellular surface.

11.2 Membrane Dynamics

One remarkable feature of all biological membranes is their flexibility—their ability to change shape without losing their integrity and becoming leaky. The basis for this property is the noncovalent interactions among lipids in the bilayer and the mobility allowed to individual lipids because they are not covalently anchored to one another. We turn now to the dynamics of membranes: the motions that occur and the transient structures allowed by these motions.

Acyl Groups in the Bilayer Interior Are Ordered to Varying Degrees

Although the lipid bilayer structure is stable, its individual phospholipid molecules have much freedom of motion **(Fig. 11–16)**, depending on the temperature and the lipid composition. Below normal physiological temperatures, the lipids in a bilayer form a semisolid **liquid-ordered (L_o) state**, in which all types of motion of individual lipid molecules are strongly constrained;

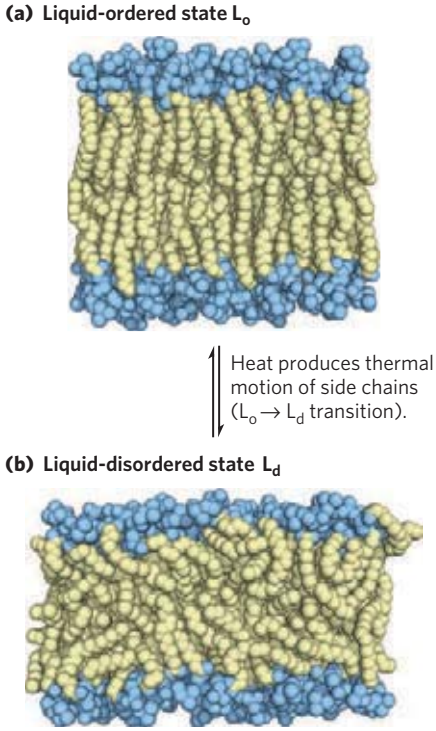

FIGURE 11–16 Two extreme states of bilayer lipids. (a) In the liquid-ordered (L_o) state, polar head groups are uniformly arrayed at the surface, and the acyl chains are nearly motionless and packed with regular geometry. **(b)** In the liquid-disordered (L_d) state, or fluid state, acyl chains undergo much thermal motion and have no regular organization. The state of membrane lipids in biological membranes is maintained somewhere between these extremes.

the bilayer is paracrystalline (Fig. 11–16a). Above physiological temperatures, individual hydrocarbon chains of fatty acids are in constant motion produced by rotation about the carbon–carbon bonds of the long acyl side chains and by lateral diffusion of individual lipid molecules in the plane of the bilayer. This is the **liquid-disordered (L_d) state** (Fig. 11–16b). In the transition from the L_o state to the L_d state, the general shape and dimensions of the bilayer are maintained; what changes is the degree of motion (lateral and rotational) allowed to individual lipid molecules.

At temperatures in the physiological range for a mammal (about 20 to 40 °C), long-chain saturated fatty acids (such as 16:0 and 18:0) tend to pack into an L_o gel phase, but the kinks in unsaturated fatty acids (see Fig. 10–2) interfere with packing, favoring the L_d state. Shorter-chain fatty acyl groups have the same effect. The sterol content of a membrane (which varies greatly with organism and organelle; Table 11–1) is another important determinant of lipid state. Sterols (such as cholesterol) have paradoxical effects on bilayer fluidity: they interact with phospholipids containing unsaturated fatty acyl chains, compacting them and constraining their motion in bilayers. Sterol association with sphingolipids and phospholipids with long, saturated fatty acyl chains tends, rather, to fluidize the bilayer, which, without

TABLE 11–2 Fatty Acid Composition of *E. coli* Cells Cultured at Different Temperatures

	Percentage of total fatty acids*			
	10 °C	20 °C	30 °C	40 °C
Myristic acid (14:0)	4	4	4	8
Palmitic acid (16:0)	18	25	29	48
Palmitoleic acid (16:1)	26	24	23	9
Oleic acid (18:1)	38	34	30	12
Hydroxymyristic acid	13	10	10	8
Ratio of unsaturated to saturated†	2.9	2.0	1.6	0.38

Source: Data from Marr, A.G. & Ingraham, J.L. (1962) Effect of temperature on the composition of fatty acids in *Escherichia coli*. *J. Bacteriol.* 84, 1260.

*The exact fatty acid composition depends not only on growth temperature but on growth stage and growth medium composition.

†Ratios calculated as the total percentage of 16:1 plus 18:1 divided by the total percentage of 14:0 plus 16:0. Hydroxymyristic acid was omitted from this calculation.

cholesterol, would adopt the L_o state. In biological membranes composed of a variety of phospholipids and sphingolipids, cholesterol tends to associate with sphingolipids and to form regions in the L_o state surrounded by cholesterol-poor regions in the L_d state (see the discussion of membrane rafts below).

Cells regulate their lipid composition to achieve a constant membrane fluidity under various growth conditions. For example, bacteria synthesize more unsaturated fatty acids and fewer saturated ones when cultured at low temperatures than when cultured at higher temperatures (Table 11–2). As a result of this adjustment in lipid composition, membranes of bacteria cultured at high or low temperatures have about the same degree of fluidity. This is presumably essential for the function of many proteins—enzymes, transporters, and receptors—that act within the lipid bilayer.

Transbilayer Movement of Lipids Requires Catalysis

At physiological temperatures, transbilayer—or "flip-flop"—diffusion of a lipid molecule from one leaflet of the bilayer to the other **(Fig. 11–17a)** occurs very slowly if at all in most membranes, although lateral diffusion *in the plane* of the bilayer is very rapid (Fig. 11–17b). Transbilayer movement requires that a polar or charged head group leave its aqueous environment and move into the hydrophobic interior of the bilayer, a process with a large, positive free-energy change. There are, however, situations in which such movement is essential. For example, in the ER, membrane glycerophospholipids are synthesized on the cytosolic surface, whereas sphingolipids are synthesized or modified on the lumenal surface. To get from their site of synthesis to their eventual point of deposition, these lipids must undergo flip-flop diffusion.

The asymmetric disposition of lipid types in the bilayer predicts the existence of flippases, floppases, and scramblases (Fig. 11–17c), which facilitate the transbilayer movement of lipids, providing a path that is energetically more favorable and much faster than the uncatalyzed movement. The combination of asymmetric biosynthesis of membrane lipids, very slow uncatalyzed flip-flop diffusion, and the presence of selective, energy-dependent lipid translocators could account for the transbilayer asymmetry in lipid composition shown in Figure 11–5. Besides contributing to this asymmetry of composition, the energy-dependent transport of lipids to one bilayer leaflet may, by creating a larger surface on one side of the bilayer, be important in generating the membrane curvature essential in the budding of vesicles.

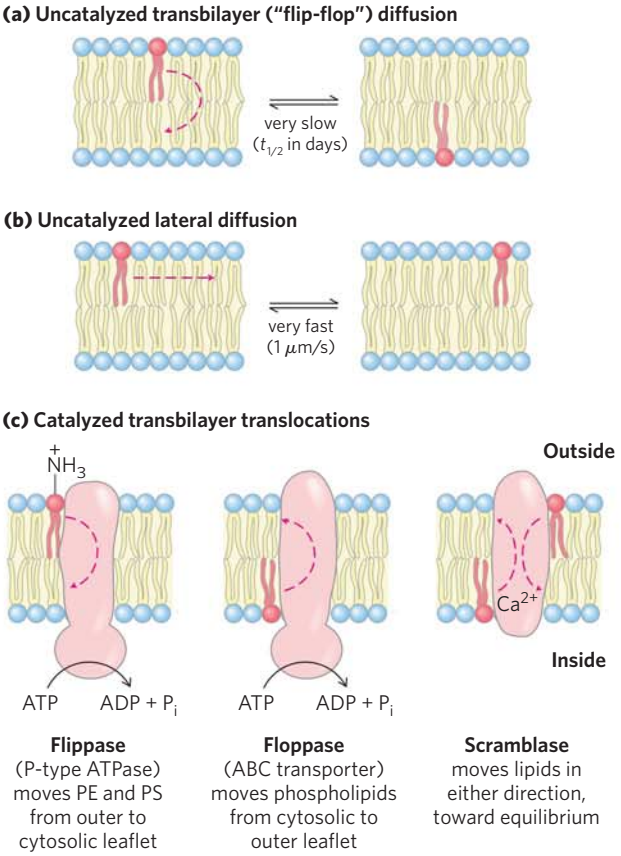

FIGURE 11–17 **Motion of single phospholipids in a bilayer. (a)** Uncatalyzed movement from one leaflet to the other is very slow, but **(b)** lateral diffusion within the leaflet is very rapid, requiring no catalysis. **(c)** Three types of phospholipid translocaters in the plasma membrane. PE is phosphatidylethanolamine; PS is phosphatidylserine.

Flippases catalyze translocation of the *amino*-phospholipids phosphatidylethanolamine and phosphatidylserine from the extracellular to the cytosolic leaflet of the plasma membrane, contributing to the asymmetric distribution of phospholipids: phosphatidylethanolamine and phosphatidylserine primarily in the cytosolic leaflet, and the sphingolipids and phosphatidylcholine in the outer leaflet. Keeping phosphatidylserine out of the extracellular leaflet is important: its exposure on the outer surface triggers apoptosis (programmed cell death; see Chapter 12) and engulfment by macrophages that carry phosphatidylserine receptors. Flippases also act in the ER, where they move newly synthesized phospholipids from their site of synthesis in the cytosolic leaflet to the lumenal leaflet. Flippases consume about one ATP per molecule of phospholipid translocated, and they are structurally and functionally related to the P-type ATPases (active transporters) described on page 410.

Two other types of lipid-translocating activities are known but less well characterized. **Floppases** move plasma membrane phospholipids from the cytosolic to the extracellular leaflet and like flippases are ATP-dependent. Floppases are members of the ABC transporter family described on page 413, all of which actively transport hydrophobic substrates outward across the plasma membrane. **Scramblases** are proteins that move any membrane phospholipid across the bilayer down its concentration gradient (from the leaflet where it has a higher concentration to the leaflet where it has a lower concentration); their activity is not dependent on ATP. Scramblase activity leads to controlled randomization of the head-group composition on the two faces of the bilayer. The activity rises sharply with an increase in cytosolic Ca^{2+} concentration, which may result from cell activation, cell injury, or apoptosis; as noted above, exposure of phosphatidylserine on the outer surface marks a cell for apoptosis and engulfment by macrophages. Finally, a group of proteins that act primarily to move phosphatidylinositol lipids across lipid bilayers, the phosphatidylinositol transfer proteins, are believed to have important roles in lipid signaling and membrane trafficking.

Lipids and Proteins Diffuse Laterally in the Bilayer

Individual lipid molecules can move laterally in the plane of the membrane by changing places with neighboring lipid molecules; that is, they undergo Brownian movement within the bilayer (Fig. 11–17b), which can be quite rapid. A molecule in the outer leaflet of the erythrocyte plasma membrane, for example, can diffuse laterally so fast that it circumnavigates the erythrocyte in seconds. This rapid lateral diffusion in the plane of the bilayer tends to randomize the positions of individual molecules in a few seconds.

Lateral diffusion can be shown experimentally by attaching fluorescent probes to the head groups of lipids and using fluorescence microscopy to follow the probes over time **(Fig. 11–18)**. In one technique, a small region (5 μm^2) of a cell surface with fluorescence-tagged lipids

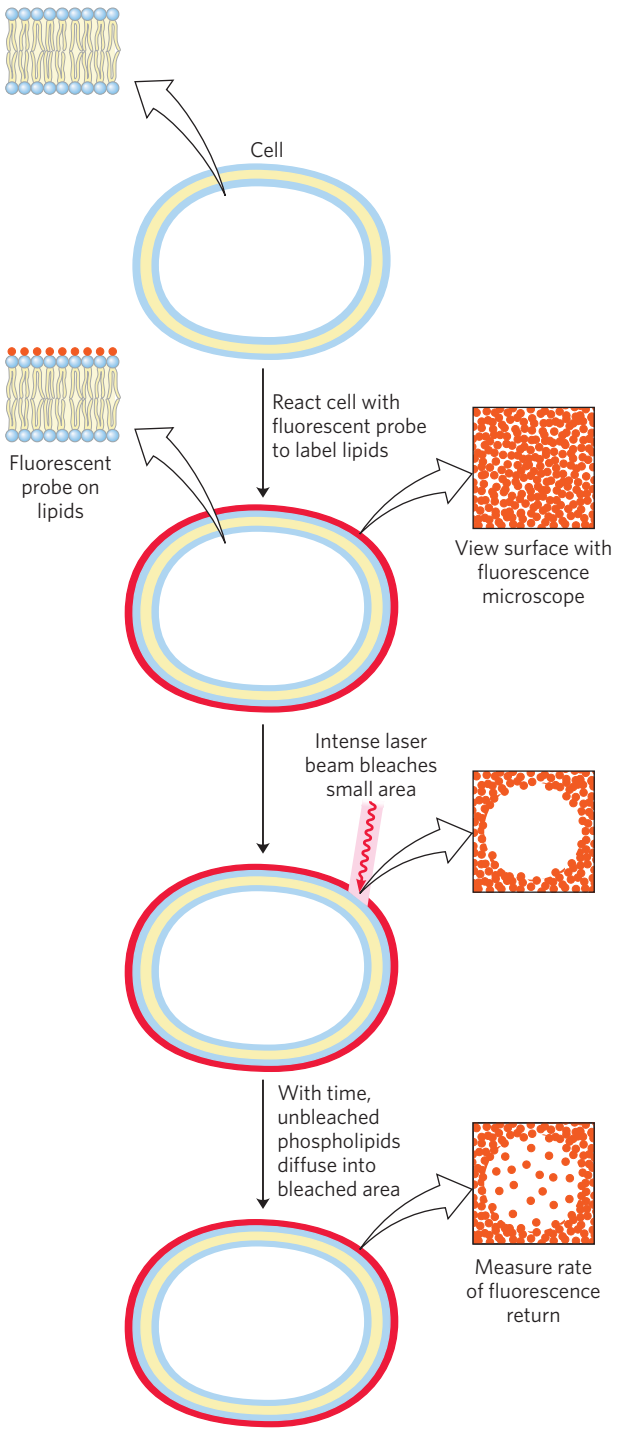

FIGURE 11–18 Measurement of lateral diffusion rates of lipids by fluorescence recovery after photobleaching (FRAP). Lipids in the outer leaflet of the plasma membrane are labeled by reaction with a membrane-impermeant fluorescent probe (red) so that the surface is uniformly labeled when viewed with a fluorescence microscope. A small area is bleached by irradiation with an intense laser beam and becomes nonfluorescent. With the passage of time, labeled lipid molecules diffuse into the bleached region, and it again becomes fluorescent. Researchers can track the time course of fluorescence return and determine a diffusion coefficient for the labeled lipid. The diffusion rates are typically high; a lipid moving at this speed could circumnavigate an *E. coli* cell in one second. (The FRAP method can also be used to measure lateral diffusion of membrane proteins.)

is bleached by intense laser radiation so that the irradiated patch no longer fluoresces when viewed with less-intense (nonbleaching) light in the fluorescence microscope. However, within milliseconds, the region recovers its fluorescence as unbleached lipid molecules diffuse into the bleached patch and bleached lipid molecules diffuse away from it. The rate of *f*luorescence *r*ecovery *a*fter *p*hotobleaching, or **FRAP**, is a measure of the rate of lateral diffusion of the lipids. Using the FRAP technique, researchers have shown that some membrane lipids diffuse laterally at rates of up to 1 μm/s.

Another technique, single particle tracking, allows one to follow the movement of a *single* lipid molecule in the plasma membrane on a much shorter time scale. Results from these studies confirm rapid lateral diffusion within small, discrete regions of the cell surface and show that movement from one such region to a nearby region ("hop diffusion") is inhibited; membrane lipids behave as though corralled by fences that they can occasionally cross by hop diffusion **(Fig. 11–19)**.

Many membrane proteins move as if afloat in a sea of lipids. Like membrane lipids, these proteins are free to diffuse laterally in the plane of the bilayer and are in constant motion, as shown by the FRAP technique with fluorescence-tagged surface proteins. Some membrane proteins associate to form large aggregates ("patches") on the surface of a cell or organelle in which individual protein molecules do not move relative to one another; for example, acetylcholine receptors form dense, near-crystalline patches on neuronal plasma membranes at synapses. Other membrane proteins are anchored to

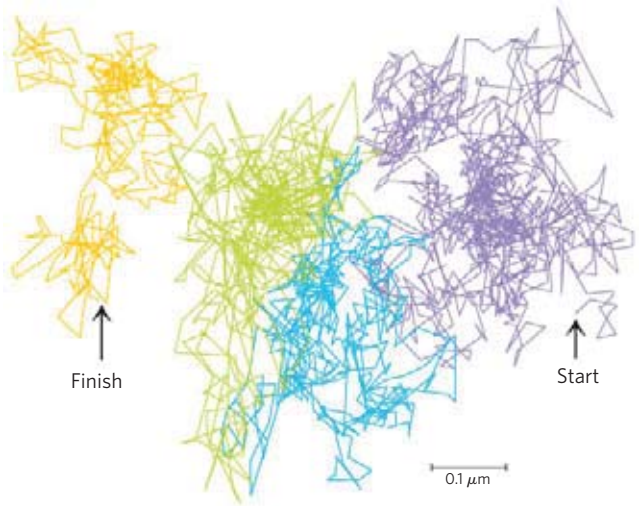

FIGURE 11–19 Hop diffusion of individual lipid molecules. The motion of a single fluorescently labeled lipid molecule in a cell surface is recorded on video by fluorescence microscopy, with a time resolution of 25 μs (equivalent to 40,000 frames/s). The track shown here represents a molecule followed for 56 ms (2,250 frames); the trace begins in the purple area and continues through blue, green, and orange. The pattern of movement indicates rapid diffusion within a confined region (about 250 nm in diameter, shown by a single color), with occasional hops into an adjoining region. This finding suggests that the lipids are corralled by molecular fences that they occasionally jump.

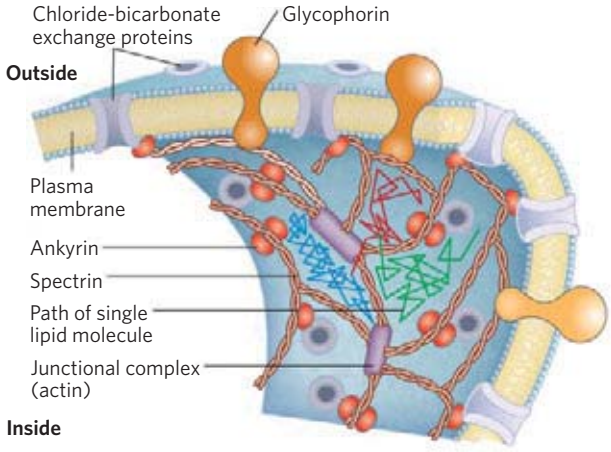

FIGURE 11–20 Restricted motion of the erythrocyte chloride-bicarbonate exchanger and glycophorin. The proteins span the membrane and are tethered to spectrin, a cytoskeletal protein, by another protein, ankyrin, limiting their lateral mobility. Ankyrin is anchored in the membrane by a covalently bound palmitoyl side chain (see Fig. 11–15). Spectrin, a long, filamentous protein, is cross-linked at junctional complexes containing actin. A network of cross-linked spectrin molecules attached to the cytoplasmic face of the plasma membrane stabilizes the membrane, making it resistant to deformation. This network of anchored membrane proteins may form the "corral" suggested by the experiment shown in Figure 11–19; the lipid tracks shown here are confined to different regions defined by the tethered membrane proteins. Occasionally a lipid molecule (green track) jumps from one corral to another (blue track), then another (red track).

internal structures that prevent their free diffusion. In the erythrocyte membrane, both glycophorin and the chloride-bicarbonate exchanger (p. 407) are tethered to spectrin, a filamentous cytoskeletal protein **(Fig. 11–20)**. One possible explanation for the pattern of lateral diffusion of lipid molecules shown in Figure 11–19 is that membrane proteins immobilized by their association with spectrin form the "fences" that define the regions of relatively unrestricted lipid motion.

Sphingolipids and Cholesterol Cluster Together in Membrane Rafts

We have seen that diffusion of membrane lipids from one bilayer leaflet to the other is very slow unless catalyzed and that the different lipid species of the plasma membrane are asymmetrically distributed in the two leaflets of the bilayer (Fig. 11–5). Even within a single leaflet, the lipid distribution is not uniform. Glycosphingolipids (cerebrosides and gangliosides), which typically contain long-chain saturated fatty acids, form transient clusters in the outer leaflet that largely exclude glycerophospholipids, which typically contain one unsaturated fatty acyl group and a shorter saturated acyl group. The long, saturated acyl groups of sphingolipids can form more compact, more stable associations with the long ring system of cholesterol than can the shorter, often unsaturated, chains of phospholipids. The cholesterol-sphingolipid **microdomains** in the outer monolayer of the plasma

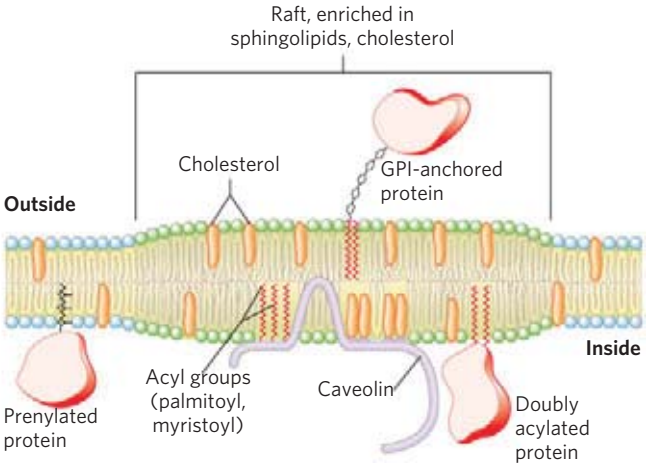

FIGURE 11–21 Membrane microdomains (rafts). Stable associations of sphingolipids and cholesterol in the outer leaflet produce a microdomain, slightly thicker than other membrane regions, that is enriched with specific types of membrane proteins. GPI-anchored proteins are prominent in the outer leaflet of these rafts, and proteins with one or several covalently attached long-chain acyl groups are common in the inner leaflet. Inwardly curved rafts called caveolae are especially enriched in the protein caveolin (see Fig. 11–22). Proteins with attached prenyl groups (such as Ras; see Box 12–2) tend to be excluded from rafts.

membrane are slightly thicker and more ordered (less fluid) than neighboring microdomains rich in phospholipids and are more difficult to dissolve with nonionic detergents; they behave like liquid-ordered sphingolipid **rafts** adrift on an ocean of liquid-disordered phospholipids **(Fig. 11–21)**.

These lipid rafts are remarkably enriched in two classes of integral membrane proteins: those anchored to the membrane by two covalently attached long-chain saturated fatty acids attached through Cys residues (two palmitoyl groups or a palmitoyl and a myristoyl group) and **GPI-anchored proteins** (Fig. 11–15). Presumably these lipid anchors, like the long, saturated acyl chains of sphingolipids, form more stable associations with the cholesterol and long acyl groups in rafts than with the surrounding phospholipids. (It is notable that other lipid-linked proteins, those with covalently attached isoprenyl groups such as farnesyl, are *not* preferentially associated with the outer leaflet of sphingolipid/cholesterol rafts (Fig. 11–21).) The "raft" and "sea" domains of the plasma membrane are not rigidly separated; membrane proteins can move into and out of lipid rafts on a time scale of seconds. But in the shorter time scale (microseconds) more relevant to many membrane-mediated biochemical processes, many of these proteins reside primarily in a raft.

We can estimate the fraction of the cell surface occupied by rafts from the fraction of the plasma membrane that resists detergent solubilization, which can be as high as 50% in some cases: the rafts cover half of the ocean. Indirect measurements in cultured fibroblasts suggest a diameter of roughly 50 nm for an individual raft, which corresponds to a patch containing a few thousand sphingolipids and perhaps 10 to 50 membrane proteins. Because most cells express more than 50 different kinds of plasma membrane proteins, it is likely that a single raft contains only a subset of membrane proteins and that this segregation of membrane proteins is functionally significant. For a process that involves interaction of two membrane proteins, their presence in a single raft would hugely increase the likelihood of their collision. Certain membrane receptors and signaling proteins, for example, seem to be segregated together in membrane rafts. Experiments show that signaling through these proteins can be disrupted by manipulations that deplete the plasma membrane of cholesterol and destroy lipid rafts.

Caveolin is an integral membrane protein with two globular domains connected by a hairpin-shaped hydrophobic domain, which binds the protein to the cytoplasmic leaflet of the plasma membrane. Three palmitoyl groups attached to the carboxyl-terminal globular domain further anchor it to the membrane. Caveolin (actually, a family of related caveolins) forms dimers and associates with cholesterol-rich regions in the membrane, and the presence of caveolin dimers forces the associated lipid bilayer to curve inward, forming **caveolae** ("little caves") in the surface of the cell **(Fig. 11–22)**. Caveolae are unusual rafts: they involve *both* leaflets of the bilayer—the cytoplasmic leaflet, from which the caveolin globular domains project, and the extracellular leaflet, a typical sphingolipid/cholesterol raft with associated GPI-anchored proteins. Caveolae are implicated in a variety of cellular functions, including membrane trafficking within cells and the transduction of external signals into cellular responses. The receptors for insulin and other growth factors, as well as certain GTP-binding proteins and protein kinases associated with transmembrane signaling, seem to be localized in rafts and perhaps in caveolae. We discuss some possible roles of rafts in signaling in Chapter 12.

Membrane Curvature and Fusion Are Central to Many Biological Processes

Caveolin is not unique in its ability to induce curvature in membranes. Changes of curvature are central to one of the most remarkable features of biological membranes: their ability to undergo fusion with other membranes without losing their continuity. Although membranes are stable, they are by no means static. Within the eukaryotic endomembrane system (which includes the nuclear membrane, endoplasmic reticulum, Golgi complex, and various small vesicles), the membranous compartments constantly reorganize. Vesicles bud from the ER to carry newly synthesized lipids and proteins to other organelles and to the plasma membrane. Exocytosis, endocytosis, cell division, fusion of egg and sperm cells, and entry of a membrane-enveloped virus into its host cell all involve membrane reorganization in which the fundamental operation is fusion of two membrane

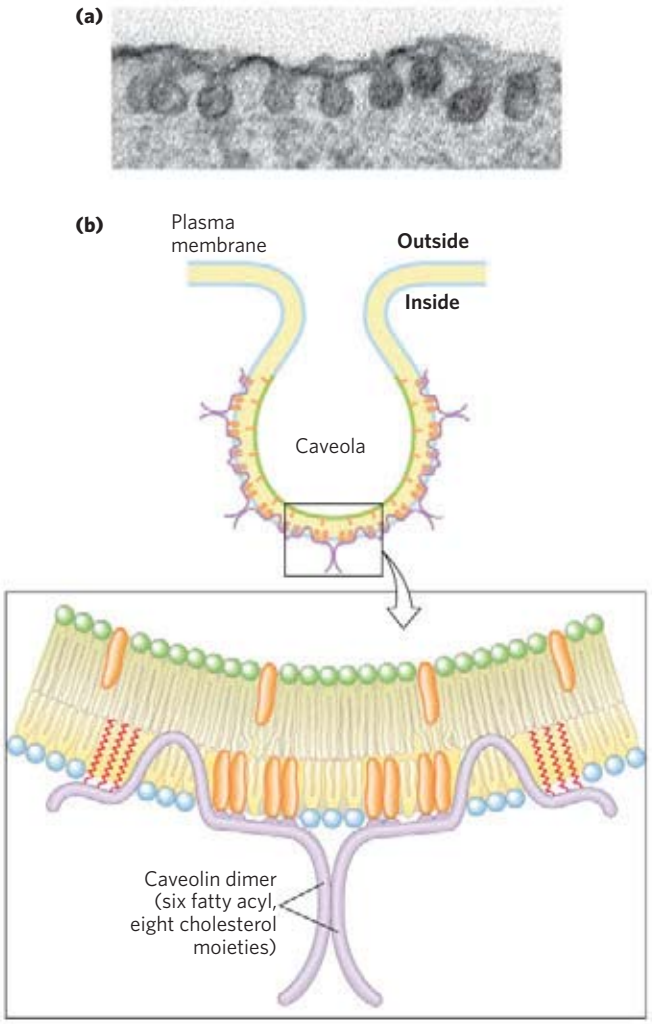

FIGURE 11–22 Caveolin forces inward curvature of a membrane. Caveolae are small invaginations in the plasma membrane, as seen in **(a)** an electron micrograph of an adipocyte that is surface-labeled with an electron-dense marker. **(b)** Cartoon showing the location and role of caveolin in causing inward membrane curvature. Each caveolin monomer has a central hydrophobic domain and three long-chain acyl groups (red), which hold the molecule to the inside of the plasma membrane. When several caveolin dimers are concentrated in a small region (a raft), they force a curvature in the lipid bilayer, forming a caveola. Cholesterol molecules in the bilayer are shown in orange.

segments without loss of continuity **(Fig. 11–23)**. Most of these processes begin with a local increase in membrane curvature. A protein that is intrinsically curved may force curvature in a bilayer by binding to it **(Fig. 11–24)**; the binding energy provides the driving force for the increase in bilayer curvature. Alternatively, multiple subunits of a scaffold protein may assemble into curved supramolecular complexes and stabilize curves that spontaneously form in the bilayer. For example, a superfamily of proteins containing **BAR domains** (named for the first three members of the family to be identified: *B*IN1, *a*mphiphysin, and *R*VS167) can assemble into a crescent-shaped scaffold that binds to the membrane surface, forcing or favoring membrane curvature.

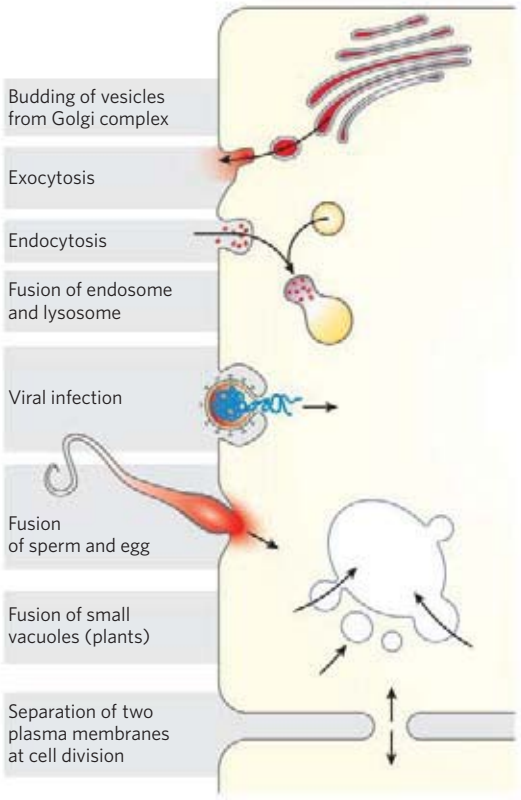

FIGURE 11–23 Membrane fusion. The fusion of two membranes is central to a variety of cellular processes involving organelles and the plasma membrane.

BAR domains consist of coiled coils that form long, thin, curved dimers with a positively charged concave surface that tends to form ionic interactions with the negatively charged head groups of membrane phospholipids (Fig. 11–24). Some of these BAR proteins also have a helical region that inserts into one leaflet of the bilayer, expanding its area relative to the other leaflet and thereby forcing curvature.

Specific fusion of two membranes requires that (1) they recognize each other; (2) their surfaces become closely apposed, which requires the removal of water molecules normally associated with the polar head groups of lipids; (3) their bilayer structures become locally disrupted, resulting in fusion of the outer leaflet of each membrane (hemifusion); and (4) their bilayers fuse to form a single continuous bilayer. The fusion occurring in receptor-mediated endocytosis, or regulated secretion, also requires that (5) the process is triggered at the appropriate time or in response to a specific signal. Integral proteins called **fusion proteins** mediate these events, bringing about specific recognition and a transient local distortion of the bilayer structure that favors membrane fusion. (Note that these fusion proteins are unrelated to the products encoded by two fused genes, also called fusion proteins, discussed in Chapter 9.)

A well-studied example of membrane fusion is that occurring at synapses, when intracellular vesicles loaded

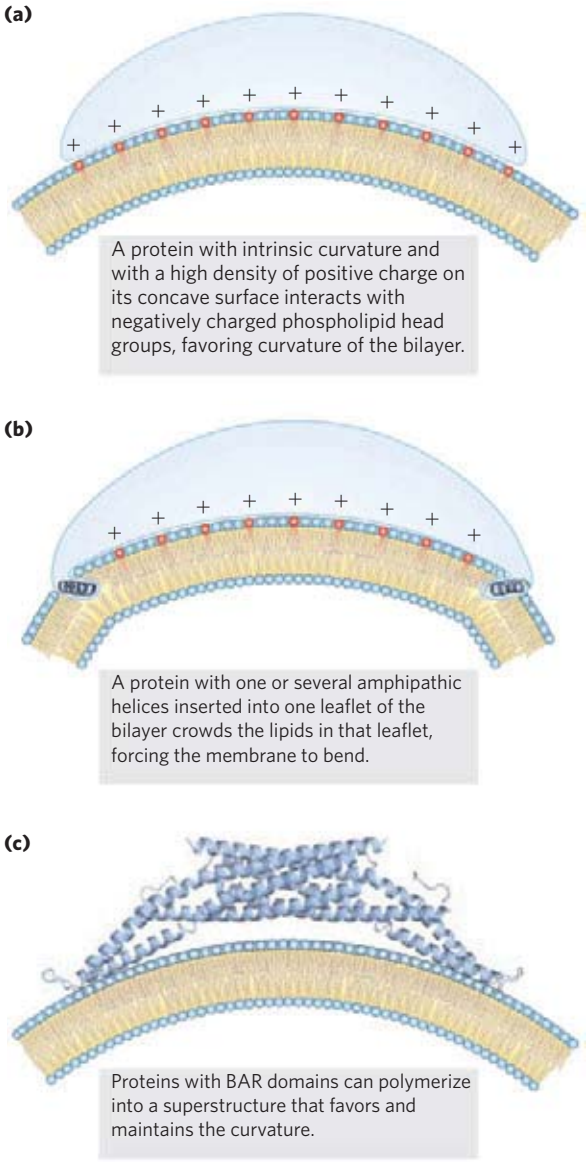

FIGURE 11–24 **Three models for protein-induced curvature of membranes.**

with neurotransmitter fuse with the plasma membrane. This process involves a family of proteins called SNARES **(Fig. 11–25)**. SNAREs in the cytoplasmic face of the intracellular vesicle are called **v-SNAREs**; those in the target membrane with which the vesicle fuses (the plasma membrane during exocytosis) are **t-SNAREs**. Two other proteins, SNAP25 and NSF, are also involved. During fusion, a v-SNARE and t-SNARE bind to each other and undergo a structural change that produces a bundle of long, thin rods made up of helices from both SNARES and two helices from SNAP25 (Fig. 11–25). The two SNAREs initially interact at their ends, then zip up into the bundle of helices. This structural change pulls the two membranes into contact and initiates the fusion of their lipid bilayers.

The complex of SNAREs and SNAP25 is the target of the powerful *Clostridium botulinum* toxin, a protease that cleaves specific bonds in these proteins,

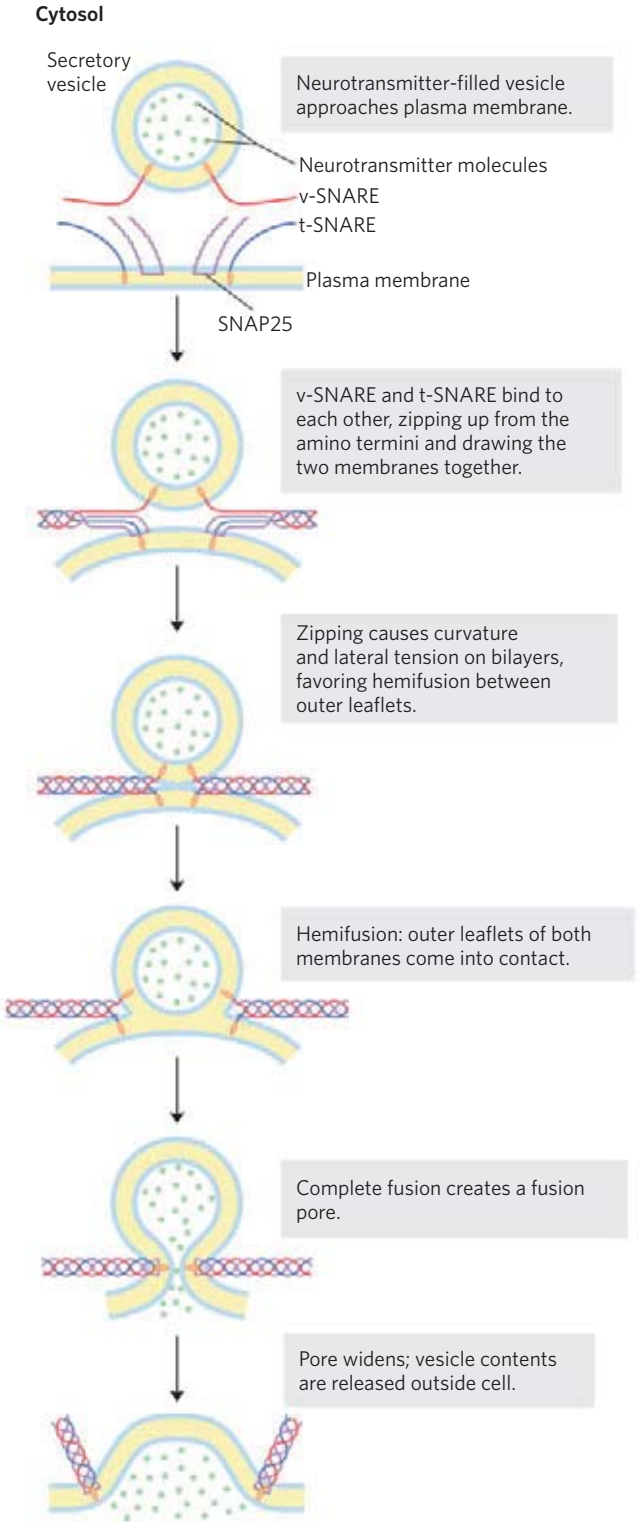

FIGURE 11–25 **Membrane fusion during neurotransmitter release at a synapse.** The secretory vesicle membrane contains the v-SNARE synaptobrevin (red). The target (plasma) membrane contains the t-SNAREs syntaxin (blue) and SNAP25 (violet). When a local increase in $[Ca^{2+}]$ signals release of neurotransmitter, the v-SNARE, SNAP25, and t-SNARE interact, forming a coiled bundle of four α helices, pulling the two membranes together and disrupting the bilayer locally. This leads first to hemifusion, joining the outer leaflets of the two membranes, then to complete membrane fusion and neurotransmitter release. NSF (*N*-ethylmaleimide-sensitive *f*usion factor) acts in disassembly of the SNARE complex when fusion is complete.

preventing neurotransmission and thereby causing the death of the organism. Because of its very high specificity for these proteins, purified botulinum toxin has served as a powerful tool for dissecting the mechanism of neurotransmitter release in vivo and in vitro.

Integral Proteins of the Plasma Membrane Are Involved in Surface Adhesion, Signaling, and Other Cellular Processes

Several families of integral proteins in the plasma membrane provide specific points of attachment between cells or between a cell and extracellular matrix proteins. **Integrins** are surface adhesion proteins that mediate a cell's interaction with the extracellular matrix and with other cells, including some pathogens. Integrins also carry signals in both directions across the plasma membrane, integrating information about the extracellular and intracellular environments. All integrins are heterodimeric proteins composed of two unlike subunits, α and β, each anchored to the plasma membrane by a single transmembrane helix. The large extracellular domains of the α and β subunits combine to form a specific binding site for extracellular proteins such as collagen and fibronectin, which contain a common determinant of integrin binding, the sequence Arg–Gly–Asp (RGD). We discuss the signaling functions of integrins in more detail in Chapter 12 (p. 470).

Other plasma membrane proteins involved in surface adhesion are the **cadherins**, which undergo homophilic ("with same kind") interactions with identical cadherins in an adjacent cell. **Selectins** have extracellular domains that, in the presence of Ca^{2+}, bind specific polysaccharides on the surface of an adjacent cell. Selectins are present primarily in the various types of blood cells and in the endothelial cells that line blood vessels (see Fig. 7–32). They are an essential part of the blood-clotting process.

Integral membrane proteins play roles in many other cellular processes. They serve as transporters and ion channels (discussed in Section 11.3) and as receptors for hormones, neurotransmitters, and growth factors (Chapter 12). They are central to oxidative phosphorylation and photophosphorylation (Chapter 19) and to cell-cell and cell-antigen recognition in the immune system (Chapter 5). Integral proteins are also important players in the membrane fusion that accompanies exocytosis, endocytosis, and the entry of many types of viruses into host cells.

SUMMARY 11.2 Membrane Dynamics

- Lipids in a biological membrane can exist in liquid-ordered or liquid-disordered states; in the latter state, thermal motion of acyl chains makes the interior of the bilayer fluid. Fluidity is affected by temperature, fatty acid composition, and sterol content.
- Flip-flop diffusion of lipids between the inner and outer leaflets of a membrane is very slow except when specifically catalyzed by flippases, floppases, or scramblases.
- Lipids and proteins can diffuse laterally within the plane of the membrane, but this mobility is limited by interactions of membrane proteins with internal cytoskeletal structures and interactions of lipids with lipid rafts. One class of lipid rafts consists of sphingolipids and cholesterol with a subset of membrane proteins that are GPI-linked or attached to several long-chain fatty acyl moieties.
- Caveolin is an integral membrane protein that associates with the inner leaflet of the plasma membrane, forcing it to curve inward to form caveolae, probably involved in membrane transport and signaling.
- Specific proteins containing BAR domains cause local membrane curvature and mediate the fusion of two membranes, which accompanies processes such as endocytosis, exocytosis, and viral invasion.
- Integrins are transmembrane proteins of the plasma membrane that act both to attach cells to each other and to carry messages between the extracellular matrix and the cytoplasm.

11.3 Solute Transport across Membranes

Every living cell must acquire from its surroundings the raw materials for biosynthesis and for energy production, and must release the byproducts of metabolism to its environment. A few nonpolar compounds can dissolve in the lipid bilayer and cross the membrane unassisted, but for transmembrane movement of any polar compound or ion, a membrane protein is essential. In some cases a membrane protein simply facilitates the diffusion of a solute down its concentration gradient, but transport can also occur against a gradient of concentration, electric charge, or both, in which case the process requires energy **(Fig. 11–26)**. The energy may come directly from ATP hydrolysis or may be supplied in the form of one solute moving down its electrochemical gradient, which provides sufficient energy to drive another solute up its gradient. Ions may also move across membranes via ion channels formed by proteins, or they may be carried across by ionophores, small molecules that mask the charge of ions and allow them to diffuse through the lipid bilayer. With very few exceptions, the traffic of small molecules across the plasma membrane is mediated by proteins such as transmembrane channels, carriers, or pumps. Within the eukaryotic cell, different compartments have different concentrations of ions and of metabolic intermediates and products, and these, too, must move across intracellular membranes in tightly regulated, protein-mediated processes.

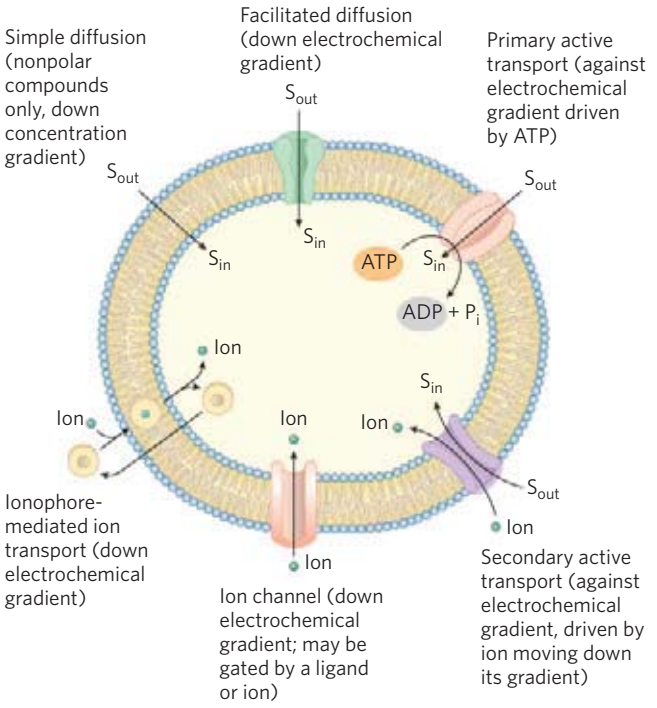

FIGURE 11–26 Summary of transporter types. Some types (ionophores, ion channels, and passive transporters) simply speed transmembrane movement of solutes down their electrochemical gradients, whereas others (active transporters) can pump solutes against a gradient, using ATP or a gradient of a second solute to provide the energy.

Passive Transport Is Facilitated by Membrane Proteins

When two aqueous compartments containing unequal concentrations of a soluble compound or ion are separated by a permeable divider (membrane), the solute moves by **simple diffusion** from the region of higher concentration, through the membrane, to the region of lower concentration, until the two compartments have equal solute concentrations **(Fig. 11–27a)**. When ions of opposite charge are separated by a permeable membrane, there is a transmembrane electrical gradient, a **membrane potential, V_m** (expressed in millivolts). This membrane potential produces a force opposing ion movements that increase V_m and driving ion movements that reduce V_m (Fig. 11–27b). Thus, the direction in which a charged solute tends to move spontaneously across a membrane depends on both the chemical gradient (the difference in solute concentration) and the electrical gradient (V_m) across the membrane. Together these two factors are referred to as the **electrochemical gradient** or **electrochemical potential**. This behavior of solutes is in accord with the second law of thermodynamics: molecules tend to spontaneously assume the distribution of greatest randomness and lowest energy.

To pass through a lipid bilayer, a polar or charged solute must first give up its interactions with the water molecules in its hydration shell, then diffuse about 3 nm (30 Å) through a substance (lipid) in which it is poorly soluble **(Fig. 11–28)**. The energy used to strip away the hydration shell and to move the polar compound from water into lipid, then through the lipid bilayer, is regained as the compound leaves the membrane on the other side and is rehydrated. However, the intermediate stage of transmembrane passage is a high-energy state comparable to the transition state in an enzyme-catalyzed chemical reaction. In both cases, an activation barrier must be overcome to reach the intermediate stage (Fig. 11–28; compare with Fig. 6–3). The energy of activation ($\Delta G^{\ddagger}$) for translocation of a polar solute across the bilayer is so large that pure lipid bilayers are virtually impermeable to polar and charged species over periods relevant to cell growth and division.

Membrane proteins lower the activation energy for transport of polar compounds and ions by providing an alternative path across the membrane for specific solutes. Proteins that bring about this **facilitated diffusion**, or

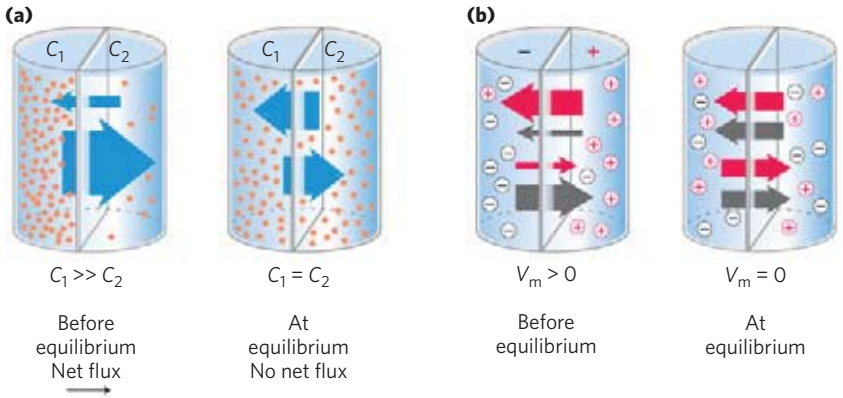

FIGURE 11–27 Movement of solutes across a permeable membrane. **(a)** Net movement of an electrically neutral solute is toward the side of lower solute concentration until equilibrium is achieved. The solute concentrations on the left and right sides of the membrane are designated C_1 and C_2. The rate of transmembrane solute movement (indicated by the arrows) is proportional to the concentration ratio. **(b)** Net movement of an electrically charged solute is dictated by a combination of the electrical potential (V_m) and the ratio of chemical concentrations (C_2/C_1) across the membrane; net ion movement continues until this electrochemical potential reaches zero.

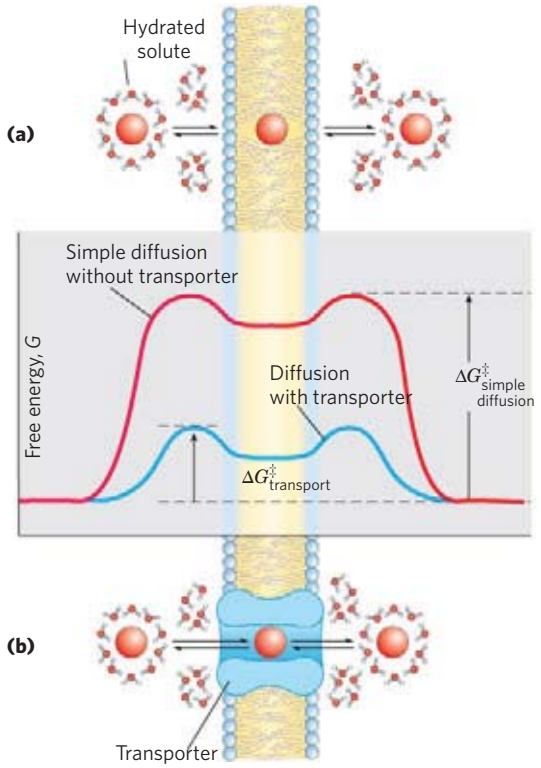

FIGURE 11–28 Energy changes accompanying passage of a hydrophilic solute through the lipid bilayer of a biological membrane. (a) In simple diffusion, removal of the hydration shell is highly endergonic, and the energy of activation ($\Delta G^{\ddagger}$) for diffusion through the bilayer is very high. **(b)** A transporter protein reduces the $\Delta G^{\ddagger}$ for transmembrane diffusion of the solute. It does this by forming noncovalent interactions with the dehydrated solute to replace the hydrogen bonding with water and by providing a hydrophilic transmembrane pathway.

passive transport, are not enzymes in the usual sense; their "substrates" are moved from one compartment to another but are not chemically altered. Membrane proteins that speed the movement of a solute across a membrane by facilitating diffusion are called **transporters** or **permeases**.

Like enzymes, transporters bind their substrates with stereochemical specificity through multiple weak, noncovalent interactions. The negative free-energy change associated with these weak interactions, $\Delta G_{\text{binding}}$, counterbalances the positive free-energy change that accompanies loss of the water of hydration from the substrate, $\Delta G_{\text{dehydration}}$, thereby lowering $\Delta G^{\ddagger}$ for transmembrane passage (Fig. 11–28). Transporters span the lipid bilayer several times, forming a transmembrane pathway lined with hydrophilic amino acid side chains. The pathway provides an alternative route for a specific substrate to move across the lipid bilayer without its having to dissolve in the bilayer, further lowering $\Delta G^{\ddagger}$ for transmembrane diffusion. The result is an increase of several to many orders of magnitude in the rate of transmembrane passage of the substrate.

Transporters and Ion Channels Are Fundamentally Different

We know from genomic studies that transporters constitute a significant fraction of all proteins encoded in the genomes of both simple and complex organisms. There are probably a thousand or more different genes in the human genome encoding proteins that allow molecules and ions to cross membranes. These proteins fall within two very broad categories: transporters and channels **(Fig. 11–29)**. **Transporters** for molecules and ions bind their substrates with high specificity, catalyze transport at rates well below the limits of free diffusion, and are saturable in the same sense as are enzymes: there is some substrate concentration above which further increases will not produce a greater rate of transport. **Channels** generally allow transmembrane movement of ions at rates that are orders of magnitude greater than those typical of transporters, approaching the limit of unhindered diffusion (tens of millions of ions per second per channel). Channels typically show some specificity for an ion, but are not saturable with the ion substrate, in contrast to the saturation kinetics seen with transporters. The direction of ion movement through an ion channel is dictated by the ion's charge and the electrochemical

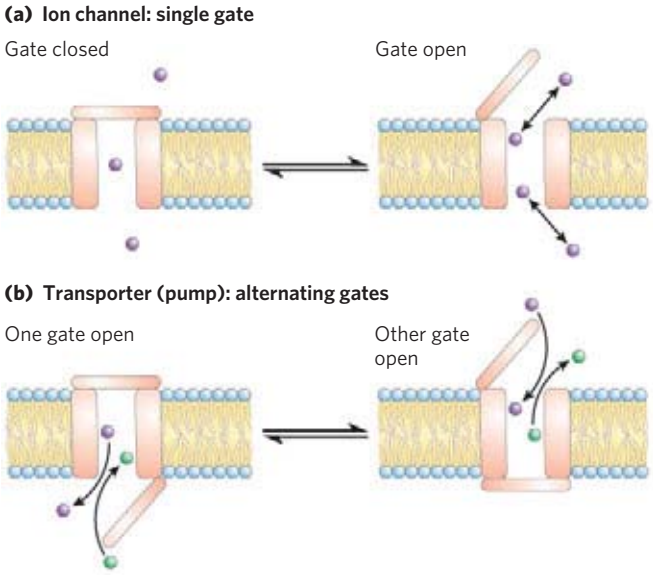

FIGURE 11–29 Differences between channels and transporters. (a) In an ion channel, a transmembrane pore is either open or closed, depending on the position of the single gate. When it is open, ions move through at a rate limited only by the maximum rate of diffusion. **(b)** Transporters (pumps) have two gates, and they are never both open. Movement of a substrate (an ion or a small molecule) through the membrane is therefore limited by the time needed for one gate to open and close (on one side of the membrane) and for the second gate to open. Rates of movement through ion channels can be orders of magnitude greater than rates through pumps, but channels simply allow the ion to flow down the electrochemical gradient, whereas pumps can move a substrate against a concentration gradient.

gradient across the membrane. Within each of these categories are families of various types, defined not only by their primary sequences but by their secondary structures. Among the transporters, some simply facilitate diffusion down a concentration gradient; they are the **passive transporters**. **Active transporters** can drive substrates across the membrane against a concentration gradient, some using energy provided directly by a chemical reaction (primary active transporters) and some coupling uphill transport of one substrate with downhill transport of another (secondary active transporters). We now consider some well-studied representatives of the main transporter and channel families. You will encounter some of these in Chapter 12 when we discuss transmembrane signaling and again in later chapters in the context of the metabolic pathways in which they participate.

The Glucose Transporter of Erythrocytes Mediates Passive Transport

Energy-yielding metabolism in erythrocytes depends on a constant supply of glucose from the blood plasma, where the glucose concentration is maintained at about 5 mM. Glucose enters the erythrocyte by facilitated diffusion via a specific glucose transporter, at a rate about 50,000 times greater than uncatalyzed transmembrane diffusion. The glucose transporter of erythrocytes (called GLUT1 to distinguish it from related glucose transporters in other tissues) is a type III integral protein (M_r ~45,000) with 12 hydrophobic segments, each of which is believed to form a membrane-spanning helix. The detailed structure of GLUT1 is not yet known, but one plausible model suggests that the side-by-side assembly of several helices produces a transmembrane channel lined with hydrophilic residues that can hydrogen-bond with glucose as it moves through the aqueous pore **(Fig. 11–30)**.

The process of glucose transport can be described by its analogy with an enzymatic reaction in which the "substrate" is glucose outside the cell (S_{out}), the "product" is glucose inside (S_{in}), and the "enzyme" is the transporter, T. When the initial rate of glucose uptake is measured as a function of external glucose concentration **(Fig. 11–31)**, the resulting plot is hyperbolic: at high external glucose concentrations the rate of uptake approaches V_{max}. Formally, such a transport process can be described by the equations

$$\begin{array}{ccc} S_{out} + T_1 & \underset{k_{-1}}{\overset{k_1}{\rightleftharpoons}} & S_{out} \bullet T_1 \\ k_{-4} \downarrow \uparrow k_4 & & k_{-2} \downarrow \uparrow k_2 \\ S_{in} + T_2 & \underset{k_{-3}}{\overset{k_3}{\rightleftharpoons}} & S_{in} \bullet T_2 \end{array}$$

in which k_1, k_{-1}, and so forth are the forward and reverse rate constants for each step; T_1 is the transporter conformation in which the glucose-binding site faces out, and T_2 is the conformation in which it faces in.

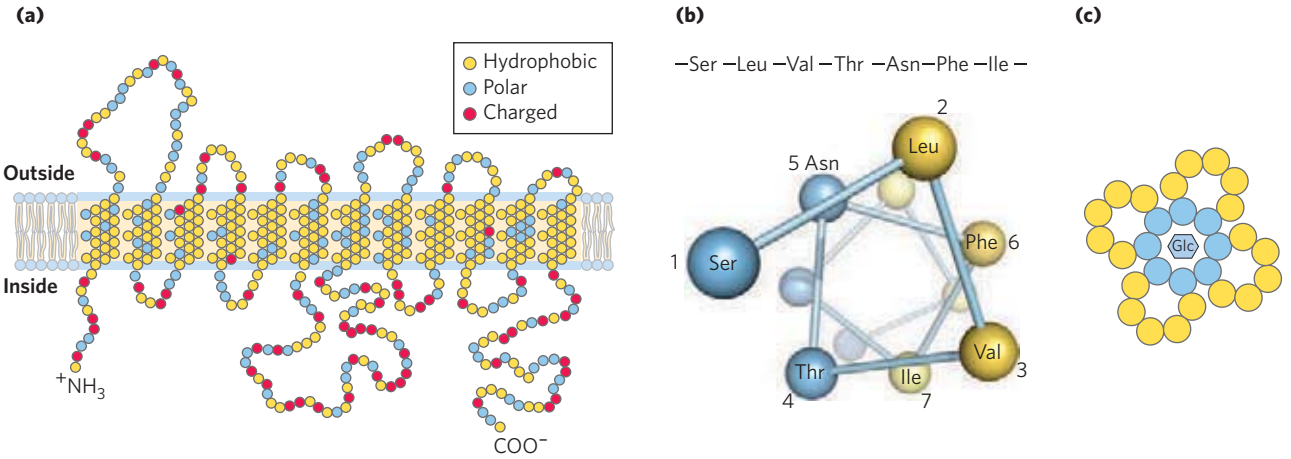

FIGURE 11–30 Membrane topology of the glucose transporter GLUT1. **(a)** Transmembrane helices are represented here as oblique (angled) rows of three or four amino acid residues, each row depicting one turn of the α helix. Nine of the 12 helices contain three or more polar or charged residues (blue or red), often separated by several hydrophobic residues (yellow). This representation of topology is not intended to depict three-dimensional structure. **(b)** A helical wheel diagram shows the distribution of polar and nonpolar residues on the surface of a helical segment. The helix is diagrammed as though observed along its axis from the amino terminus. Adjacent residues in the linear sequence are connected, and each residue is placed around the wheel in the position it occupies in the helix; recall that 3.6 residues are required to make one complete turn of the α helix. In this example, the polar residues (blue) are on one side of the helix and the hydrophobic residues (yellow) on the other. This is, by definition, an amphipathic helix. **(c)** Side-by-side association of four amphipathic helices, each with its polar face oriented toward the central cavity, can produce a transmembrane channel lined with polar (and charged) residues. This channel provides many opportunities for hydrogen bonding with glucose as it moves through.

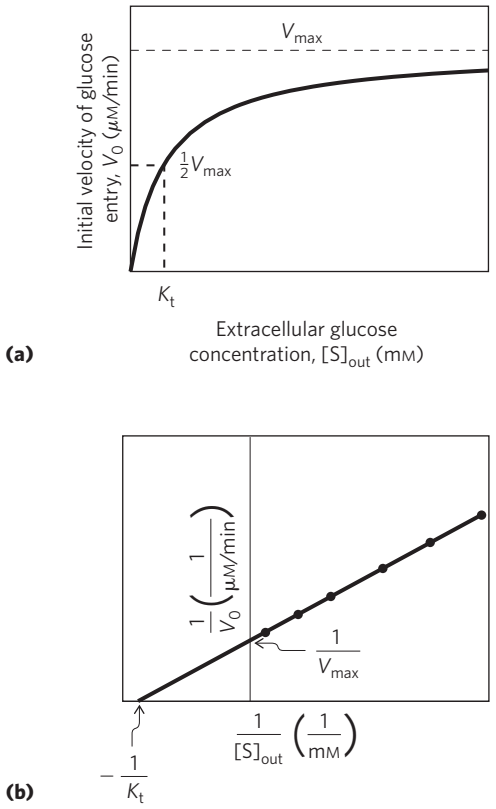

FIGURE 11–31 Kinetics of glucose transport into erythrocytes. (a) The initial rate of glucose entry into an erythrocyte, V_0, depends on the initial concentration of glucose on the outside, $[S]_{out}$. **(b)** Double-reciprocal plot of the data in (a). The kinetics of facilitated diffusion is analogous to the kinetics of an enzyme-catalyzed reaction. Compare these plots with Figure 6–11 and with Figure 1 in Box 6–1. Note that K_t is analogous to K_m, the Michaelis constant.

The steps are summarized in **Figure 11–32**. Given that every step in this sequence is reversible, the transporter is, in principle, equally able to move glucose into or out of the cell. However, with GLUT1, glucose always moves down its concentration gradient, which normally means *into* the cell. Glucose that enters a cell is generally metabolized immediately, and the intracellular glucose concentration is thereby kept low relative to its concentration in the blood.

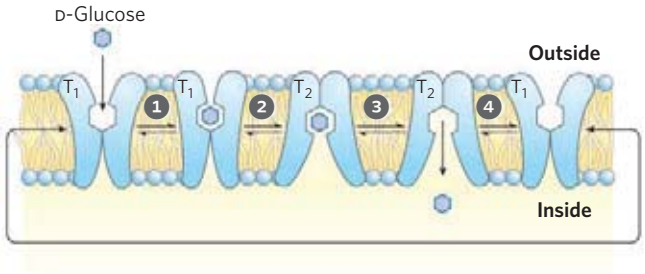

FIGURE 11–32 Model of glucose transport into erythrocytes by GLUT1. The transporter exists in two conformations: T_1, with the glucose-binding site exposed on the outer surface of the plasma membrane, and T_2, with the binding site exposed on the inner surface. Glucose transport occurs in four steps. ❶ Glucose in blood plasma binds to a stereospecific site on T_1; this lowers the activation energy for ❷ a conformational change from $glucose_{out} \cdot T_1$ to $glucose_{in} \cdot T_2$, effecting the transmembrane passage of the glucose. ❸ Glucose is released from T_2 into the cytoplasm, and ❹ the transporter returns to the T_1 conformation, ready to transport another glucose molecule.

The rate equations for glucose transport can be derived exactly as for enzyme-catalyzed reactions (Chapter 6), yielding an expression analogous to the Michaelis-Menten equation:

$$V_0 = \frac{V_{max}[S]_{out}}{K_t + [S]_{out}} \qquad (11\text{–}1)$$

in which V_0 is the initial velocity of accumulation of glucose inside the cell when its concentration in the surrounding medium is $[S]_{out}$ and $\boldsymbol{K_t}$ **(**$\boldsymbol{K_{transport}}$**)** is a constant analogous to the Michaelis constant, a combination of rate constants that is characteristic of each transport system. This equation describes the *initial* velocity, the rate observed when $[S]_{in} = 0$. As is the case for enzyme-catalyzed reactions, the slope-intercept form of the equation describes a linear plot of $1/V_0$ against $1/[S]_{out}$, from which we can obtain values of K_t and V_{max} (Fig. 11–31b). When $[S]_{out} = K_t$, the rate of uptake is $\frac{1}{2}V_{max}$; the transport process is half-saturated. The concentration of glucose in blood is 4.5 to 5 mM, close to the K_t, which ensures that GLUT1 is nearly saturated with substrate and operates near V_{max}.

Because no chemical bonds are made or broken in the conversion of S_{out} to S_{in}, neither "substrate" nor "product" is intrinsically more stable, and the process of entry is therefore fully reversible. As $[S]_{in}$ approaches $[S]_{out}$, the rates of entry and exit become equal. Such a system is therefore incapable of accumulating glucose within a cell at concentrations above that in the surrounding medium; it simply equilibrates glucose on the two sides of the membrane much faster than would occur in the absence of a specific transporter. GLUT1 is specific for D-glucose, with a measured K_t of about 6 mM. For the close analogs D-mannose and D-galactose, which differ only in the position of one hydroxyl group, the values of K_t are 20 and 30 mM, respectively, and for L-glucose, K_t exceeds 3,000 mM. Thus, GLUT1 shows the three hallmarks of passive transport: high rates of diffusion down a concentration gradient, saturability, and specificity.

Twelve passive glucose transporters are encoded in the human genome, each with its unique kinetic properties, patterns of tissue distribution, and function (Table 11–3). In the liver, GLUT2 transports glucose out of hepatocytes when liver glycogen is broken down to replenish blood glucose. GLUT2 has a large K_t (17 mM or greater) and can therefore respond to increased levels of intracellular glucose (produced by glycogen breakdown) by increasing outward transport. Skeletal and heart muscle and adipose tissue have yet another glucose transporter, GLUT4

TABLE 11–3 Glucose Transporters in Humans

Transporter	Tissue(s) where expressed	K_t (mM)*	Role†
GLUT1	Ubiquitous	3	Basal glucose uptake
GLUT2	Liver, pancreatic islets, intestine	17	In liver and kidney, removal of excess glucose from blood; in pancreas, regulation of insulin release
GLUT3	Brain (neuronal), testis (sperm)	1.4	Basal glucose uptake
GLUT4	Muscle, fat, heart	5	Activity increased by insulin
GLUT5	Intestine (primarily), testis, kidney	6‡	Primarily fructose transport
GLUT6	Spleen, leukocytes, brain	>5	Possibly no transporter function
GLUT7	Small intestine, colon	0.3	—
GLUT8	Testis	~2	—
GLUT9	Liver, kidney	0.6	—
GLUT10	Heart, lung, brain, liver, muscle, pancreas, kidney	0.3§	—
GLUT11	Heart, skeletal muscle, kidney	0.16	—
GLUT12	Skeletal muscle, heart, prostate, small intestine	—	—

*K_t for glucose, except as noted, from Augustin, R. (2010) The protein family of glucose transport facilitators: it's not only about glucose after all. *IUBMB Life* 62, 315–333.

†Dash indicates role uncertain.

‡K_m for fructose.

§K_m for 2-deoxyglucose.

(K_t = 5 mM), which is distinguished by its response to insulin: its activity increases when insulin signals a high blood glucose concentration, thus increasing the rate of glucose uptake into muscle and adipose tissue (Box 11–1 describes the effect of insulin on this transporter).

The Chloride-Bicarbonate Exchanger Catalyzes Electroneutral Cotransport of Anions across the Plasma Membrane

The erythrocyte contains another facilitated diffusion system, an anion exchanger that is essential in CO_2 transport to the lungs from tissues such as skeletal muscle and liver. Waste CO_2 released from respiring tissues into the blood plasma enters the erythrocyte, where it is converted to bicarbonate (HCO_3^-) by the enzyme carbonic anhydrase. (Recall that HCO_3^- is the primary buffer of blood pH; see Fig. 2–21.) The HCO_3^- reenters the blood plasma for transport to the lungs **(Fig. 11–33)**. Because HCO_3^- is much more soluble in blood plasma than is CO_2, this roundabout route increases the capacity of the blood to carry carbon dioxide from the tissues to the lungs. In the lungs, HCO_3^- reenters the erythrocyte and is converted to CO_2, which is eventually released into the lung space and exhaled. To be effective, this shuttle requires very rapid movement of HCO_3^- across the erythrocyte membrane.

The **chloride-bicarbonate exchanger**, also called the **anion exchange (AE) protein**, increases the rate of HCO_3^- transport across the erythrocyte membrane more than a millionfold. Like the glucose transporter, it is an integral protein that probably

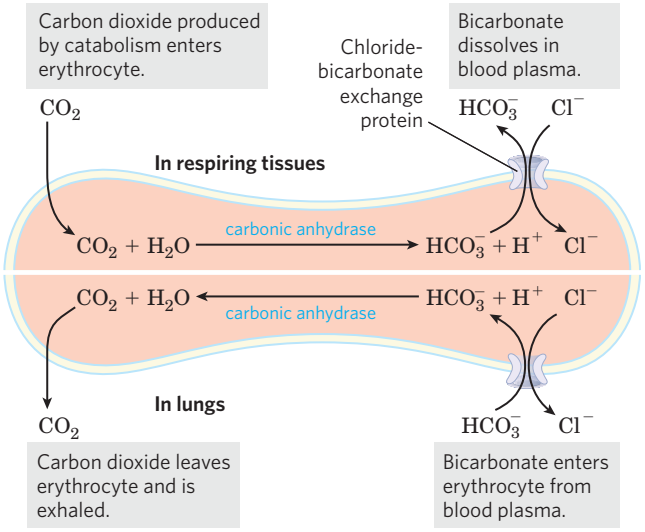

FIGURE 11–33 Chloride-bicarbonate exchanger of the erythrocyte membrane. This cotransport system allows the entry and exit of HCO_3^- without changing the membrane potential. Its role is to increase the CO_2-carrying capacity of the blood. The top half of the figure illustrates the events that take place in respiring tissues; the bottom half, the events in the lungs.

BOX 11–1 MEDICINE Defective Glucose and Water Transport in Two Forms of Diabetes

When ingestion of a carbohydrate-rich meal causes blood glucose to exceed the usual concentration between meals (about 5 mM), excess glucose is taken up by the myocytes of cardiac and skeletal muscle (which store it as glycogen) and by adipocytes (which convert it to triacylglycerols). Glucose uptake into myocytes and adipocytes is mediated by the glucose transporter GLUT4. Between meals, some GLUT4 is present in the plasma membrane, but most is sequestered in the membranes of small intracellular vesicles (Fig. 1). Insulin released from the pancreas in response to high blood glucose triggers the movement of these intracellular vesicles to the plasma membrane, with which they fuse, bringing GLUT4 molecules to the plasma membrane (see Fig. 12–16). With more GLUT4 molecules in action, the rate of glucose uptake increases 15-fold or more. When blood glucose levels return to normal, insulin release slows and most GLUT4 molecules are removed from the plasma membrane and stored in vesicles.

In type 1 (insulin-dependent) diabetes mellitus, the inability to release insulin (and thus to mobilize glucose transporters) results in low rates of glucose uptake into muscle and adipose tissue. One consequence is a prolonged period of high blood glucose after a carbohydrate-rich meal. This condition is the basis for the glucose tolerance test used to diagnose diabetes (Chapter 23).

The water permeability of epithelial cells lining the renal collecting duct in the kidney is due to the presence of an aquaporin (AQP2) in their apical plasma membranes (facing the lumen of the duct). Vasopressin (antidiuretic hormone, ADH) regulates the retention of water by mobilizing AQP2 molecules stored in vesicle membranes within the epithelial cells, much as insulin mobilizes GLUT4 in muscle and adipose tissue. When the vesicles fuse with the epithelial cell plasma membrane, water permeability greatly increases and more water is reabsorbed from the collecting duct and returned to the blood. When the vasopressin level drops, AQP2 is resequestered within vesicles, reducing water retention. In the relatively rare human disease diabetes insipidus, a genetic defect in AQP2 leads to impaired water reabsorption by the kidney. The result is excretion of copious volumes of very dilute urine. If the individual drinks enough water to replace that lost in the urine, there are no serious medical consequences, but insufficient water intake leads to dehydration and imbalances in blood electrolytes, which can lead to fatigue, headache, muscle pain, or even death.

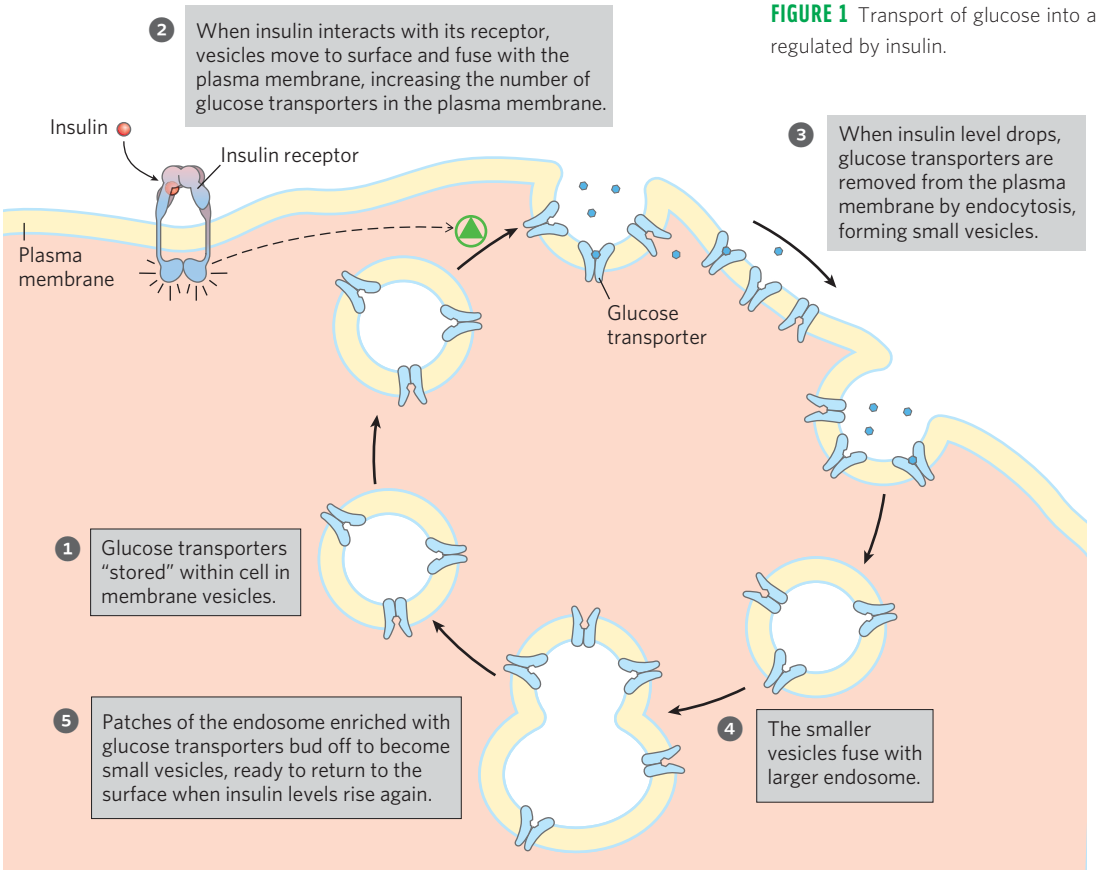

FIGURE 1 Transport of glucose into a myocyte by GLUT4 is regulated by insulin.

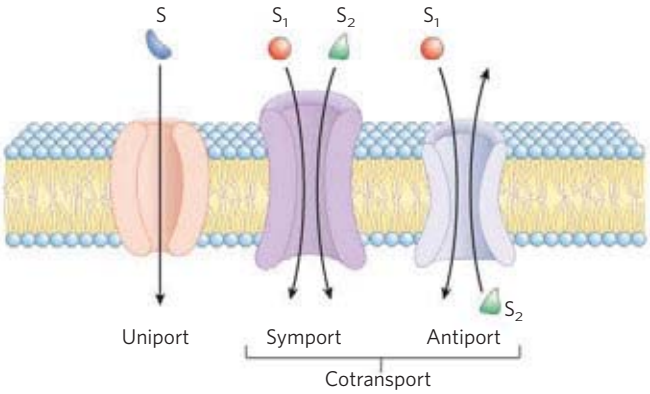

FIGURE 11–34 Three general classes of transport systems. Transporters differ in the number of solutes (substrates) transported and the direction in which each solute moves. Examples of all three types of transporter are discussed in the text. Note that this classification tells us nothing about whether these are energy-requiring (active transport) or energy-independent (passive transport) processes.

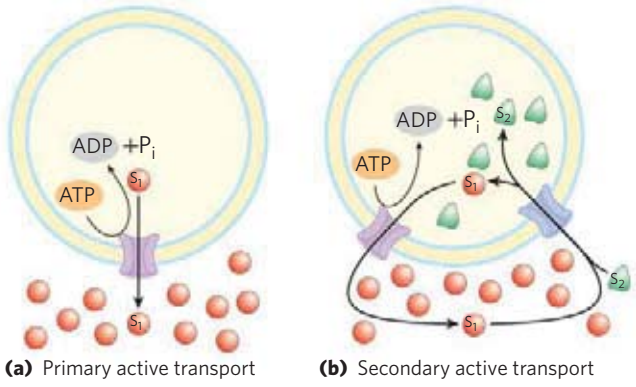

FIGURE 11–35 Two types of active transport. (a) In primary active transport, the energy released by ATP hydrolysis drives solute (S_1) movement against an electrochemical gradient. **(b)** In secondary active transport, a gradient of ion X (S_1) (often Na^+) has been established by primary active transport. Movement of X (S_1) down its electrochemical gradient now provides the energy to drive cotransport of a second solute (S_2) against its electrochemical gradient.

spans the membrane at least 12 times. This protein mediates the simultaneous movement of two anions: for each HCO_3^- ion that moves in one direction, one Cl^- ion moves in the opposite direction, with no net transfer of charge; the exchange is **electroneutral**. The coupling of Cl^- and HCO_3^- movements is obligatory; in the absence of chloride, bicarbonate transport stops. In this respect, the anion exchanger is typical of those systems, called **cotransport systems**, that simultaneously carry two solutes across a membrane **(Fig. 11–34)**. When, as in this case, the two substrates move in opposite directions, the process is **antiport**. In **symport**, two substrates are moved simultaneously in the same direction. Transporters that carry only one substrate, such as the erythrocyte glucose transporter, are known as **uniport** systems.

The human genome has genes for three closely related chloride-bicarbonate exchangers, all with the same predicted transmembrane topology. Erythrocytes contain the AE1 transporter, AE2 is prominent in the liver, and AE3 is present in plasma membranes of the brain, heart, and retina. Similar anion exchangers are also found in plants and microorganisms.

Active Transport Results in Solute Movement against a Concentration or Electrochemical Gradient

In passive transport, the transported species always moves down its electrochemical gradient and is not accumulated above the equilibrium concentration. **Active transport**, by contrast, results in the accumulation of a solute above the equilibrium point. Active transport is thermodynamically unfavorable (endergonic) and takes place only when coupled (directly or indirectly) to an exergonic process such as the absorption of sunlight, an oxidation reaction, the breakdown of ATP, or the concomitant flow of some other chemical species down its electrochemical gradient. In **primary active transport**, solute accumulation is coupled directly to an exergonic chemical reaction, such as conversion of ATP to ADP + P_i **(Fig. 11–35)**. **Secondary active transport** occurs when endergonic (uphill) transport of one solute is coupled to the exergonic (downhill) flow of a different solute that was originally pumped uphill by primary active transport.

The amount of energy needed for the transport of a solute against a gradient can be calculated from the initial concentration gradient. The general equation for the free-energy change in the chemical process that converts S to P is

$$\Delta G = \Delta G'^\circ + RT \ln ([P]/[S]) \qquad (11\text{–}2)$$

where $\Delta G'^\circ$ is the standard free-energy change, R is the gas constant, 8.315 J/mol · K, and T is the absolute temperature. When the "reaction" is simply transport of a solute from a region where its concentration is C_1 to a region where its concentration is C_2, no bonds are made or broken and $\Delta G'^\circ$ is zero. The free-energy change for transport, ΔG_t, is then

$$\Delta G_t = RT \ln (C_2/C_1) \qquad (11\text{–}3)$$

If there is a 10-fold difference in concentration between two compartments, the cost of moving 1 mol of an uncharged solute at 25 °C uphill across a membrane separating the compartments is

$$\Delta G_t = (8.315 \text{ J/mol·K})(298 \text{ K}) \ln (10/1) = 5{,}700 \text{ J/mol} = 5.7 \text{ kJ/mol}$$

Equation 11–3 holds for all uncharged solutes.

WORKED EXAMPLE 11–1 Energy Cost of Pumping an Uncharged Solute

Calculate the energy cost (free-energy change) of pumping an uncharged solute against a 1.0×10^4–fold concentration gradient at 25 °C.

Solution: Begin with Equation 11–3. Substitute 1.0×10^4 for (C_2/C_1), 8.315 J/mol · K for R, and 298 K for T:

$$\begin{aligned}\Delta G_t &= RT \ln (C_2/C_1) \\ &= (8.315 \text{ J/mol·K})(298 \text{ K}) \ln (1.0 \times 10^4) \\ &= 23 \text{ kJ/mol}\end{aligned}$$

When the solute is an *ion*, its movement without an accompanying counterion results in the endergonic separation of positive and negative charges, producing an electrical potential; such a transport process is said to be **electrogenic**. The energetic cost of moving an ion depends on the electrochemical potential (Fig 11–27), the sum of the chemical and electrical gradients:

$$\Delta G_t = RT \ln (C_2/C_1) + Z\mathcal{F}\Delta\psi \quad (11\text{–}4)$$

where Z is the charge on the ion, $\mathcal{F}$ is the Faraday constant (96,480 J/V · mol), and $\Delta\psi$ is the transmembrane electrical potential (in volts). Eukaryotic cells typically have plasma membrane potentials of about 0.05 V (with the inside negative relative to the outside), so the second term of Equation 11–4 can make a significant contribution to the total free-energy change for transporting an ion. Most cells maintain more than a 10-fold difference in ion concentrations across their plasma or intracellular membranes, and for many cells and tissues active transport is therefore a major energy-consuming process.

WORKED EXAMPLE 11–2 Energy Cost of Pumping a Charged Solute

Calculate the energy cost (free-energy change) of pumping Ca^{2+} from the cytosol, where its concentration is about 1.0×10^{-7} M, to the extracellular fluid, where its concentration is about 1.0 mM. Assume a temperature of 37 °C (body temperature in a mammal) and a standard transmembrane potential of 50 mV (inside negative) for the plasma membrane.

Solution: In this calculation, both the concentration gradient and the electrical potential must be taken into account. In Equation 11–4, substitute 8.315 J/mol · K for R, 310 K for T, 1.0×10^{-3} for C_2, 1.0×10^{-7} for C_1, 96,500 J/V · mol for $\mathcal{F}$, +2 (the charge on a Ca^{2+} ion) for Z, and 0.050 V for $\Delta\psi$. Note that the transmembrane potential is 50 mV (inside negative), so the change in potential when an ion moves from inside to outside is 50 mV.

$$\begin{aligned}\Delta G_t &= RT \ln (C_2/C_1) + Z\mathcal{F}\Delta\psi \\ &= (8.315 \text{ J/mol·K})(310 \text{ K}) \ln \frac{1.0 \times 10^{-3}}{1.0 \times 10^{-7}} + \\ &\quad 2(96{,}500 \text{ J/V·mol})(0.050 \text{ V}) \\ &= 33 \text{ kJ/mol}\end{aligned}$$

The mechanism of active transport is of fundamental importance in biology. As we shall see in Chapter 19, ATP is formed in mitochondria and chloroplasts by a mechanism that is essentially ATP-driven ion transport operating in reverse. The energy made available by the spontaneous flow of protons across a membrane is calculable from Equation 11–4; remember that ΔG for flow *down* an electrochemical gradient has a negative value and ΔG for transport of ions *against* an electrochemical gradient has a positive value.

P-Type ATPases Undergo Phosphorylation during Their Catalytic Cycles

The family of active transporters called **P-type ATPases** are cation transporters that are reversibly phosphorylated by ATP (thus the name P-type) as part of the transport cycle. Phosphorylation forces a conformational change that is central to movement of the cation across the membrane. The human genome encodes at least 70 P-type ATPases that share similarities in amino acid sequence and topology, especially near the Asp residue that undergoes phosphorylation. All are integral proteins with 8 or 10 predicted membrane-spanning regions in a single polypeptide (type III in Fig. 11–9), and all are sensitive to inhibition by the phosphate analog **vanadate**.

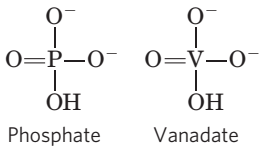

Phosphate Vanadate

The P-type ATPases are widespread in eukaryotes and bacteria. The Na^+K^+ ATPase of animal cells (an antiporter for Na^+ and K^+ ions) and the plasma membrane H^+ ATPase of plants and fungi set the transmembrane electrochemical potential in cells by establishing ion gradients across the plasma membrane. These gradients provide the driving force for secondary active transport and are also the basis for electrical signaling in neurons. In animal tissues, the ***s*arcoplasmic/*e*ndoplasmic *r*eticulum *Ca*$^{2+}$ *A*TPase (SERCA) pump** and the plasma membrane Ca^{2+} ATPase pump are uniporters for Ca^{2+} ions, which together maintain the cytosolic level of Ca^{2+} below 1 μM. Parietal cells in the lining of the mammalian stomach have a P-type ATPase that pumps H^+ and K^+ across the plasma membrane, thereby acidifying the stomach contents. Lipid flippases, as we noted earlier, are structurally and functionally

related to P-type transporters. Bacteria and eukaryotes use P-type ATPases to pump out toxic heavy metal ions such as Cd^{2+} and Cu^{2+}.

The P-type pumps have similar structures **(Fig. 11–36)** and similar mechanisms. The mechanism postulated for P-type ATPases takes into account the large conformational changes and the phosphorylation-dephosphorylation of the critical Asp residue in the P domain that is known to occur during a catalytic cycle. For the SERCA pump **(Fig. 11–37)**, each catalytic cycle moves two Ca^{2+} ions across the membrane and converts an ATP to ADP and P_i. ATP has two roles in this mechanism, one catalytic and one modulatory. The role of ATP binding and phosphoryl transfer to the enzyme is to bring about the interconversion of two conformations (E1 and E2) of the transporter. In the E1 conformation, the two Ca^{2+}-binding sites are exposed on the cytosolic side of the ER or sarcoplasmic reticulum and bind Ca^{2+} with high affinity. ATP binding and Asp phosphorylation drive a conformational change from E1 to E2 in which the Ca^{2+}-binding sites are now exposed on the lumenal side of the membrane and their affinity for Ca^{2+} is greatly reduced, causing Ca^{2+} release into the lumen. By this mechanism, the energy released by hydrolysis of ATP during one phosphorylation-dephosphorylation cycle drives Ca^{2+} across the membrane against a large electrochemical gradient.

Jens Skou

A variation on this basic mechanism is seen in the **Na^+K^+ ATPase** of the plasma membrane, discovered by Jens Skou in 1957. This cotransporter couples phosphorylation-dephosphorylation of the critical Asp residue to the simultaneous movement of both Na^+ and K^+ against their electrochemical gradients. The Na^+K^+ ATPase is responsible for maintaining low Na^+ and high K^+ concentrations in the cell relative to the extracellular fluid **(Fig. 11–38)**. For each molecule of ATP converted to ADP and P_i, the transporter moves two K^+ ions inward

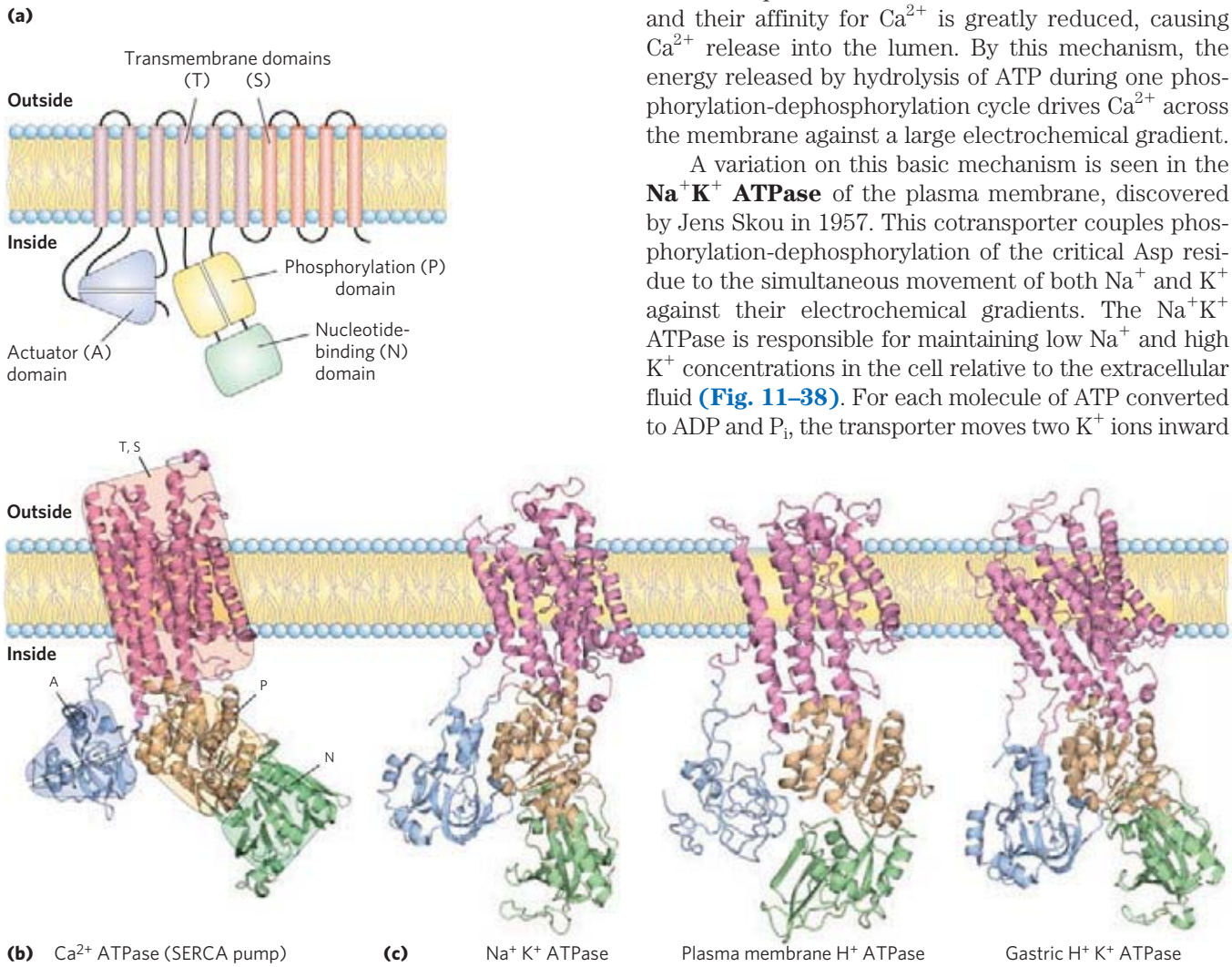

FIGURE 11–36 The general structure of the P-type ATPases. (a) P-type ATPases have three cytoplasmic domains (A, N, and P) and two transmembrane domains (T and S) consisting of multiple helices. The N (nucleotide) domain binds ATP and Mg^{2+}, and it has protein kinase activity that phosphorylates the specific Asp residue found in the P (phosphorylated) domain of all P-type ATPases. The A (actuator) domain has protein phosphatase activity and removes the phosphoryl group from the Asp residue with each catalytic cycle of the pump. A transport domain with six transmembrane helices (T) includes the ion-transporting structure, and four more transmembrane helices make up the support (S) domain, which provides physical support to the transport domain and may have other specialized function in certain P-type ATPases. The binding sites for the ions to be transported are near the middle of the membrane, 40 to 50 Å from the phosphorylated Asp residue—thus Asp phosphorylation-dephosphorylation does not *directly* affect ion binding. The A domain communicates movements of the N and P domains to the ion-binding sites. **(b)** A ribbon representation of the Ca^{2+} ATPase (SERCA pump) (PDB 1T5S). ATP binds to the N domain and the Ca^{2+} ions to be transported bind to the T domain. **(c)** Other P-type ATPases have domain structures, and presumably mechanisms, like the SERCA pump: Na^+K^+ ATPase (PDB ID 3KDP), the plasma membrane H^+ ATPase (PDB ID 3B8C), and the gastric H^+K^+ ATPase (derived from PDB ID 3IXZ).

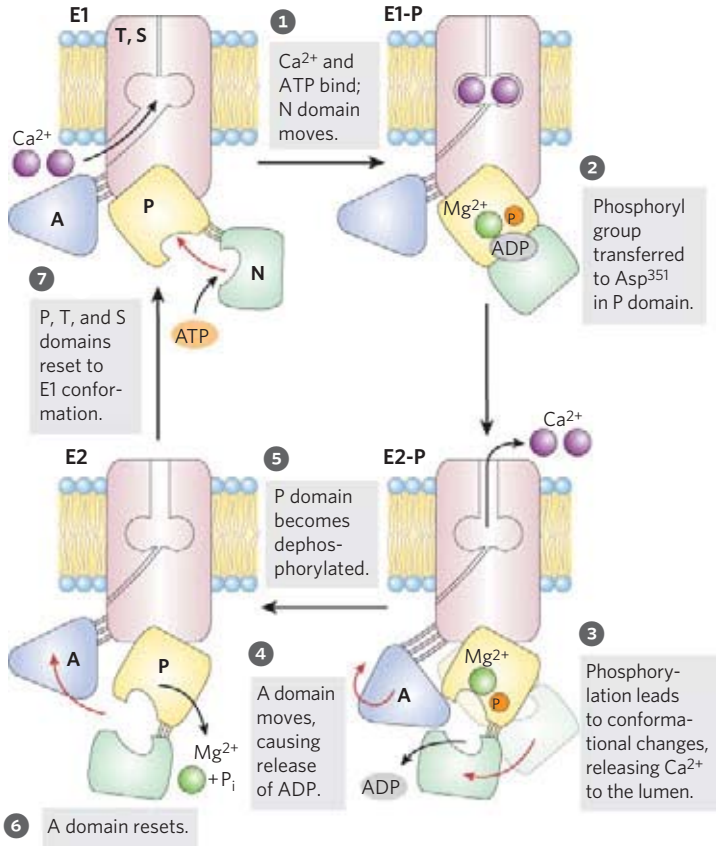

FIGURE 11–37 Postulated mechanism of the SERCA pump. The transport cycle begins with the protein in the E1 conformation, with the Ca^{2+}-binding sites facing the cytosol. Two Ca^{2+} ions bind, then ATP binds to the transporter and phosphorylates Asp^{351}, forming E1-P. Phosphorylation favors the second conformation, E2-P, in which the Ca^{2+}-binding sites, now with a reduced affinity for Ca^{2+}, are accessible on the other side of the membrane (the lumen or extracellular space), and the released Ca^{2+} diffuses away. Finally, E2-P is dephosphorylated, returning the protein to the E1 conformation for another round of transport.

and three Na^+ ions outward across the plasma membrane. Cotransport is therefore electrogenic—it creates a net separation of charge across the membrane; in animals, this produces the membrane potential of −50 to −70 mV (inside negative relative to outside) that is characteristic of most cells and is essential to the conduction of action potentials in neurons. The central role of the Na^+K^+ ATPase is reflected in the energy invested in this single reaction: about 25% of the total energy consumption of a human at rest!

V-Type and F-Type ATPases Are ATP-Driven Proton Pumps

V-type ATPases, a class of proton-transporting ATPases, are responsible for acidifying intracellular compartments in many organisms (thus *V* for *v*acuolar). Proton pumps of this type maintain the vacuoles of fungi and higher plants at a pH between 3 and 6, well below that of the surrounding cytosol (pH 7.5). V-type ATPases are also responsible for the acidification of lysosomes, endosomes, the Golgi complex, and secretory vesicles in animal cells. All V-type ATPases have a similar complex structure, with an integral (transmembrane) domain (V_o) that serves as a proton channel and a peripheral domain (V_1) that contains the ATP-binding site and the ATPase activity **(Fig 11–39a)**. The structure is similar to that of the well-characterized F-type ATPases.

F-type ATPase active transporters catalyze the uphill transmembrane passage of protons driven by ATP hydrolysis. The "F-type" designation derives from the identification of these ATPases as energy-coupling *f*actors. The F_o integral membrane protein complex (Fig. 11–39b; subscript *o* denotes its inhibition by the drug *o*ligomycin) provides a transmembrane pathway for protons, and the peripheral protein F_1 (subscript *1* indicating this was the first of several factors isolated from mitochondria) uses the energy of ATP to drive protons uphill (into a region of higher H^+ concentration). The

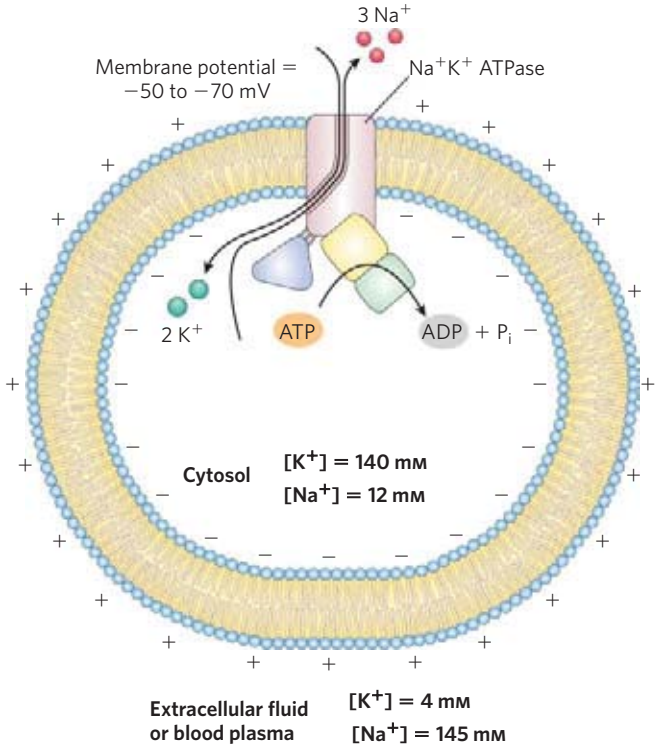

FIGURE 11–38 Role of the Na^+K^+ ATPase in animal cells. This active transport system is primarily responsible for setting and maintaining the intracellular concentrations of Na^+ and K^+ in animal cells and for generating the membrane potential. It does this by moving three Na^+ out of the cell for every two K^+ it moves in. The electrical potential across the plasma membrane is central to electrical signaling in neurons, and the gradient of Na^+ is used to drive the uphill cotransport of solutes in many cell types.

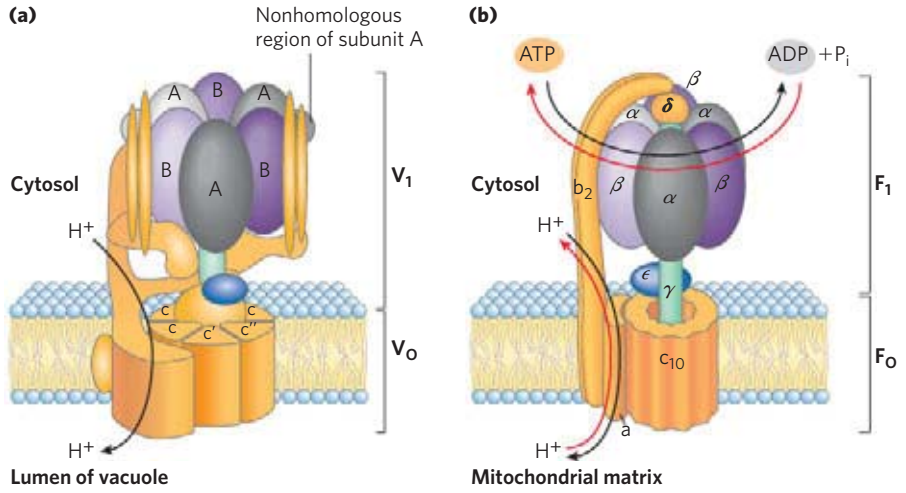

FIGURE 11–39 Two proton pumps with similar structures. (a) The V_oV_1 H^+ ATPase uses ATP to pump protons into vacuoles and lysosomes, creating their low internal pH. It has an integral (membrane-embedded) domain, V_o (orange), that includes multiple identical c subunits, and a peripheral domain that projects into the cytosol and contains the ATP hydrolysis sites, located on three identical B subunits (purple). **(b)** The F_oF_1 ATPase/ATP synthase of mitochondria has an integral domain, F_o (orange), with multiple copies of the c subunit, and a peripheral domain, F_1, consisting of three α subunits, three β subunits, and a central shaft joined to the integral domain. F_o, and presumably V_o, provides a transmembrane channel through which protons are pumped as ATP is hydrolyzed on the β subunits of F_1 (B subunits of V_1). The remarkable mechanism by which ATP hydrolysis is coupled to proton movement is described in detail in Chapter 19. It involves rotation of F_o in the plane of the membrane. The structures of the V_oV_1 ATPase and its analogs A_oA_1 ATPase (of archaea) and CF_oCF_1 ATPase (of chloroplasts) are essentially similar to that of F_oF_1, and the mechanisms are also conserved. An ATP-driven proton transporter also can catalyze ATP synthesis (red arrows) as protons flow *down* their electrochemical gradient. This is the central reaction in the processes of oxidative phosphorylation and photophosphorylation, both described in detail in Chapter 19.

F_oF_1 organization of proton-pumping transporters must have developed very early in evolution. Bacteria such as *E. coli* use an F_oF_1 ATPase complex in their plasma membrane to pump protons outward, and archaea have a closely homologous proton pump, the A_oA_1 ATPase.

Like all enzymes, F-type ATPases catalyze their reactions in both directions. Therefore, a sufficiently large proton gradient can supply the energy to drive the reverse reaction, ATP synthesis (Fig. 11–39b). When functioning in this direction, the F-type ATPases are more appropriately named **ATP synthases**. ATP synthases are central to ATP production in mitochondria during oxidative phosphorylation and in chloroplasts during photophosphorylation, as well as in bacteria and archaea. The proton gradient needed to drive ATP synthesis is produced by other types of proton pumps powered by substrate oxidation or sunlight. We provide a detailed description of these processes in Chapter 19 (p. 750).

ABC Transporters Use ATP to Drive the Active Transport of a Wide Variety of Substrates

ABC transporters (Fig. 11–40) constitute a large family of ATP-dependent transporters that pump amino acids, peptides, proteins, metal ions, various lipids, bile salts, and many hydrophobic compounds, including drugs, out of cells against a concentration gradient. One ABC transporter in humans, the **multidrug transporter** (**MDR1**; also called **P glycoprotein**), is responsible for the striking resistance of certain tumors to some generally effective antitumor drugs. MDR1 has broad substrate specificity for hydrophobic compounds, including, for example, the chemotherapeutic drugs adriamycin, doxorubicin, and vinblastine. By pumping these drugs out of the cell, the transporter prevents their accumulation within a tumor and thus blocks their therapeutic effects. MDR1 (Fig. 11–40a) is an integral membrane protein (M_r 170,000) with two homologous halves, each with six transmembrane helices and a cytoplasmic ATP-binding domain ("cassette"), which give the family its name: *A*TP-*b*inding *c*assette transporters. Overexpression of MDR1 is associated with treatment failure in cancers of the liver, kidney, and colon. A related ABC transporter, ABCC1, is overexpressed in drug-resistant prostate, lung, and breast cancer cells. Highly selective inhibitors of multidrug transporters, which would be expected to enhance the effectiveness of antitumor drugs that are otherwise pumped out of tumor cells, are the objects of current drug discovery and design. Why have multidrug transporters been conserved in evolution? MDR1 in the placental membrane and in the blood-brain barrier keep out toxic compounds that would damage the fetus or the brain.

ABC transporters are also present in simpler animals and in plants and microorganisms. Yeast has 31 genes that encode ABC transporters, *Drosophila* has 56, and *E. coli* has 80, representing 2% of its entire genome. ABC transporters, used by *E. coli* and other bacteria to import

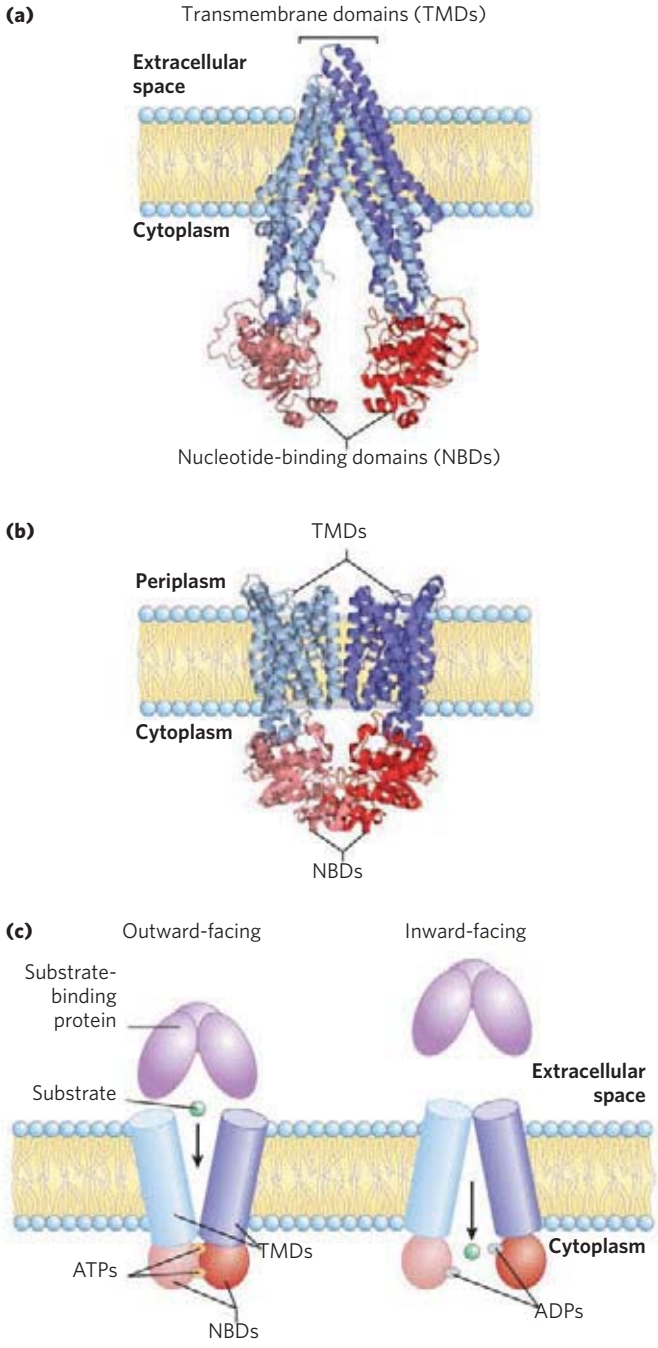

FIGURE 11–40 Two ABC transporters. (a) The multidrug transporter of animal cells (MDR1, also called P glycoprotein; PDB ID 3G60), responsible for pumping a variety of antitumor drugs out of human cells, has two homologous halves (blue and light blue), each with six transmembrane helices in two transmembrane domains (TMDs; blue), and a cytoplasmic nucleotide-binding domain (NBD; red). **(b)** The vitamin B_{12} importer BtuCD (PDB ID 1L7V) of *E. coli* is a homodimer with 10 transmembrane helices (blue, light blue) in each monomer and two NBDs (red) that extend into the cytoplasm. **(c)** Mechanisms proposed for the *E. coli* vitamin B_{12} ABC transporter coupling of ATP hydrolysis to transport. Substrate is brought to the transporter on the periplasmic side by a substrate-specific binding protein. With ATP bound to the NBD sites, the transporter is open to the outside (periplasm), but on substrate binding and ATP hydrolysis to ADP, a conformational change exposes the substrate to the inside surface, and it diffuses away from the transporter and into the cytosol.

essentials such as vitamin B_{12} (Fig. 11–40b), are the presumed evolutionary precursors of the MDRs of animal cells. The presence of ABC transporters that confer antibiotic resistance in pathogenic microbes (*Pseudomonas aeruginosa*, *Staphylococcus aureus*, *Candida albicans*, *Neisseria gonorrhoeae*, and *Plasmodium falciparum*) is a serious public health concern and makes these transporters attractive targets for drug design. ■

All ABC transporters have two nucleotide-binding domains (NBDs) and two transmembrane domains containing multiple transmembrane helices. In some cases, all these domains are in a single long polypeptide; other ABC transporters have two subunits, each contributing an NBD and a domain with six transmembrane helices. Many ABC transporters are in the plasma membrane, but some types are also found in the endoplasmic reticulum and in the membranes of mitochondria and lysosomes. The CFTR protein (see Box 11–2) is an interesting case of an ion channel (for Cl^-), operated by ATP hydrolysis, that is apparently derived from an ABC transporter in which evolution has eliminated the pumping function but left a functional channel.

The NBDs of all ABC proteins are similar in sequence and presumably in three-dimensional structure; they are the conserved molecular motor that can be coupled to a wide variety of pumps and channels. When coupled with a pump, the ATP-driven motor moves solutes against a concentration gradient. The stoichiometry of ABC pumps is approximately one ATP hydrolyzed per molecule of substrate transported, but neither the mechanism of coupling nor the site of substrate binding is fully understood (Fig. 11–40c).

Some ABC transporters have very high specificity for a single substrate; others are more promiscuous. The human genome contains at least 48 genes that encode ABC transporters, many of which are involved in maintaining the lipid bilayer and in transporting sterols, sterol derivatives, and fatty acids throughout the body. The flippases that move membrane lipids from one leaflet of the bilayer to the other are ABC transporters, and the cellular machinery for exporting excess cholesterol includes an ABC transporter. Mutations in the genes that encode some of these proteins contribute to several genetic diseases, including cystic fibrosis (Box 11–2), Tangier disease (p. 874), retinal degeneration, anemia, and liver failure. ■

Ion Gradients Provide the Energy for Secondary Active Transport

The ion gradients formed by primary transport of Na^+ or H^+ can in turn provide the driving force for cotransport of other solutes. Many cell types contain transport systems that couple the spontaneous, downhill flow of these ions to the simultaneous uphill pumping of another ion, sugar, or amino acid (Table 11–4).

BOX 11–2 MEDICINE A Defective Ion Channel in Cystic Fibrosis

Cystic fibrosis (CF) is a serious and relatively common hereditary human disease. About 5% of white Americans are carriers, having one defective and one normal copy of the gene. Only individuals with two defective copies show the severe symptoms of the disease: obstruction of the gastrointestinal and respiratory tracts, commonly leading to bacterial infection of the airways and death due to respiratory insufficiency before the age of 30. In CF, the thin layer of mucus that normally coats the internal surfaces of the lungs is abnormally thick, obstructing air flow and providing a haven for pathogenic bacteria, particularly *Staphylococcus aureus* and *Pseudomonas aeruginosa*.

The defective gene in CF patients was discovered in 1989. It encodes a membrane protein called *c*ystic *f*ibrosis *t*ransmembrane conductance *r*egulator, or CFTR. This protein has two segments, each containing six transmembrane helices, two nucleotide-binding domains (NBDs), and a regulatory region (Fig. 1). CFTR is therefore very similar to other ABC transporter proteins except that it functions as an *ion channel* (for Cl^- ion), not as a pump. The channel conducts Cl^- across the plasma membrane when both NBDs have bound ATP, and it closes when the ATP on one of the NBDs is broken down to ADP and P_i. The Cl^- channel is further regulated by phosphorylation of several Ser residues in the regulatory domain, catalyzed by cAMP-dependent protein kinase (Chapter 12). When the regulatory domain is not phosphorylated, the Cl^- channel is closed. The mutation responsible for CF in 70% of cases results in deletion of a Phe residue at position 508. The mutant protein folds incorrectly, which interferes with its insertion in the plasma membrane, resulting in reduced Cl^- and H_2O movement across the plasma membranes of epithelial cells that line the airways (Fig. 2), the digestive tract, and exocrine glands (pancreas, sweat glands, bile ducts, and vas deferens). Liquid secretion is essential to keep the mucus on the surface of alveoli of the lung at just the right viscosity to trap and clear microorganisms that are inhaled.

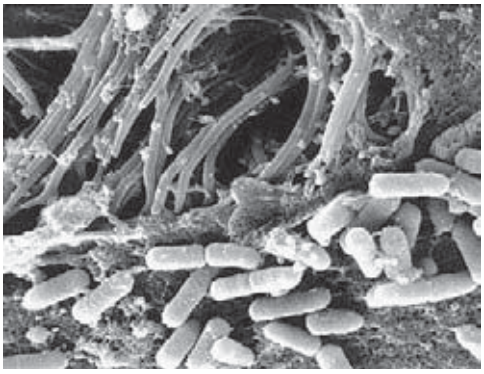

FIGURE 2 Mucus lining the surface of the lungs traps bacteria. In healthy lungs (shown here), these bacteria are killed and swept away by the action of cilia. In CF, this mechanism is impaired, resulting in recurring infections and progressive damage to the lungs.

Diminished export of Cl^- is accompanied by diminished export of water from cells, causing the mucus on the surfaces of the cells to become dehydrated, thick, and excessively sticky. In normal circumstances, cilia on the epithelial cells that line the inner surface of the lungs constantly sweep away bacteria that settle in this mucus, but the thick mucus in individuals with CF hinders this process. Frequent infections by bacteria such as *S. aureus* and *P. aeruginosa* result, causing progressive damage to the lungs and reduced respiratory efficiency. Respiratory failure is commonly the cause of death in people with CF.

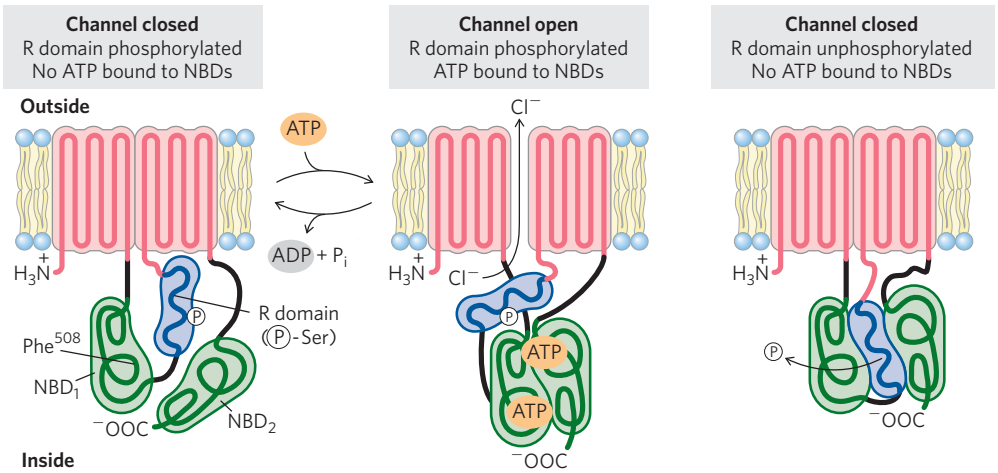

FIGURE 1 Three states of the cystic fibrosis transmembrane conductance regulator, CFTR. The protein has two segments, each with six transmembrane helices, and three functionally significant domains extend from the cytoplasmic surface: NBD_1 and NBD_2 (green) are nucleotide-binding domains that bind ATP, and a regulatory R domain (blue) is the site of phosphorylation by cAMP-dependent protein kinase. When this R domain is phosphorylated but no ATP is bound to the NBDs (left), the channel is closed. The binding of ATP opens the channel (middle) until the bound ATP is hydrolyzed. When the regulatory domain is unphosphorylated (right), it binds the NBD domains and prevents ATP binding and channel opening. The most commonly occurring mutation leading to CF is the deletion of Phe^{508} in the NBD_1 domain (left). CFTR is a typical ABC transporter in all but two respects: most ABC transporters lack the regulatory domain, and CFTR acts as an ion channel (for Cl^-), not as a typical transporter.

TABLE 11–4 Cotransport Systems Driven by Gradients of Na^+ or H^+

Organism/ tissue/cell type	Transported solute (moving against its gradient)	Cotransported solute (moving down its gradient)	Type of transport
E. coli	Lactose	H^+	Symport
	Proline	H^+	Symport
	Dicarboxylic acids	H^+	Symport
Intestine, kidney (vertebrates)	Glucose	Na^+	Symport
	Amino acids	Na^+	Symport
Vertebrate cells (many types)	Ca^{2+}	Na^+	Antiport
Higher plants	K^+	H^+	Antiport
Fungi (*Neurospora*)	K^+	H^+	Antiport

The **lactose transporter** (**lactose permease**, or **galactoside permease**) of *E. coli* is the well-studied prototype for proton-driven cotransporters. This protein consists of a single polypeptide chain (417 residues) that functions as a monomer to transport one proton and one lactose molecule into the cell, with the net accumulation of lactose **(Fig. 11–41)**. *E. coli* normally produces a gradient of protons and charge across its plasma membrane by oxidizing fuels and using the energy of oxidation to pump protons outward. (This mechanism is discussed in detail in Chapter 19.) The lipid bilayer is impermeable to protons, but the lactose transporter provides a route for proton reentry, and lactose is simultaneously carried into the cell by symport. The endergonic accumulation of lactose is thereby coupled to the exergonic flow of protons into the cell, with a negative overall free-energy change.

The lactose transporter is one member of the **major facilitator superfamily (MFS)** of transporters, which comprises 28 families. Almost all proteins in this superfamily have 12 transmembrane domains (the few exceptions have 14). The proteins share relatively little sequence homology, but the similarity of their secondary structures and topology suggests a common tertiary structure. The crystallographic solution of the *E. coli* lactose transporter provides a glimpse of this general structure **(Fig. 11–42a)**. The protein has 12 transmembrane helices, and connecting loops protrude into the cytoplasm or the periplasmic space (between the plasma membrane and outer membrane or cell wall). The six amino-terminal and six carboxyl-terminal helices form very similar domains to produce a structure with a rough twofold symmetry. In the crystallized form of the protein, a large aqueous cavity is exposed on the cytoplasmic side of the membrane. The substrate-binding site is in this cavity, more or less in the middle of the membrane. The side of the transporter facing outward (the periplasmic face) is closed tightly, with no channel big enough for lactose to enter. The proposed mechanism for transmembrane passage of the substrate (Fig. 11–42b) involves a rocking motion between the two domains, driven by substrate binding and proton movement, alternately exposing the substrate-binding domain to the cytoplasm and to the periplasm. This "rocking banana" model is similar to that shown in Figure 11–32 for GLUT1.

How is proton movement into the cell coupled with lactose uptake? Extensive genetic studies of the lactose transporter have established that of the 417 residues in the protein, only 6 are absolutely essential for cotransport of H^+ and lactose—some for lactose binding, others for

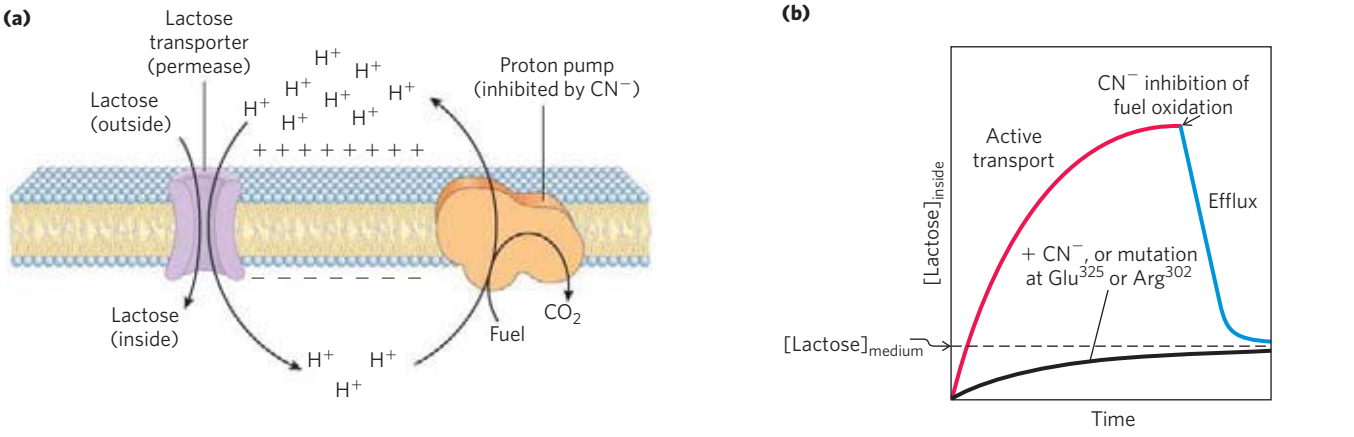

FIGURE 11–41 **Lactose uptake in *E. coli*.** **(a)** The primary transport of H^+ out of the cell, driven by the oxidation of a variety of fuels, establishes both a proton gradient and an electrical potential (inside negative) across the membrane. Secondary active transport of lactose into the cell involves symport of H^+ and lactose by the lactose transporter. The uptake of lactose against its concentration gradient is entirely dependent on this inflow of protons driven by the electrochemical gradient. **(b)** When the energy-yielding oxidation reactions of metabolism are blocked by cyanide (CN^-), the lactose transporter allows equilibration of lactose across the membrane via passive transport. Mutations that affect Glu^{325} or Arg^{302} have the same effect as cyanide. The dashed line represents the concentration of lactose in the surrounding medium.

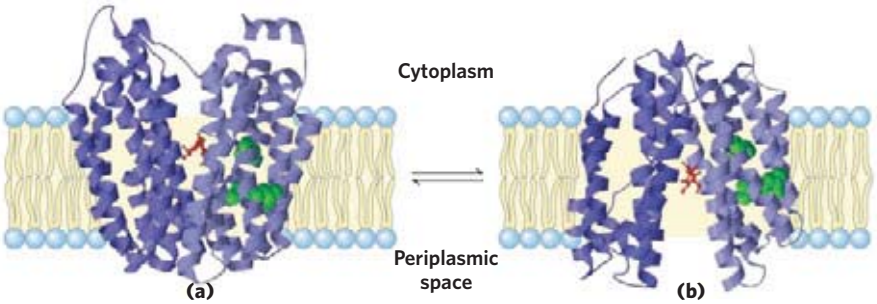

FIGURE 11–42 The lactose transporter (lactose permease) of *E. coli*. **(a)** Ribbon representation viewed parallel to the plane of the membrane shows the 12 transmembrane helices arranged in two nearly symmetric domains, shown in different shades of purple. In the form of the protein for which the crystal structure was determined, the substrate sugar (red) is bound near the middle of the membrane where the sugar is exposed to the cytoplasm (derived from PDB ID 1PV7). **(b)** The postulated second conformation of the transporter (PDB ID 2CFQ), related to the first by a large, reversible conformational change in which the substrate-binding site is exposed first to the periplasm, where lactose is picked up, then to the cytoplasm, where the lactose is released. The interconversion of the two forms is driven by changes in the pairing of charged (protonatable) side chains such as those of Glu^{325} and Arg^{302} (green), which is affected by the transmembrane proton gradient.

proton transport. Mutation in either of two residues (Glu^{325} and Arg^{302}; Fig. 11–42) results in a protein still able to catalyze facilitated diffusion of lactose but incapable of coupling H^+ flow to uphill lactose transport. A similar effect is seen in wild-type (unmutated) cells when their ability to generate a proton gradient is blocked with CN^-: the transporter carries out facilitated diffusion normally, but it cannot pump lactose against a concentration gradient (Fig. 11–41b). The balance between the two conformations of the lactose transporter is affected by changes in charge pairing between the side chains of Glu^{325} and Arg^{302}.

In intestinal epithelial cells, glucose and certain amino acids are accumulated by symport with Na^+, down the Na^+ gradient established by the Na^+K^+ ATPase of the plasma membrane **(Fig. 11–43)**. The apical surface of the intestinal epithelial cell is covered with microvilli, long, thin projections of the plasma membrane that greatly increase the surface area exposed to the intestinal contents. **Na^+-glucose symporters** in the apical plasma membrane take up glucose from the intestine in a process driven by the downhill flow of Na^+:

$$2Na^+_{out} + glucose_{out} \longrightarrow 2Na^+_{in} + glucose_{in}$$

The energy required for this process comes from two sources: the greater concentration of Na^+ outside than inside (the chemical potential) and the membrane (electrical) potential, which is inside negative and therefore draws Na^+ inward.

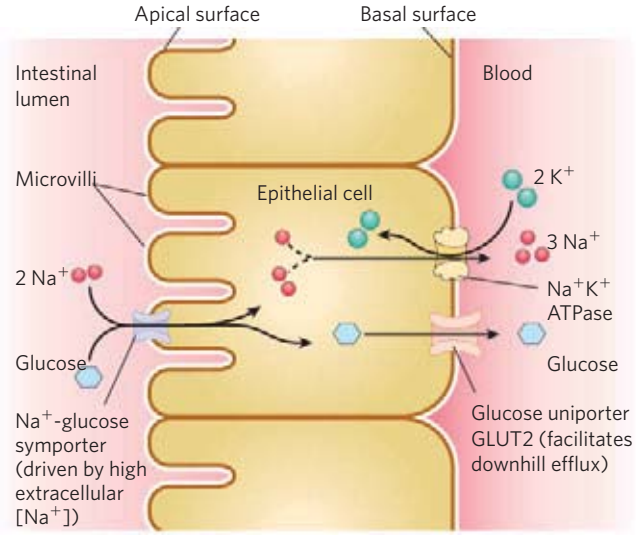

WORKED EXAMPLE 11–3 Energetics of Pumping by Symport

Calculate the maximum $\frac{[glucose]_{in}}{[glucose]_{out}}$ ratio that can be achieved by the plasma membrane Na^+-glucose symporter of an epithelial cell when $[Na^+]_{in}$ is 12 mM, $[Na^+]_{out}$ is 145 mM, the membrane potential is −50 mV (inside negative), and the temperature is 37°C.

Solution: Using Equation 11–4 (p. 412), we can calculate the energy inherent in an electrochemical Na^+ gradient—that is, the cost of moving one Na^+ ion up this gradient:

$$\Delta G_t = RT \ln \frac{[Na^+]_{out}}{[Na^+]_{in}} + Z\mathcal{F}\Delta\psi$$

We then substitute standard values for R, T, and $\mathcal{F}$; the given values for $[Na^+]$ (expressed as molar concentrations); +1 for Z (because Na^+ has a positive charge); and 0.050 V for $\Delta\psi$. Note that the membrane potential

FIGURE 11–43 Glucose transport in intestinal epithelial cells. Glucose is cotransported with Na^+ across the apical plasma membrane into the epithelial cell. It moves through the cell to the basal surface, where it passes into the blood via GLUT2, a passive glucose uniporter. The Na^+K^+ ATPase continues to pump Na^+ outward to maintain the Na^+ gradient that drives glucose uptake.

is −50 mV (inside negative), so the change in potential when an ion moves from inside to outside is 50 mV.

$$\Delta G_t = (8.315\ \text{J/mol·K})(310\ \text{K}) \ln \frac{1.45 \times 10^{-1}}{1.2 \times 10^{-2}} + 1(96{,}500\ \text{J/V·mol})(0.050\ \text{V})$$
$$= 11.2\ \text{kJ/mol}$$

When Na^+ reenters the cell, it releases the electrochemical potential created by pumping it out; ΔG for reentry is −11.2 kJ/mol of Na^+. This is the potential energy per mole of Na^+ that is available to pump glucose. Given that two Na^+ ions pass down their electrochemical gradient and into the cell for each glucose carried in by symport, the energy available to pump 1 mole of glucose is 2 × 11.2 kJ/mol = 22.4 kJ/mol. We can now calculate the maximum concentration ratio of glucose that can be achieved by this pump (from Equation 11–3, p. 411):

$$\Delta G_t = RT \ln \frac{[\text{glucose}]_{in}}{[\text{glucose}]_{out}}$$

Rearranging, then substituting the values of ΔG_t, R, and T, gives

$$\ln \frac{[\text{glucose}]_{in}}{[\text{glucose}]_{out}} = \frac{\Delta G_t}{RT} = \frac{22.4\ \text{kJ/mol}}{(8.315\ \text{J/mol·K})(310\ \text{K})} = 8.69$$
$$\frac{[\text{glucose}]_{in}}{[\text{glucose}]_{out}} = e^{8.69}$$
$$= 5.94 \times 10^3$$

Thus the cotransporter can pump glucose inward until its concentration inside the epithelial cell is about 6,000 times that outside (in the intestine). (This is the maximum theoretical ratio, assuming a perfectly efficient coupling of Na^+ reentry and glucose uptake.)

As glucose is pumped from the intestine into the epithelial cell at the apical surface, it is simultaneously moved from the cell into the blood by passive transport through a glucose transporter (GLUT2) in the basal surface (Fig. 11–43). The crucial role of Na^+ in symport and antiport systems such as this requires the continued outward pumping of Na^+ to maintain the transmembrane Na^+ gradient.

Because of the essential role of ion gradients in active transport and energy conservation, compounds that collapse ion gradients across cellular membranes are effective poisons, and those that are specific for infectious microorganisms can serve as antibiotics. One such substance is valinomycin, a small cyclic peptide that neutralizes the K^+ charge by surrounding it with six carbonyl oxygens **(Fig. 11–44)**. The hydrophobic peptide then acts as a shuttle, carrying K^+ across membranes down its concentration gradient and deflating that gradient. Compounds that shuttle ions across membranes in this way are called **ionophores** ("ion bearers"). Both valinomycin and monensin (a Na^+-carrying ionophore) are antibiotics; they kill microbial cells by disrupting secondary transport processes and energy-conserving reactions. Monensin is widely used as an antifungal and antiparasitic agent. ■

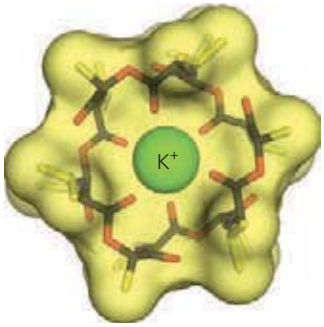

FIGURE 11–44 Valinomycin, a peptide ionophore that binds K^+. In this image, the surface contours are shown as a yellow envelope, through which a stick structure of the peptide and a K^+ ion (green) are visible. The oxygen atoms (red) that bind K^+ are part of a central hydrophilic cavity. Hydrophobic amino acid side chains (yellow) coat the outside of the molecule. Because the exterior of the K^+-valinomycin complex is hydrophobic, the complex readily diffuses through membranes, carrying K^+ down its concentration gradient. The resulting dissipation of the transmembrane ion gradient kills microbial cells, making valinomycin a potent antibiotic.

Aquaporins Form Hydrophilic Transmembrane Channels for the Passage of Water


Peter Agre

A family of integral membrane proteins discovered by Peter Agre, the **aquaporins (AQPs)**, provide channels for rapid movement of water molecules across all plasma membranes. Aquaporins are found in all organisms, and multiple aquaporin genes are generally present, encoding similar but not identical proteins. Eleven aquaporins are known in mammals, each with a specific localization and role (Table 11–5). Erythrocytes, which swell or shrink rapidly in response to abrupt changes in extracellular osmolarity as blood travels through the renal medulla, have a high density of aquaporin in their plasma membrane (2×10^5 copies of AQP1 per cell). Water secretion by the exocrine glands that produce sweat, saliva, and tears occurs through aquaporins. Seven different aquaporins play roles in urine production and water retention in the nephron (the functional unit of the kidney). Each renal AQP has a specific localization in the nephron, and each has specific properties and regulatory features. For example, AQP2 in the epithelial cells of the renal collecting duct is regulated by vasopressin (also called antidiuretic hormone): more water is reabsorbed in the kidney when the vasopressin level is high. Mutant mice with no AQP2 gene have increased urine output (polyuria) and decreased urine-concentrating ability, the

TABLE 11–5 Permeability Characteristics and Predominant Distribution of Known Mammalian Aquaporins

Aquaporin	Permeant (permeability)	Tissue distribution	Subcellular distribution*
AQP0	Water (low)	Lens	Plasma membrane
AQP1	Water (high)	Erythrocyte, kidney, lung, vascular endothelium, brain, eye	Plasma membrane
AQP2	Water (high)	Kidney, vas deferens	Apical plasma membrane, intracellular vesicles
AQP3	Water (high), glycerol (high), urea (moderate)	Kidney, skin, lung, eye, colon	Basolateral plasma membrane
AQP4	Water (high)	Brain, muscle, kidney, lung, stomach, small intestine	Basolateral plasma membrane
AQP5	Water (high)	Salivary gland, lacrimal gland, sweat gland, lung, cornea	Apical plasma membrane
AQP6	Water (low), anions ($NO_3^- > Cl^-$)	Kidney	Intracellular vesicles
AQP7	Water (high), glycerol (high), urea (high)	Adipose tissue, kidney, testis	Plasma membrane
AQP8†	Water (high)	Testis, kidney, liver, pancreas, small intestine, colon	Plasma membrane, intracellular vesicles
AQP9	Water (low), glycerol (high), urea (high), arsenite	Liver, leukocyte, brain, testis	Plasma membrane
AQP10	Water (low), glycerol (high), urea (high)	Small intestine	Intracellular vesicles

Source: Data from King, L.S., Kozono, D., & Agre, P. (2004) From structure to disease: the evolving tale of aquaporin biology. *Nat. Rev. Mol. Cell Biol.* 5, 688.

*Aquaporins that are present primarily in the apical or in the basolateral membrane are noted as localized in one of these membranes; those present in both membranes are described as localized in the plasma membrane.

†AQP8 might also be permeated by urea.

result of decreased water permeability of the proximal tubule. In humans, genetically defective AQPs are known to be responsible for a variety of diseases, including a relatively rare form of diabetes that is accompanied by polyuria (Box 11–1).

Water molecules flow through an AQP1 channel at a rate of about $10^9\ s^{-1}$. For comparison, the highest known turnover number for an enzyme is that for catalase, $4 \times 10^7\ s^{-1}$, and many enzymes have turnover numbers between $1\ s^{-1}$ and $10^4\ s^{-1}$ (see Table 6–7). The low activation energy for passage of water through aquaporin channels ($\Delta G^{\ddagger} < 15$ kJ/mol) suggests that water moves through the channels in a continuous stream, in the direction dictated by the osmotic gradient. (For a discussion of osmosis, see p. 56.) Aquaporins do not allow passage of protons (hydronium ions, H_3O^+), which would collapse membrane electrochemical gradients. What is the basis for this extraordinary selectivity?

We find an answer in the structure of AQP1, as determined by x-ray crystallography. AQP1 **(Fig. 11–45a)** consists of four identical monomers (each M_r 28,000), each of which forms a transmembrane pore with a diameter sufficient to allow passage of water molecules in single file. Each monomer has six transmembrane helical segments and two shorter helices, both of which contain the sequence Asn–Pro–Ala (NPA). The six transmembrane helices form the pore through the monomer, and the two short loops containing the NPA sequences extend toward the middle of the bilayer from opposite sides. Their NPA regions overlap in the middle of the membrane to form part of the specificity filter—the structure that allows only water to pass (Fig. 11–45b).

The water channel narrows to a diameter of 2.8 Å near the center of the membrane, severely restricting the size of molecules that can travel through. The positive charge of a highly conserved Arg residue at this bottleneck discourages the passage of cations such as H_3O^+. The residues that line the channel of each AQP1 monomer are generally nonpolar, but carbonyl oxygens in the peptide backbone, projecting into the narrow part of the channel at intervals, can hydrogen-bond with individual water molecules as they pass through; the two Asn residues (Asn^{76} and Asn^{192}) in the NPA loops also form hydrogen bonds with the water. The structure of the channel does not permit formation of a chain of water molecules close enough to allow proton hopping (see Fig. 2–14), which would effectively move protons across the membrane. Critical Arg and His residues and

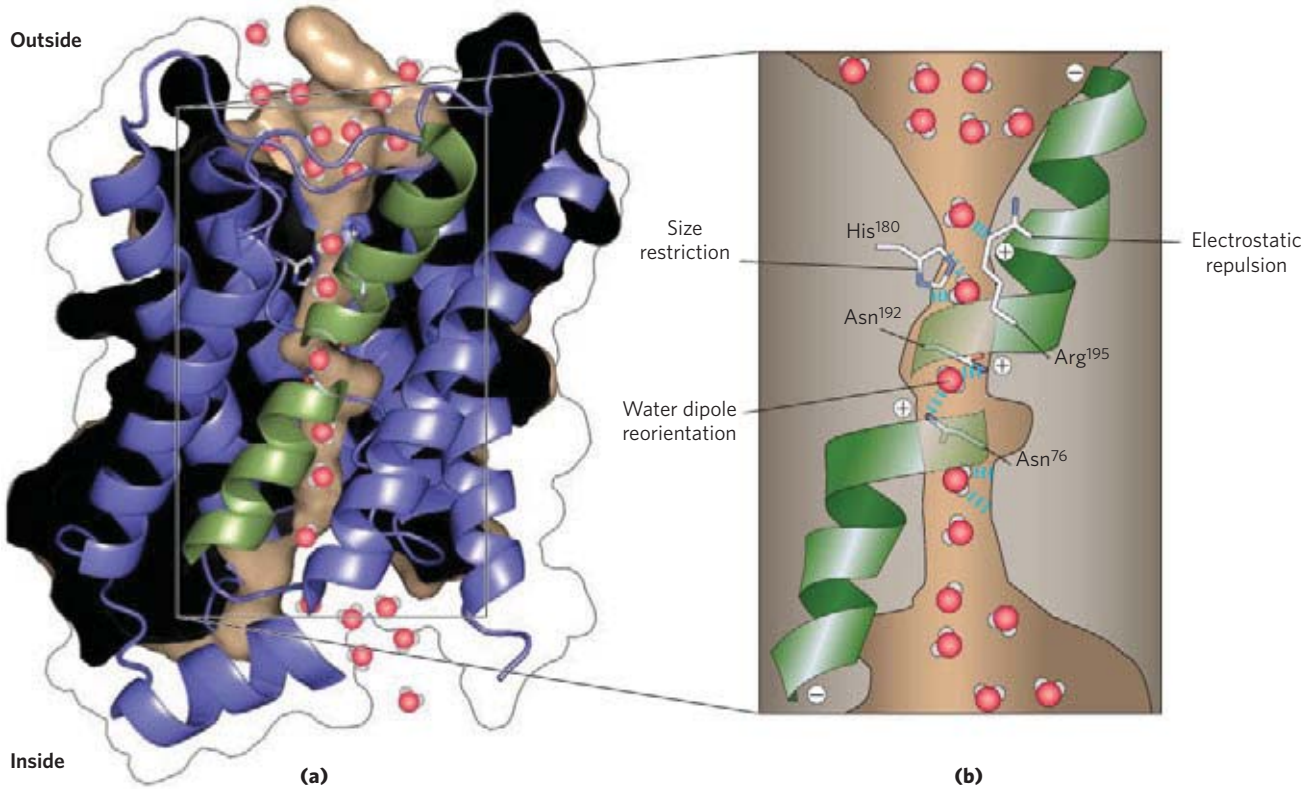

FIGURE 11–45 **Aquaporin.** The protein is a tetramer of identical subunits, each with a transmembrane pore. **(a)** A monomer of spinach aquaporin SoPIP2;1 (derived from PDB ID 2B5F), viewed in the plane of the membrane. The helices form a central pore, and two short helical segments (green) contain the Asn-Pro-Ala (NPA) sequences, found in all aquaporins, that form part of the water channel. **(b)** This cartoon of bovine aquaporin 1 (derived from PDB ID 1J4N) shows that the pore (brown; filled with water molecules shown in red and white) narrows at His^{180} to a diameter of 2.8 Å (about the size of a water molecule), limiting passage of molecules larger than H_2O. The positive charge of Arg^{195} repels cations, including H_3O^+, preventing their passage through the pore. The two short helices shown in green are oriented with their positively charged dipoles pointed at the pore in such a way as to force a water molecule to reorient as it passes through; this breaks up hydrogen-bonded chains of water molecules, preventing proton passage by "proton hopping."

electric dipoles formed by the short helices of the NPA loops provide positive charges in positions that repel any protons that might leak through the pore and prevent hydrogen bonding between adjacent water molecules.

An aquaporin isolated from spinach is known to be "gated"—open when two critical Ser residues near the intracellular end of the channel are phosphorylated, and closed when they are dephosphorylated. Both the open and closed structures have been determined by crystallography. Phosphorylation favors a conformation that presses two nearby Leu residues and a His residue into the channel, blocking the movement of water past that point and effectively closing the channel. Other aquaporins are regulated in other ways, allowing rapid changes in membrane permeability to water.

Although generally highly specific for water, some AQPs also allow glycerol or urea to pass at high rates (Table 11–5); these AQPs are believed to be important in the metabolism of glycerol. AQP7, for example, found in the plasma membranes of adipocytes (fat cells), transports glycerol efficiently. Mice with defective AQP7 develop obesity and non–insulin-dependent diabetes, presumably as a result of their inability to move glycerol into or out of adipocytes as triacylglycerols are converted to free fatty acids and glycerol, and as glycerol is acylated to triacylglycerol.

Ion-Selective Channels Allow Rapid Movement of Ions across Membranes

Ion-selective channels—first recognized in neurons and now known to be present in the plasma membranes of all cells, as well as in the intracellular membranes of eukaryotes—provide another mechanism for moving inorganic ions across membranes. Ion channels, together with ion pumps such as the Na^+K^+ ATPase, determine a plasma membrane's permeability to specific ions and regulate the cytosolic concentration of ions and the membrane potential. In neurons, very rapid changes in the activity of ion channels cause the changes in membrane potential (action potentials) that carry signals from one end of a neuron to the other. In myocytes, rapid opening of Ca^{2+} channels in the sarcoplasmic reticulum releases the Ca^{2+} that triggers muscle contraction. We discuss

the signaling functions of ion channels in Chapter 12. Here we describe the structural basis for ion-channel function, using as examples a voltage-gated K^+ channel, the neuronal Na^+ channel, and the acetylcholine receptor ion channel.

Ion channels are distinct from ion transporters in at least three ways. First, the rate of flux through channels can be several orders of magnitude greater than the turnover number for a transporter—10^7 to 10^8 ions/s for an ion channel, approaching the theoretical maximum for unrestricted diffusion. By contrast, the turnover rate of the Na^+K^+ ATPase is about 100 s^{-1}. Second, ion channels are not saturable: rates do not approach a maximum at high substrate concentration. Third, they are gated in response to some cellular event. In **ligand-gated channels** (which are generally oligomeric), binding of an extracellular or intracellular small molecule forces an allosteric transition in the protein, which opens or closes the channel. In **voltage-gated ion channels**, a change in transmembrane electrical potential (V_m) causes a charged protein domain to move relative to the membrane, opening or closing the channel. Both types of gating can be very fast. A channel typically opens in a fraction of a millisecond and may remain open for only milliseconds, making these molecular devices effective for very fast signal transmission in the nervous system.

Ion-Channel Function Is Measured Electrically

Because a single ion channel typically remains open for only a few milliseconds, monitoring this process is beyond the limit of most biochemical measurements. Ion fluxes must therefore be measured electrically, either as changes in V_m (in the millivolt range) or as electric current I (in the microampere or picoampere range), using microelectrodes and appropriate amplifiers. In **patch-clamping**, a technique developed by Erwin Neher and Bert Sakmann in 1976, very small currents are measured through a tiny region of the membrane surface containing only one or a few ion-channel molecules **(Fig. 11–46)**. The researcher can measure the size and duration of the current that flows during one opening of an ion channel and can determine how often a channel opens and how that frequency is affected by membrane potential, regulatory ligands, toxins, and other agents. Patch-clamp studies have revealed that as many as 10^4 ions can move through a single ion channel in 1 ms. Such an ion flux represents a huge amplification of the initial signal; for example, only two acetylcholine molecules are needed to open an acetylcholine receptor channel (as described below).

Erwin Neher

Bert Sakmann

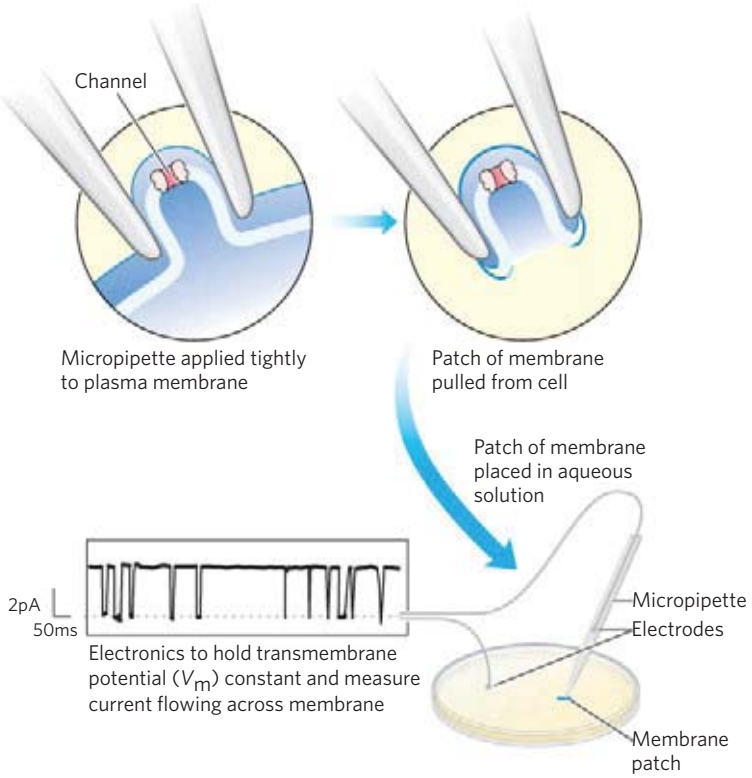

FIGURE 11–46 Electrical measurements of ion-channel function. The "activity" of an ion channel is estimated by measuring the flow of ions through it, using the patch-clamp technique. A finely drawn-out pipette (micropipette) is pressed against the cell surface, and negative pressure in the pipette forms a pressure seal between pipette and membrane. As the pipette is pulled away from the cell, it pulls off a tiny patch of membrane (which may contain one or a few ion channels). After placing the pipette and attached patch in an aqueous solution, the researcher can measure channel activity as the electric current that flows between the contents of the pipette and the aqueous solution. In practice, a circuit is set up that "clamps" the transmembrane potential at a given value and measures the current that must flow to maintain this voltage. With highly sensitive current detectors, researchers can measure the current flowing through a single ion channel, typically a few picoamperes. The trace shows the current through a single acetylcholine receptor channel as a function of time (in milliseconds), revealing how fast the channel opens and closes, how frequently it opens, and how long it stays open. Downward deflection represents channel opening. Clamping the V_m at different values permits determination of the effect of membrane potential on these parameters of channel function.

The Structure of a K^+ Channel Reveals the Basis for Its Specificity

Roderick MacKinnon

The structure of a potassium channel from the bacterium *Streptomyces lividans*, determined crystallographically by Roderick MacKinnon in 1998, provides important insight into the way ion channels work. This bacterial ion channel is related in sequence to all other known K^+ channels and serves as the prototype for such channels, including the voltage-gated K^+ channel of neurons. Among the members of this protein family, the similarities in sequence are greatest in the "pore region," which contains the ion selectivity filter that allows K^+ (radius 1.33 Å) to pass 10^4 times more readily than Na^+ (radius 0.95 Å)—at a rate (about 10^8 ions/s) approaching the theoretical limit for unrestricted diffusion.

The K^+ channel consists of four identical subunits that span the membrane and form a cone within a cone surrounding the ion channel, with the wide end of the double cone facing the extracellular space **(Fig. 11–47a)**. Each subunit has two transmembrane α helices as well as a third, shorter helix that contributes to the pore region. The outer cone is formed by one of the transmembrane helices of each subunit. The inner cone, formed by the other four transmembrane helices, surrounds the ion channel and cradles the ion selectivity filter. Viewed perpendicular to the plane of the membrane, the central channel is seen to be just wide enough to accommodate an unhydrated metal ion such as potassium (Fig. 11–47b).

Both the ion specificity and the high flux through the channel are understandable from what we know of the channel's structure (Fig. 11–47c). At the inner and outer plasma membrane surfaces, the entryways to the channel have several negatively charged amino acid residues, which presumably increase the local concentration of cations such as K^+ and Na^+. The ion path through the membrane begins (on the inner surface) as a wide, water-filled channel in which the ion can retain its hydration sphere. Further stabilization is provided by the short helices in the pore region of each subunit, with the partial negative charges of their electric dipoles pointed at K^+ in the channel. About two-thirds of the way through the membrane, this channel narrows in the region of the selectivity filter, forcing the ion to give up its hydrating water molecules. Carbonyl oxygen atoms in the backbone of the selectivity filter replace the water molecules in the hydration sphere, forming a series of perfect coordination shells through which the K^+ moves. This favorable interaction with the filter is not possible for Na^+, which is too small to make contact with all the potential oxygen ligands. The preferential stabilization of K^+ is the basis for the ion selectivity of the filter, and mutations that change residues in this part of the protein eliminate the channel's ion selectivity. The K^+-binding sites of the filter are flexible enough to collapse to fit any

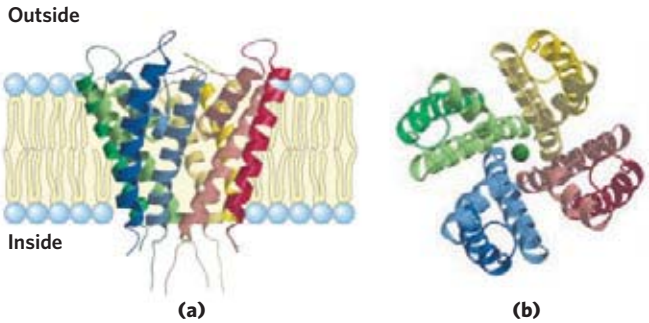

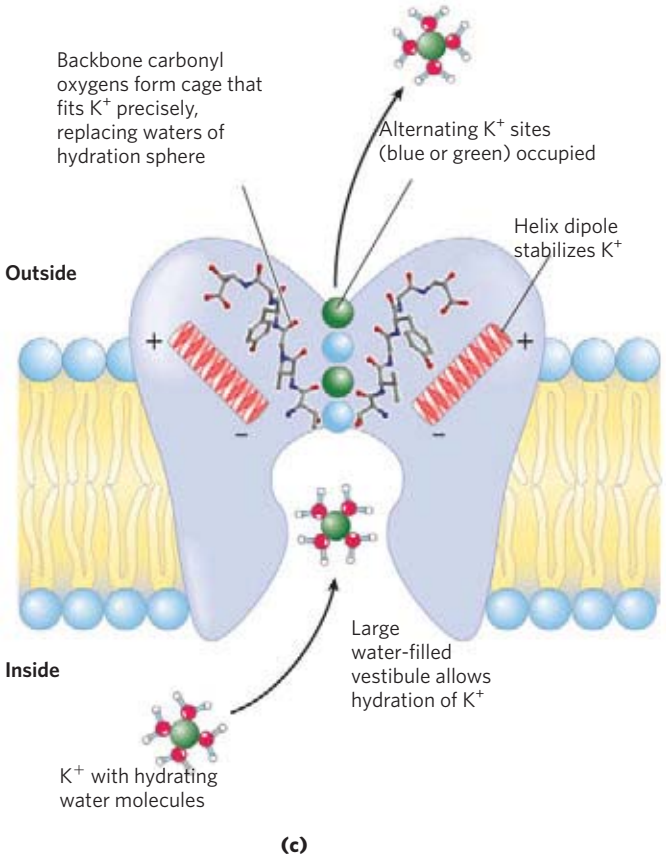

FIGURE 11–47 The K^+ channel of *Streptomyces lividans*. (PDB ID 1BL8) **(a)** Viewed in the plane of the membrane, the channel consists of eight transmembrane helices (two from each of four identical subunits), forming a cone with its wide end toward the extracellular space. The inner helices of the cone (lighter colored) line the transmembrane channel, and the outer helices interact with the lipid bilayer. Short segments of each subunit converge in the open end of the cone to make a selectivity filter. **(b)** This view, perpendicular to the plane of the membrane, shows the four subunits arranged around a central channel just wide enough for a single K^+ ion to pass. **(c)** Diagram of a K^+ channel in cross section, showing the structural features critical to function. Carbonyl oxygens (red) of the peptide backbone in the selectivity filter protrude into the channel, interacting with and stabilizing a K^+ ion passing through. These ligands are perfectly positioned to interact with each of four K^+ ions but not with the smaller Na^+ ions. This preferential interaction with K^+ is the basis for the ion selectivity.

Na^+ that enters the channel, and this conformational change closes the channel.

There are four potential K^+-binding sites along the selectivity filter, each composed of an oxygen "cage" that provides ligands for the K^+ ions (Fig. 11–47c). In the crystal structure, two K^+ ions are visible within the selectivity filter, about 7.5 Å apart, and two water molecules occupy the unfilled positions. K^+ ions pass through the filter in single file; their mutual electrostatic repulsion most likely just balances the interaction of each ion with the selectivity filter and keeps them moving. Movement of the two K^+ ions is concerted: first they occupy positions 1 and 3, then they hop to positions 2 and 4. The energetic difference between these two configurations (1, 3 and 2, 4) is very small; energetically, the selectivity pore is not a series of hills and valleys but a flat surface, which is ideal for rapid ion movement through the channel. The structure of the channel seems to have been optimized during evolution to give maximal flow rates and high specificity.

Voltage-gated K^+ channels are more complex structures than that illustrated in Figure 11–47, but they are variations on the same theme. For example, the mammalian voltage-gated K^+ channels in the *Shaker* family have an ion channel like that of the bacterial channel shown in Figure 11–47, but with additional protein domains that sense the membrane potential, move in response to a change in potential, and in moving trigger the opening or closing of the K^+ channel **(Fig. 11–48)**. The critical transmembrane helix in the voltage-sensing domain of

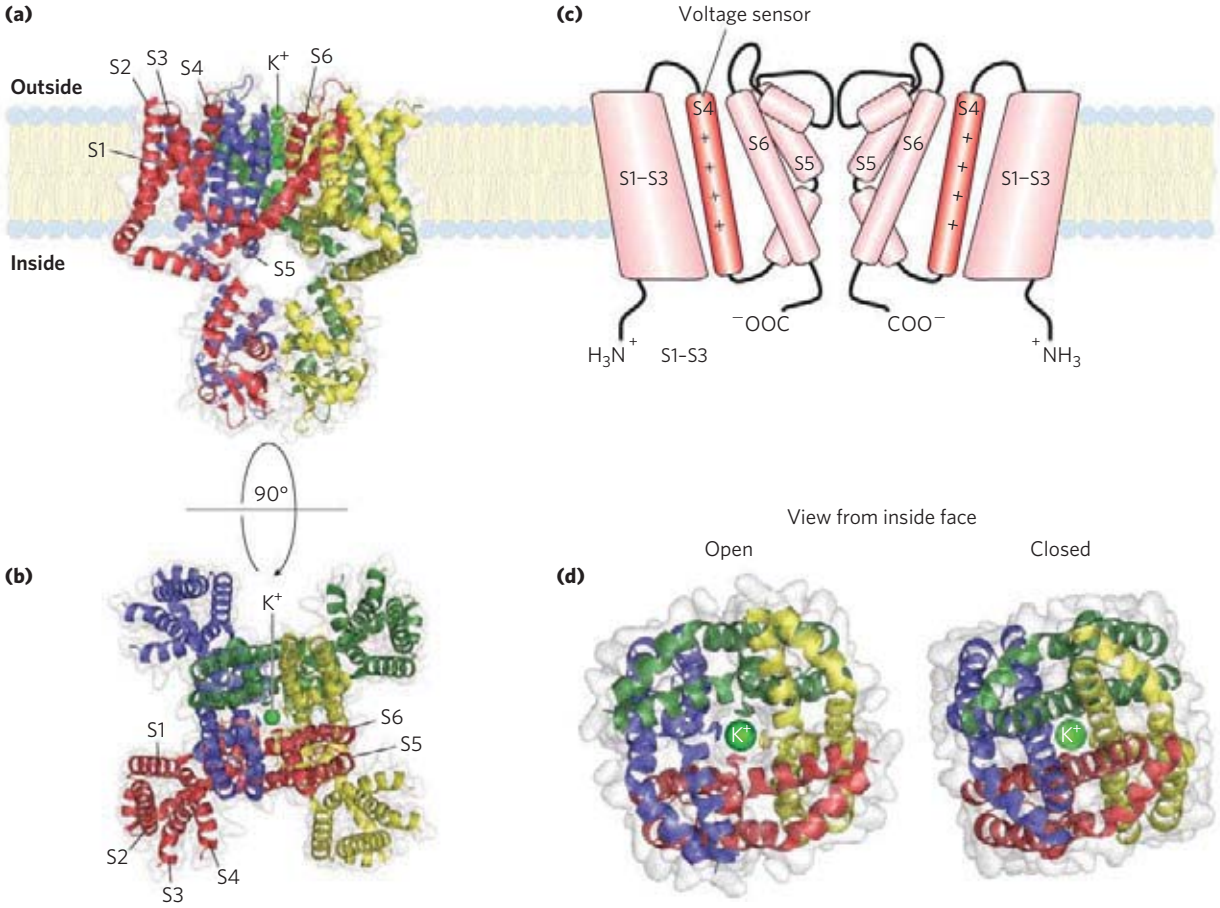

FIGURE 11–48 Structural basis for voltage gating in the K^+ channel. (PDB ID 2A79) This crystal structure of the Kv1.2-β2 subunit complex from rat brain shows the basic K^+ channel (corresponding to that shown in Fig. 11–47) with the extra machinery necessary to make the channel sensitive to gating by membrane potential: four transmembrane helical extensions of each subunit and four β subunits. The entire complex, viewed **(a)** in the plane of the membrane and **(b)** perpendicular to the plane (as viewed from outside the membrane), is represented as in Figure 11–47, with each subunit in a different color; each of the four β subunits is the same color as the subunit with which it associates. In (b), each transmembrane helix of one subunit (red) is numbered, S1 to S6. S5 and S6 from each of four subunits form the channel itself and are comparable to the two transmembrane helices of each subunit in Figure 11–47. S1 to S4 are four transmembrane helices. The S4 helix contains the highly conserved Arg residues and is believed to be the chief moving part of the voltage-sensing mechanism. **(c)** A schematic diagram of the voltage-gated channel, showing the basic pore structure (center) and the extra structures that make the channel voltage-sensitive; S4, the Arg-containing helix, is orange. For clarity, the β subunits are not shown in this view. In the resting membrane, the transmembrane electrical potential (inside negative) exerts a pull on positively charged Arg side chains in S4, toward the cytosolic side. When the membrane is depolarized, the pull is lessened, and with complete reversal of the membrane potential, S4 is drawn toward the extracellular side. **(d)** This movement of S4 is physically coupled to opening and closing of the K^+ channel, which is shown here in its open and closed conformations. Although K^+ is present in the closed channel, the pore closes on the bottom, near the cytosol, preventing K^+ passage.

Shaker K^+ channels contains four Arg residues; the positive charges on these residues cause the helix to move relative to the membrane in response to changes in the transmembrane electric field (the membrane potential).

Cells also have channels that specifically conduct Na^+ or Ca^{2+} and exclude K^+. In each case, the ability to discriminate among cations requires both a cavity in the binding site of just the right size (neither too large nor too small) to accommodate the ion and the precise positioning within the cavity of carbonyl oxygens that can replace the ion's hydration shell. This fit can be achieved with molecules smaller than proteins; for example, valinomycin (Fig. 11–44) can provide the precise fit that gives high specificity for the binding of one ion rather than another. Chemists have designed small molecules with very high specificity for binding of Li^+ (radius 0.60 Å), Na^+ (radius 0.95 Å), K^+ (radius 1.33 Å), or Rb^+ (radius 1.48 Å). The biological versions, however—the channel proteins—not only *bind* specifically but *conduct* ions across membranes in a *gated* fashion.

Gated Ion Channels Are Central in Neuronal Function

Virtually all rapid signaling between neurons and their target tissues (such as muscle) is mediated by the rapid opening and closing of ion channels in plasma membranes. For example, Na^+ channels in neuronal plasma membranes sense the transmembrane electrical gradient and respond to changes by opening or closing. These voltage-gated ion channels are typically very selective for Na^+ over other monovalent or divalent cations (by factors of 100 or more) and have very high flux rates ($>10^7$ ions/s). Closed in the resting state, Na^+ channels are opened—activated—by a reduction in the membrane potential; they then undergo very rapid inactivation. Within milliseconds of opening, a channel closes and remains inactive for many milliseconds. Activation followed by inactivation of Na^+ channels is the basis for signaling by neurons (see Fig. 12–26).

Another very well-studied ion channel is the **nicotinic acetylcholine receptor**, which functions in the passage of an electric signal from a motor neuron to a muscle fiber at the neuromuscular junction (signaling the muscle to contract). Acetylcholine released by the motor neuron diffuses a few micrometers to the plasma membrane of a myocyte, where it binds to an acetylcholine receptor. This forces a conformational change in the receptor, causing its ion channel to open. The resulting inward movement of positively charged ions into the myocyte depolarizes its plasma membrane and triggers contraction. The acetylcholine receptor allows Na^+, Ca^{2+}, and K^+ to pass through its channel with equal ease, but other cations and all anions are unable to pass. Movement of Na^+ through an acetylcholine receptor ion channel is unsaturable (its rate is linear with respect to extracellular $[Na^+]$) and very fast—about 2×10^7 ions/s under physiological conditions.

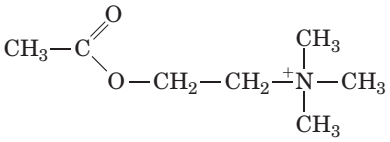

Acetylcholine

The acetylcholine receptor channel is typical of many other ion channels that produce or respond to electric signals: it has a "gate" that opens in response to stimulation by a signal molecule (in this case acetylcholine) and an intrinsic timing mechanism that closes the gate after a split second. Thus the acetylcholine signal is transient—an essential feature of all electric signal conduction.

Based on similarities between the amino acid sequences of other ligand-gated ion channels and the acetylcholine receptor, neuronal receptor channels that respond to the extracellular signals γ-aminobutyric acid (GABA), glycine, and serotonin are grouped in the acetylcholine receptor superfamily and probably share three-dimensional structure and gating mechanisms. The $GABA_A$ and glycine receptors are anion channels specific for Cl^- or HCO_3^-, whereas the serotonin receptor, like the acetylcholine receptor, is cation-specific.

Another class of ligand-gated ion channels respond to *intracellular* ligands: 3′,5′-cyclic guanosine mononucleotide (cGMP) in the vertebrate eye, cGMP and cAMP in olfactory neurons, and ATP and inositol 1,4,5-trisphosphate (IP_3) in many cell types. These channels are composed of multiple subunits, each with six transmembrane helical domains. We discuss the signaling functions of these ion channels in Chapter 12.

Table 11–6 shows some transporters discussed in other chapters in the context of the pathways in which they act.

Defective Ion Channels Can Have Severe Physiological Consequences

The importance of ion channels to physiological processes is clear from the effects of mutations in specific ion-channel proteins (Table 11–7, Box 11–2). Genetic defects in the voltage-gated Na^+ channel of the myocyte plasma membrane result in diseases in which muscles are periodically either paralyzed (as in hyperkalemic periodic paralysis) or stiff (as in paramyotonia congenita). Cystic fibrosis is the result of a mutation that changes one amino acid in the protein CFTR, a Cl^- ion channel; the defective process here is not neurotransmission but secretion by various exocrine gland cells with activities tied to Cl^- ion fluxes.

Many naturally occurring toxins act on ion channels, and the potency of these toxins further illustrates the importance of normal ion-channel function. Tetrodotoxin (produced by the puffer fish, *Sphaeroides rubripes*) and saxitoxin (produced by the marine

TABLE 11–6 Transport Systems Described Elsewhere in This Text

Transport system and location	Figure	Role
Adenine nucleotide antiporter of mitochondrial inner membrane	19–30	Imports substrate ADP for oxidative phosphorylation and exports product ATP
Acetylcholine receptor/channel	12–28	Signals muscle contraction
Acyl-carnitine/carnitine transporter of mitochondrial inner membrane	17–6	Imports fatty acids into matrix for β oxidation
P_i-H^+ symporter of mitochondrial inner membrane	19–30	Supplies P_i for oxidative phosphorylation
Malate–α-ketoglutarate transporter of mitochondrial inner membrane	19–31	Shuttles reducing equivalents (as malate) from matrix to cytosol
Glutamate-aspartate transporter of mitochondrial inner membrane	19–31	Completes shuttling begun by malate–α-ketoglutarate shuttle
Citrate transporter of mitochondrial inner membrane	21–10	Provides cytosolic citrate as source of acetyl-CoA for lipid synthesis
Pyruvate transporter of mitochondrial inner membrane	21–10	Is part of mechanism for shuttling citrate from matrix to cytosol
Fatty acid transporter of myocyte plasma membrane	17–3	Imports fatty acids for fuel
Complex I, III, and IV proton transporters of mitochondrial inner membrane	19–16	Act as energy-conserving mechanism in oxidative phosphorylation, converting electron flow into proton gradient
Thermogenin (uncoupling protein 1), a proton pore of mitochondrial inner membrane	19–36, 23–34	Allows dissipation of proton gradient in mitochondria as means of thermogenesis and/or disposal of excess fuel
Cytochrome *bf* complex, a proton transporter of chloroplast thylakoid	19–61	Acts as proton pump, driven by electron flow through the Z scheme; source of proton gradient for photosynthetic ATP synthesis
Bacteriorhodopsin, a light-driven proton pump	19–69	Is light-driven source of proton gradient for ATP synthesis in halophilic bacterium
F_oF_1 ATPase/ATP synthase of mitochondrial inner membrane, chloroplast thylakoid, and bacterial plasma membrane	19–25, 19–62a, 19–66	Interconverts energy of proton gradient and ATP during oxidative phosphorylation and photophosphorylation
P_i–triose phosphate antiporter of chloroplast inner membrane	20–15, 20–16	Exports photosynthetic product from stroma; imports P_i for ATP synthesis
Bacterial protein transporter	27–44	Exports secreted proteins through plasma membrane
Protein translocase of ER	27–38	Transports into ER proteins destined for plasma membrane, secretion, or organelles
Nuclear pore protein translocase	27–42	Shuttles proteins between nucleus and cytoplasm
LDL receptor in animal cell plasma membrane	21–41	Imports, by receptor-mediated endocytosis, lipid-carrying particles
Glucose transporter of animal cell plasma membrane; regulated by insulin	12–16	Increases capacity of muscle and adipose tissue to take up excess glucose from blood
IP_3-gated Ca^{2+} channel of ER	12–10	Allows signaling via changes in cytosolic [Ca^{2+}]
cGMP-gated Ca^{2+} channel of retinal rod and cone cells	12–37	Allows signaling via rhodopsin linked to cAMP-dependent phosphodiesterase in vertebrate eye
Voltage-gated Na^+ channel of neuron	12–26	Creates action potentials in neuronal signal transmission

TABLE 11–7 Some Diseases Resulting from Ion Channel Defects

Ion channel	Affected gene	Disease
Na^+ (voltage-gated, skeletal muscle)	*SCN4A*	Hyperkalemic periodic paralysis (or paramyotonia congenita)
Na^+ (voltage-gated, neuronal)	*SCN1A*	Generalized epilepsy with febrile seizures
Na^+ (voltage-gated, cardiac muscle)	*SCN5A*	Long QT syndrome 3
Ca^{2+} (neuronal)	*CACNA1A*	Familial hemiplegic migraine
Ca^{2+} (voltage-gated, retina)	*CACNA1F*	Congenital stationary night blindness
Ca^{2+} (polycystin-1)	*PKD1*	Polycystic kidney disease
K^+ (neuronal)	*KCNQ4*	Dominant deafness
K^+ (voltage-gated, neuronal)	*KCNQ2*	Benign familial neonatal convulsions
Nonspecific cation (cGMP-gated, retinal)	*CNCG1*	Retinitis pigmentosa
Acetylcholine receptor (skeletal muscle)	*CHRNA1*	Congenital myasthenic syndrome
Cl^-	*CFTR*	Cystic fibrosis

dinoflagellate *Gonyaulax*, which causes "red tides") act by binding to the voltage-gated Na^+ channels of neurons and preventing normal action potentials. Puffer fish is an ingredient of the Japanese delicacy fugu, which may be prepared only by chefs specially trained to separate succulent morsel from deadly poison. Eating shellfish that have fed on *Gonyaulax* can also be fatal; shellfish are not sensitive to saxitoxin, but they concentrate it in their muscles, which become highly poisonous to organisms higher up the food chain. The venom of the black mamba snake contains dendrotoxin, which interferes with voltage-gated K^+ channels. Tubocurarine, the active component of curare (used as an arrow poison in the Amazon region), and two other toxins from snake venoms, cobrotoxin and bungarotoxin, block the acetylcholine receptor or prevent the opening of its ion channel. By blocking signals from nerves to muscles, all these toxins cause paralysis and possibly death. On the positive side, the extremely high affinity of bungarotoxin for the acetylcholine receptor ($K_d = 10^{-15}$ M) has proved useful experimentally: the radiolabeled toxin was used to quantify the receptor during its purification. ■

SUMMARY 11.3 Solute Transport across Membranes

- Movement of polar compounds and ions across biological membranes requires transporter proteins. Some transporters simply facilitate passive diffusion across the membrane from the side with higher concentration to the side with lower. Others transport solutes against an electrochemical gradient; this requires a source of metabolic energy.
- Carriers, like enzymes, show saturation and stereospecificity for their substrates. Transport via these systems may be passive or active. Primary active transport is driven by ATP or electron-transfer reactions; secondary active transport is driven by coupled flow of two solutes, one of which (often H^+ or Na^+) flows down its electrochemical gradient as the other is pulled up its gradient.
- The GLUT transporters, such as GLUT1 of erythrocytes, carry glucose into cells by facilitated diffusion. These transporters are uniporters, carrying only one substrate. Symporters permit simultaneous passage of two substances in the same direction; examples are the lactose transporter of *E. coli*, driven by the energy of a proton gradient (lactose-H^+ symport), and the glucose transporter of intestinal epithelial cells, driven by a Na^+ gradient (glucose-Na^+ symport). Antiporters mediate simultaneous passage of two substances in opposite directions; examples are the chloride-bicarbonate exchanger of erythrocytes and the ubiquitous Na^+K^+ ATPase.
- In animal cells, Na^+K^+ ATPase maintains the differences in cytosolic and extracellular concentrations of Na^+ and K^+, and the resulting Na^+ gradient is used as the energy source for a variety of secondary active transport processes.
- The Na^+K^+ ATPase of the plasma membrane and the Ca^{2+} transporters of the sarcoplasmic and endoplasmic reticulum (the SERCA pumps) are examples of P-type ATPases; they undergo reversible phosphorylation during their catalytic cycle. F-type ATPase proton pumps (ATP synthases) are central to energy-conserving mechanisms in mitochondria and chloroplasts. V-type ATPases produce gradients of protons across some intracellular membranes, including plant vacuolar membranes.
- ABC transporters carry a variety of substrates (including many drugs) out of cells, using ATP as energy source.

- Ionophores are lipid-soluble molecules that bind specific ions and carry them passively across membranes, dissipating the energy of electrochemical ion gradients.
- Water moves across membranes through aquaporins. Some aquaporins are regulated; some also transport glycerol or urea.
- Ion channels provide hydrophilic pores through which select ions can diffuse, moving down their electrical or chemical concentration gradients; they characteristically are unsaturable, have very high flux rates, and are highly specific for one ion. Most are voltage- or ligand-gated. The neuronal Na^+ channel is voltage-gated, and the acetylcholine receptor ion channel is gated by acetylcholine, which triggers conformational changes that open and close the transmembrane path.

Key Terms

Terms in bold are defined in the glossary.

fluid mosaic model 387
micelle 387
bilayer 387
vesicle 388
integral proteins 389
peripheral proteins 389
amphitropic proteins 390
annular lipid 391
hydropathy index 392
positive-inside rule 393
β barrel 393
porin 393
liquid-disordered state (l_d) 395
liquid-ordered state (l_o) 395
flippases 397
floppases 397
scramblases 397
FRAP 398
microdomains 398
rafts 399
GPI-anchored protein 399
caveolin 399
caveolae 399
BAR domain 400
fusion protein 400
v-SNAREs 401
t-SNAREs 401
selectins 402
simple diffusion 403
membrane potential (V_m) 403
electrochemical gradient 403
electrochemical potential 403
facilitated diffusion 403
passive transport 404
transporters 404
permeases 404
channels 404
K_t ($K_{transport}$) 406
electroneutral 409
cotransport 409
antiport 409
symport 409
uniport 409
active transport 409
electrogenic 410
P-type ATPases 410
SERCA pump 410
Na^+K^+ ATPase 411
V-type ATPases 412
F-type ATPases 412
ATP synthase 413
ABC transporters 413
multidrug transporters 413
lactose transporter 416
major facilitator superfamily (MFS) 416
Na^+-glucose symporters 417
ionophore 418
aquaporins (AQPs) 418
ion channel 420
ligand-gated channel 421
voltage-gated channel 421
patch-clamping 421
nicotinic acetylcholine receptor 424

Further Reading

Composition and Architecture of Membranes

Dowhan, W. (1997) Molecular basis for membrane phospholipids diversity: why are there so many lipids? *Annu. Rev. Biochem.* **66**, 199–232.

Ediden, M. (2002) Lipids on the frontier: a century of cell-membrane bilayers. *Nat. Rev. Mol. Cell Biol.* **4**, 414–418.
Short review of how the notion of a lipid bilayer membrane was developed and confirmed.

Leventis, P.A. & Grinstein, S. (2010) The distribution and function of phosphatidylserine in cellular membranes. *Annu. Rev. Biophys.* **39**, 407–427.

Maxfield, R.R. & van Meer, G. (2010) Cholesterol, the central lipid of mammalian cells *Curr. Opin. Cell Biol.* **22**, 422–429.

Von Heijne, G. (2006) Membrane protein topology. *Nat. Rev. Mol. Cell Biol.* **7**, 909–918.

White, S.H., Ladokhin, A.S., Jayasinghe, S., & Hristova, K. (2001) How membranes shape protein structure. *J. Biol. Chem.* **276**, 32,395–32,398.
Brief, intermediate-level review of the forces that shape transmembrane helices.

Wimley, W.C. (2003) The versatile β barrel membrane protein. *Curr. Opin. Struct. Biol.* **13**, 1–8.
Intermediate-level review.

Zeth, K. & Thein, M. (2010) Porins in prokaryotes and eukaryotes: common themes and variations. *Biochem. J.* **431**, 13–22.
Intermediate-level review of the β-barrel porins.

Membrane Dynamics

Daleke, D.L. (2007) Phospholipid flippases. *J. Biol. Chem.* **282**, 821–825.
Intermediate-level review.

Deveaux, P.F., Lopez-Montero, I., & Bryde, S. (2006) Proteins involved in lipid translocation in eukaryotic cells. *Chem. Phys. Lipids* **141**, 119–132.

Didier, M., Lenne, P.-F., Rigneault, H., & He, H.-T. (2006) Dynamics in the plasma membrane: how to combine fluidity and order. *EMBO J.* **25**, 3446–3457.
Intermediate-level review of studies of membrane dynamics, with fluorescent and other probes.

Frost, A., Unger, V.M., & De Camilli, P. (2009) The BAR domain superfamily: membrane-molding macromolecules. *Cell* **137**, 191–196.

Frye, L.D. & Ediden, M. (1970) The rapid intermixing of cell-surface antigens after formation of mouse-human heterokaryons. *J. Cell Sci.* **7**, 319–335.
The classic demonstration of membrane protein mobility.

Graham, T.R. (2004) Flippases and vesicle-mediated protein transport. *Trends Cell Biol.* **14**, 670–677.
Intermediate-level review of flippase function.

Graham, T.R. & Kozlov, M.M. (2010) Interplay of proteins and lipids in generating membrane curvature. *Curr. Opin. Cell Biol.* **22**, 430–436.

Hannich, J.T., Umebayashi, K., & Riezman, H. (2011) Distribution and functions of sterols and sphingolipids. In *The Biology of Lipids: Trafficking, Regulation, and Function* (Simons, K., ed.), Cold Spring Harbor Laboratory Press, Cold Spring Harbor, NY; also in *CSH Perspect. Cell Biol.* doi:10.1101/cshperspect.a004762.

Jahn, R. & Scheller, R.H. (2006) SNAREs—engines for membrane fusion. *Nat. Rev. Cell Mol. Biol.* **7**, 631–643.
Excellent intermediate-level review of the role of SNAREs in membrane fusion and the fusion mechanism itself.

Janmey, P.A. & Kunnunen, P.K.J. (2006) Biophysical properties of lipids and dynamic membranes. *Trends Cell Biol.* **16**, 538–546.

Leventis, P.A. & Grinstein, S. (2010) The distribution and function of phosphatidylserine in cellular membranes. *Annu. Rev. Biophys.* **39**, 407–427.

Advanced review that includes discussion of flippases.

Lingwood, D. & Simons, K. (2010) Lipid rafts as a membrane-organizing principle. *Science* **327**, 46–50.

MacCallum, J.L. & Tieleman, D.P. (2011) Hydrophobicity scales: a thermodynamic looking glass into lipid-protein interactions. *Trends Biochem. Sci.* **36**, 653–662.

Intermediate-level review of several methods for determining an amino acid's hydrophobicity.

Marguet, D., Lenne, P.-F., Rigneault, H., & He, H.-T. (2006) Dynamics in the plasma membrane: how to combine fluidity and order. *EMBO J.* **25**, 3446–3457.

Intermediate-level review of the methods and results of studies on molecular motions in the membrane.

Martens, S. & McMahon, H.T. (2008) Mechanisms of membrane fusion: disparate players and common principles. *Nat. Rev. Mol. Cell Biol.* **9**, 543–566.

Niessen, C.M., Leckband, D., & Yap, A.S. (2011) Tissue organization by cadherin adhesion molecules: dynamic molecular and cellular mechanisms of morphogenetic regulation. *Physiol. Rev.* **91**, 691–731.

Palmgren, M.G. & Nissen, P. (2011) P-type ATPases. *Annu. Rev. Biophys.* **40**, 243–266.

Advanced review of transporters that include P4-type flippases.

Palsdottir, H. & Hunte, C. (2004) Lipids in membrane protein structures. *Biochim. Biophys. Acta* **1666**, 2–18.

Parton, R.G. & Simons, K. (2007) The multiple faces of caveolae. *Nat. Rev. Mol. Cell Biol.* **8**, 185–194.

Phillips, R., Ursell, T., Wiggins, P., & Sens, P. (2009) Emerging roles for lipids in shaping membrane-protein function. *Nature* **459**, 379–385.

Intermediate-level review.

Qualman, B., Koch, D., & Kessels, M.M. (2011) Let's go bananas: revisiting the endocytic BAR code. *EMBO J.* **30**, 3501–3515.

Intermediate-level review of the action of BAR domains in causing membrane curvature.

Quinn, P.J. & Wolf, C. (2009) The liquid ordered phase in membranes. *Biochim. Biophys. Acta* **1788**, 33–46.

Advanced review of the state of membrane lipids. This is one of 26 excellent reviews that appear in this issue of the journal on all aspects of the physical state of lipids in biological membranes.

Sanyal, S. & Menon, A.K. (2009) Flipping lipids: why an' what's the reason for? *ACS Chem. Biol.* **4**, 895–909.

Intermediate-level review of flippases in membrane biogenesis.

Sezgin, E. & Schwille, P. (2011) Fluorescence techniques to study lipid dynamics. In *The Biology of Lipids: Trafficking, Regulation, and Function* (Simons, K., ed.), Cold Spring Harbor Laboratory Press, Cold Spring Harbor, NY; also in *CSH Perspect. Cell Biol.*, doi:10.1101/cshperspect.a009803.

Simons, K. & Sampaio, J.L. (2011) Membrane organization and lipid rafts. In *The Biology of Lipids: Trafficking, Regulation, and Function* (Simons, K., ed.), Cold Spring Harbor Laboratory Press, Cold Spring Harbor, NY; also in *CSH Perspect. Cell Biol.*, doi:10.1101/cshperspect.a004697.

Tanaka, K., Fujimura-Kamada, K., & Yamamoto, T. (2011) Functions of phospholipid flippases. *J. Biochem.* **149**, 131–143.

Intermediate-level review of flippase structure and function.

van der Velden, L.M., van de Graaf, S.F.J., & Klomp, L.W.J. (2010) Biochemical and cellular functions of P_4 ATPases. *Biochem. J.* **431,** 1–11.

Intermediate-level review of the P_4 ATPase flippases.

van Deurs, B., Roepstorff, K., Hommelgaard, A.M., & Sandpit, K. (2003) Caveolae: anchored, multifunctional platforms in the lipid ocean. *Trends Cell Biol.* **13**, 92–100.

Van Meer, G. (2011) Dynamic transbilayer lipid asymmetry. In *The Biology of Lipids: Trafficking, Regulation, and Function* (Simons, K., ed.), Cold Spring Harbor Laboratory Press, Cold Spring Harbor, NY; also in *CSH Perspect. Cell Biol.*, doi:10.1101/cshperspect.a004671.

Wickner, W. & Shekmana, R. (2010) Membrane fusion *Nat. Struct. Mol. Biol.* **15**, 658–664.

Brief and accessible review of the molecules involved in membrane fusion.

Zhang, Y.-M. & Rock, C.O. (2008) Membrane lipid homeostasis in bacteria. *Nat. Rev. Microbiol.* **6**, 222–233.

Zimmerberg, J. & Kozlov, M.M. (2006) How proteins produce cellular membrane curvature. *Nat. Rev. Mol. Cell Biol.* **7**, 9–19.

Transporters

Augustin, R. (2010) The protein family of glucose transport facilitators: it's not only about glucose after all. *IUBMB Life* **62**, 315–333.

Advanced review of the GLUT proteins' structure and function.

Brini, M. & Carafoli, E. (2009) Calcium pumps in health and disease *Physiol. Rev.* **89**, 1341–1378.

Bublitz, M., Poulson, H., Preben Morth, J., & Nissen, P. (2010) In and out of the cation pumps: P-type ATPase structure revisited. *Curr. Opin. Struct. Biol.* **20**, 431–439.

Bublitz, M., Preben Morth, J., & Nissen, P. (2011) P-type ATPases at a glance. *J. Cell Sci.* **124**, 2515–2519.

Fujiyoshi, Y., Mitsuoka, K., de Groot, B.L., Philippsen, A., Grubmüller, H., Agre, P., & Engel, A. (2002) Structure and function of water channels. *Curr. Opin. Struct. Biol.* **12**, 509–515.

Guan, L. & Kaback, H.R. (2006) Lessons from lactose permease. *Annu. Rev. Biophys. Biomol. Struct.* **35**, 67–91.

Hoffman, N.J. & Elmendorf, J.S. (2011) Signaling, cytoskeletal and membrane mechanisms regulating GLUT4 exocytosis. *Trends Endocrinol. Metab.* **22**, 110–116.

Jones, P.M., O'Mara, M.L., & George, A.M. (2001) ABC transporters: a riddle wrapped in a mystery inside an enigma. *Trends Biochem. Sci.* **34**, 520–531.

Intermediate-level review of ATP transporter structure and function.

Kjellbom, P., Larsson, C., Johansson, I., Karlsson, M., & Johanson, U. (1999) Aquaporins and water homeostasis in plants. *Trends Plant Sci.* **4**, 308–314.

Intermediate-level review.

Krishnamurthy, H., Piscitelli, C.L., & Gouaus, E. (2009) Unlocking the molecular secrets of sodium-coupled transporters. *Nature* **459**, 347–355.

Intermediate-level review of the structure and function of the Na^+ cotransporters.

Preben Morth, J., Pedersen, B.P., Buch-Pedersen, M.J., Andersen, J.P., Vilsen, B., Palmgren, M.G., & Nissen, P. (2011) A structural overview of the plasma membrane Na^+,K^+-ATPase and H^+-ATPase ion pumps. *Nat. Rev. Mol. Cell Biol.* **12**, 60–70.

Rees, D.C., Johnson, E., & Lewinson, O. (2009) ABC transporters: the power to change. *Nat. Rev. Mol. Cell Biol.* **10**, 218–227.

Sui, H., Han, B.-G., Lee, J.K., Walian, P., & Jap, B.K. (2001) Structural basis of water-specific transport through the AQP1 water channel. *Nature* **414**, 872–878.

High-resolution solution of the aquaporin structure by x-ray crystallography.

Thorens, B. & Mueckler, M. (2010) Glucose transporters in the 21st century. *Am. J. Physiol. Endocrinol. Metab.* **298**, E141–E145.

Intermediate-level review of glucose facilitators.

Toyoshima, C. & Mizutani, T. (2004) Crystal structure of the calcium pump with a bound ATP analogue. *Nature* **430**, 529–535.

Toyoshima, C., Nomura, H., & Tsuda, T. (2004) Lumenal gating mechanism revealed in calcium pump crystal structures with phosphate analogs. *Nature* **432**, 361–368.

The supplementary materials available with the online version of this article include an excellent movie of the putative gating mechanism.

Watson, R.T. & Pessin, J.E. (2006) Bridging the GAP between insulin signaling and GLUT4 translocation. *Trends Biochem. Sci.* **31**, 215–222.

Intermediate-level review of the regulation of glucose transport through GLUT4.

Wright, E.M., Loo, D.D.F., & Hirayama, B.A. (2011) Biology of human sodium glucose transporters. *Physiol. Rev.* **91**, 733–794.

Advanced review of the Na^+-glucose cotransporter's biochemistry and physiology.

Zeth, K. & Thein, M. (2010) Porins in prokaryotes and eukaryotes: common themes and variations. *Biochem. J.* **431**, 13–22.

Ion Channels

Ashcroft, F.M. (2006). From molecule to malady. *Nature* **440**, 440–447.

A short review of the many known cases in which genetic defects in ion channels lead to disease in humans.

Doyle, D.A., Cabral, K.M., Pfuetzner, R.A., Kuo, A., Gulbis, J.M., Cohen, S.L., Chait, B.T., & MacKinnon, R. (1998) The structure of the potassium channel: molecular basis of K^+ conduction and selectivity. *Science* **280**, 69–77.

The first crystal structure of an ion channel is described.

Gadsby, D.C., Vergani, P., & Csanady, L. (2006) The ABC protein turned chloride channel whose failure causes cystic fibrosis. *Nature* **440**, 477–483.

This is one of seven excellent reviews of ion channels published together in this issue of *Nature*.

Gouaux, E. & MacKinnon, R. (2005) Principles of selective ion transport in channels and pumps. *Science* **310**, 1461–1465.

Short review of the architectural features of channels and pumps that give each protein its ion specificity.

Guggino, W.B. & Stanton, B.A. (2006) New insights into cystic fibrosis: molecular switches that regulate CFTR. *Nat. Rev. Mol. Cell Biol.* **7**, 426–436.

Hille, B. (2001) *Ion Channels of Excitable Membranes*, 3rd edn, Sinauer Associates, Sunderland, MA.

Intermediate-level text emphasizing the function of ion channels.

Jiang, Y., Lee, A., Chen, J., Ruta, V., Cadene, M., Chait, B.T., & MacKinnon, R. (2003) X-ray structure of a voltage-dependent K^+ channel. *Nature* **423**, 33–41.

King, L.S., Kozono, D., & Agre, P. (2004) From structure to disease: the evolving tale of aquaporin biology. *Nat. Rev. Mol. Cell Biol.* **5**, 687–698.

Intermediate-level review of the localization of aquaporins in mammalian tissues and the effects of aquaporin defects on physiology.

Lee, A.G. & East, J.M. (2001) What the structure of a calcium pump tells us about its mechanism. *Biochem J.* **356**, 665–683.

Long, S.B., Campbell, E.B., & MacKinnon, R. (2005) Crystal structure of a mammalian voltage-dependent *Shaker* family K^+ channel. *Science* **309**, 897–902.

Neher, E. & Sakmann, B. (1992) The patch clamp technique. *Sci. Am.* (March) **266**, 44–51.

Clear description of the electrophysiological methods used to measure the activity of single ion channels, by the Nobel Prize–winning developers of this technique.

Tombola, F., Pathak, M.M., & Isacoff, E.Y. (2006) How does voltage open an ion channel? *Annu. Rev. Cell Dev. Biol.* **22**, 23–52.

Advanced review of the mechanisms of voltage gating of ion channels.

Verkman, A.S. (2011) Aquaporins at a glance. *J. Cell Sci.* **124**, 2107–2112.

Intermediate-level, poster-style review of aquaporin structure and function.

Problems

1. Determining the Cross-Sectional Area of a Lipid Molecule When phospholipids are layered gently onto the surface of water, they orient at the air-water interface with their head groups in the water and their hydrophobic tails in the air. An experimental apparatus **(a)** has been devised that reduces the surface area available to a layer of lipids. By measuring the force necessary to push the lipids together, it is possible to determine when the molecules are packed tightly in a continuous monolayer; as that area is approached, the force needed to further reduce the surface area increases sharply **(b)**. How would you use this apparatus to determine the average area occupied by a single lipid molecule in the monolayer?

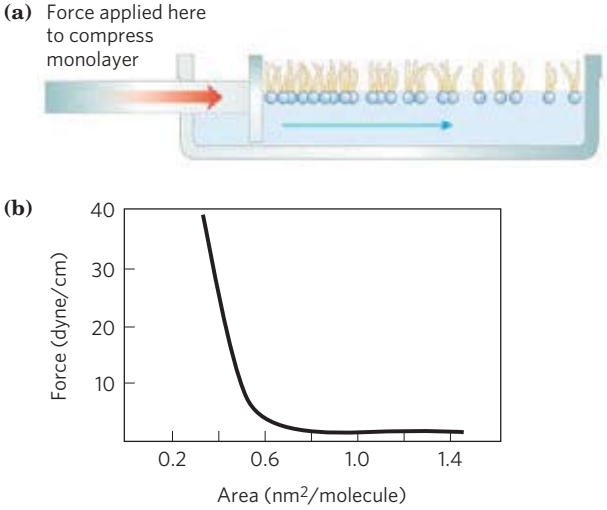

2. Evidence for a Lipid Bilayer In 1925, E. Gorter and F. Grendel used an apparatus like that described in Problem 1 to determine the surface area of a lipid monolayer formed by lipids extracted from erythrocytes of several animal species. They used a microscope to measure the dimensions of individual cells, from which they calculated the average surface area of one erythrocyte. They obtained the data shown in the table. Were these investigators justified in concluding that "chromocytes [erythrocytes] are covered by a layer of fatty substances that is two molecules thick" (i.e., a lipid bilayer)?

Animal	Volume of packed cells (mL)	Number of cells (per mm^3)	Total surface area of lipid monolayer from cells (m^2)	Total surface area of one cell (μm^2)
Dog	40	8,000,000	62	98
Sheep	10	9,900,000	6.0	29.8
Human	1	4,740,000	0.92	99.4

Source: Data from Gorter, E. & Grendel, F. (1925) On bimolecular layers of lipoids on the chromocytes of the blood. *J. Exp. Med.* 41, 439–443.

3. Number of Detergent Molecules per Micelle When a small amount of the detergent sodium dodecyl sulfate (SDS; $Na^+CH_3(CH_2)_{11}OSO_3^-$) is dissolved in water, the detergent ions enter the solution as monomeric species. As more detergent is added, a concentration is reached (the critical micelle concentration) at which the monomers associate to form micelles. The critical micelle concentration of SDS is 8.2 mM. The micelles have an average particle weight (the sum of the molecular weights of the constituent monomers) of 18,000. Calculate the number of detergent molecules in the average micelle.

4. Properties of Lipids and Lipid Bilayers Lipid bilayers formed between two aqueous phases have this important property: they form two-dimensional sheets, the edges of which close on each other and undergo self-sealing to form vesicles (liposomes).

(a) What properties of lipids are responsible for this property of bilayers? Explain.

(b) What are the consequences of this property for the structure of biological membranes?

5. Length of a Fatty Acid Molecule The carbon–carbon bond distance for single-bonded carbons such as those in a saturated fatty acyl chain is about 1.5 Å. Estimate the length of a single molecule of palmitate in its fully extended form. If two molecules of palmitate were placed end to end, how would their total length compare with the thickness of the lipid bilayer in a biological membrane?

6. Temperature Dependence of Lateral Diffusion The experiment described in Figure 11–18 was performed at 37 °C. If the experiment were carried out at 10 °C, what effect would you expect on the rate of diffusion? Why?

7. Synthesis of Gastric Juice: Energetics Gastric juice (pH 1.5) is produced by pumping HCl from blood plasma (pH 7.4) into the stomach. Calculate the amount of free energy required to concentrate the H^+ in 1 L of gastric juice at 37 °C. Under cellular conditions, how many moles of ATP must be hydrolyzed to provide this amount of free energy? The free-energy change for ATP hydrolysis under cellular conditions is about −58 kJ/mol (as explained in Chapter 13). Ignore the effects of the transmembrane electrical potential.

8. Energetics of the Na^+K^+ ATPase For a typical vertebrate cell with a membrane potential of −0.070 V (inside negative), what is the free-energy change for transporting 1 mol of Na^+ from the cell into the blood at 37 °C? Assume the concentration of Na^+ inside the cell is 12 mM and that in blood plasma is 145 mM.

9. Action of Ouabain on Kidney Tissue Ouabain specifically inhibits the Na^+K^+ ATPase activity of animal tissues but is not known to inhibit any other enzyme. When ouabain is added to thin slices of living kidney tissue, it inhibits oxygen consumption by 66%. Why? What does this observation tell us about the use of respiratory energy by kidney tissue?

10. Energetics of Symport Suppose you determined experimentally that a cellular transport system for glucose, driven by symport of Na^+, could accumulate glucose to concentrations 25 times greater than in the external medium, while the external $[Na^+]$ was only 10 times greater than the intracellular $[Na^+]$. Would this violate the laws of thermodynamics? If not, how could you explain this observation?

11. Location of a Membrane Protein The following observations are made on an unknown membrane protein, X. It can be extracted from disrupted erythrocyte membranes into a concentrated salt solution, and it can be cleaved into fragments by proteolytic enzymes. Treatment of erythrocytes with proteolytic enzymes followed by disruption and extraction of membrane components yields intact X. However, treatment of erythrocyte "ghosts" (which consist of just plasma membranes, produced by disrupting the cells and washing out the hemoglobin) with proteolytic enzymes followed by disruption and extraction yields extensively fragmented X. What do these observations indicate about the location of X in the plasma membrane? Do the properties of X resemble those of an integral or peripheral membrane protein?

12. Membrane Self-Sealing Cellular membranes are self-sealing—if they are punctured or disrupted mechanically, they quickly and automatically reseal. What properties of membranes are responsible for this important feature?

13. Lipid Melting Temperatures Membrane lipids in tissue samples obtained from different parts of a reindeer's leg have different fatty acid compositions. Membrane lipids from tissue near the hooves contain a larger proportion of unsaturated fatty acids than those from tissue in the upper leg. What is the significance of this observation?

14. Flip-Flop Diffusion The inner leaflet (monolayer) of the human erythrocyte membrane consists predominantly of phosphatidylethanolamine and phosphatidylserine. The outer leaflet consists predominantly of phosphatidylcholine and sphingomyelin. Although the phospholipid components of the membrane can diffuse in the fluid bilayer, this sidedness is preserved at all times. How?

15. Membrane Permeability At pH 7, tryptophan crosses a lipid bilayer at about one-thousandth the rate of indole, a closely related compound:

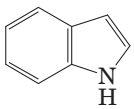

Suggest an explanation for this observation.

16. Water Flow through an Aquaporin A human erythrocyte has about 2×10^5 AQP1 monomers. If water molecules flow through the plasma membrane at a rate of 5×10^8 per AQP1 tetramer per second and the volume of an erythrocyte is 5×10^{-11} mL, how rapidly could an erythrocyte halve its volume as it encountered the high osmolarity (1 M) in the interstitial fluid of the renal medulla? Assume that the erythrocyte consists entirely of water.

17. Labeling the Lactose Transporter A bacterial lactose transporter, which is highly specific for lactose, contains a Cys residue that is essential to its transport activity. Covalent reaction of *N*-ethylmaleimide (NEM) with this Cys residue irreversibly inactivates the transporter. A high concentration of lactose in the medium prevents inactivation by NEM, presumably by sterically protecting the Cys residue, which is in or near the lactose-binding site. You know nothing else about the transporter protein. Suggest an experiment that might allow you to determine the M_r of the Cys-containing transporter polypeptide.

18. Predicting Membrane Protein Topology from Sequence You have cloned the gene for a human erythrocyte protein, which you suspect is a membrane protein. From the nucleotide sequence of the gene, you know the amino acid sequence. From this sequence alone, how would you evaluate the possibility that the protein is an integral protein? Suppose the protein proves to be an integral protein, either type I or type II. Suggest biochemical or chemical experiments that might allow you to determine which type it is.

19. Intestinal Uptake of Leucine You are studying the uptake of L-leucine by epithelial cells of the mouse intestine. Measurements of the rate of uptake of L-leucine and several of its analogs, with and without Na^+ in the assay buffer, yield the results given in the table. What can you conclude about the properties and mechanism of the leucine transporter? Would you expect L-leucine uptake to be inhibited by ouabain?

	Uptake in presence of Na^+		Uptake in absence of Na^+	
Substrate	V_{max}	K_t (mM)	V_{max}	K_t (mM)
L-Leucine	420	0.24	23	0.2
D-Leucine	310	4.7	5	4.7
L-Valine	225	0.31	19	0.31

20. Effect of an Ionophore on Active Transport Consider the leucine transporter described in Problem 19. Would V_{max} and/or K_t change if you added a Na^+ ionophore to the assay solution containing Na^+? Explain.

21. Surface Density of a Membrane Protein *E. coli* can be induced to make about 10,000 copies of the lactose transporter (M_r 31,000) per cell. Assume that *E. coli* is a cylinder 1 μm in diameter and 2 μm long. What fraction of the plasma membrane surface is occupied by the lactose transporter molecules? Explain how you arrived at this conclusion.

22. Use of the Helical Wheel Diagram A helical wheel is a two-dimensional representation of a helix, a view along its central axis (see Fig. 11–30b; see also Fig. 4–4d). Use the helical wheel diagram shown here to determine the distribution of amino acid residues in a helical segment with the sequence –Val–Asp–Arg–Val–Phe–Ser–Asn–Val–Cys–Thr–His–Leu–Lys–Thr–Leu–Gln–Asp–Lys–

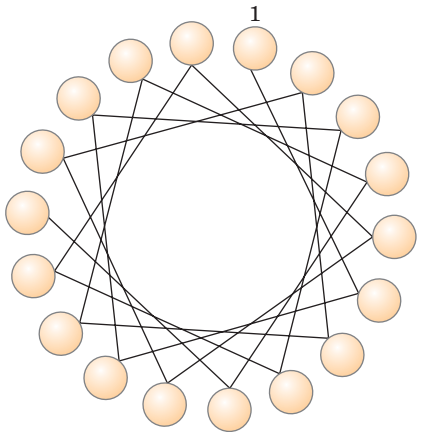

What can you say about the surface properties of this helix? How would you expect the helix to be oriented in the tertiary structure of an integral membrane protein?

23. Molecular Species in the *E. coli* Membrane The plasma membrane of *E. coli* is about 75% protein and 25% phospholipid by weight. How many molecules of membrane lipid are present for each molecule of membrane protein? Assume an average protein M_r of 50,000 and an average phospholipid M_r of 750. What more would you need to know to estimate the fraction of the membrane surface that is covered by lipids?

Using the Web

24. Membrane Protein Topology The receptor for the hormone epinephrine in animal cells is an integral membrane protein (M_r 64,000) that is believed to have seven membrane-spanning regions.

(a) Show that a protein of this size is capable of spanning the membrane seven times.

(b) Given the amino acid sequence of this protein, how would you predict which regions of the protein form the membrane-spanning helices?

(c) Go to the Protein Data Bank (www.pdb.org). Use the PDB identifier 1DEP to retrieve the data page for a portion of the β-adrenergic receptor (one type of epinephrine receptor) isolated from a turkey. Using Jmol to explore the structure, predict whether this portion of the receptor is located within the membrane or at the membrane surface. Explain.

(d) Retrieve the data for a portion of another receptor, the acetylcholine receptor of neurons and myocytes, using the PDB identifier 1A11. As in (c), predict where this portion of the receptor is located and explain your answer.

If you have not used the PDB, see Box 4–4 (p. 132) for more information.

Data Analysis Problem

25. The Fluid Mosaic Model of Biological Membrane Structure Figure 11–3 shows the currently accepted fluid mosaic model of biological membrane structure. This model was presented in detail in a review article by S. J. Singer in 1971. In the article, Singer presented the three models of membrane structure that had been proposed by that time:

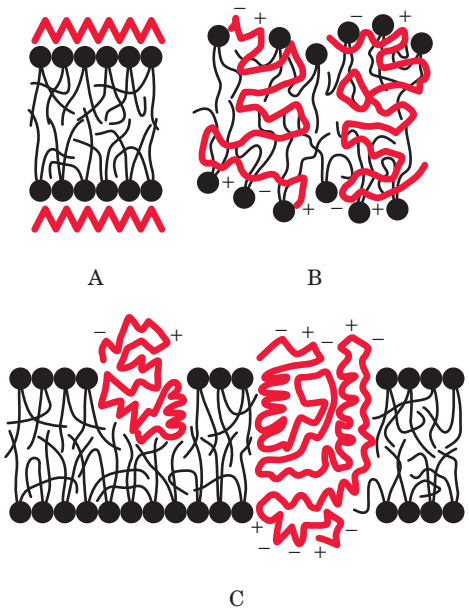

A. The Davson-Danielli-Robertson Model. This was the most widely accepted model in 1971, when Singer's review was published. In this model, the phospholipids are arranged as a bilayer. Proteins are found on both surfaces of the bilayer, attached to it by ionic interactions between the charged head groups of the phospholipids and charged groups in the proteins. Crucially, there is no protein in the interior of the bilayer.

B. The Benson Lipoprotein Subunit Model. Here the proteins are globular and the membrane is a protein-lipid mixture. The hydrophobic tails of the lipids are embedded in the hydrophobic parts of the proteins. The lipid head groups are exposed to the solvent. There is no lipid bilayer.

C. The Lipid-Globular Protein Mosaic Model. This is the model shown in Figure 11–3. The lipids form a bilayer and proteins are embedded in it, some extending through the bilayer and others not. Proteins are anchored in the bilayer by hydrophobic interactions between the hydrophobic tails of the lipids and hydrophobic portions of the protein.

For the data given below, consider how each piece of information aligns with each of the three models of membrane structure. Which model(s) are supported, which are not supported, and what reservations do you have about the data or their interpretation? Explain your reasoning.

(a) When cells were fixed, stained with osmium tetroxide, and examined in the electron microscope, the membranes showed a "railroad track" appearance, with two dark-staining lines separated by a light space.

(b) The thickness of membranes in cells fixed and stained in the same way was found to be 5 to 9 nm. The thickness of a "naked" phospholipid bilayer, without proteins, was 4 to 4.5 nm. The thickness of a single monolayer of proteins was about 1 nm.

(c) Singer wrote in his article: "The average amino acid composition of membrane proteins is not distinguishable from that of soluble proteins. In particular, a substantial fraction of the residues is hydrophobic" (p. 165).

(d) As described in Problems 1 and 2 of this chapter, researchers had extracted membranes from cells, extracted the lipids, and compared the area of the lipid monolayer with the area of the original cell membrane. The interpretation of the results was complicated by the issue illustrated in the graph of Problem 1: the area of the monolayer depended on how hard it was pushed. With very light pressures, the ratio of monolayer area to cell membrane area was about 2.0. At higher pressures—thought to be more like those found in cells—the ratio was substantially lower.

(e) Circular dichroism spectroscopy uses changes in polarization of UV light to make inferences about protein secondary structure (see Fig. 4–10). On average, this technique showed that membrane proteins have a large amount of α helix and little or no β sheet. This finding was consistent with most membrane proteins having a globular structure.

(f) Phospholipase C is an enzyme that removes the polar head group (including the phosphate) from phospholipids. In several studies, treatment of intact membranes with phospholipase C removed about 70% of the head groups without disrupting the "railroad track" structure of the membrane.

(g) Singer described in his article a study in which "a glycoprotein of molecular weight about 31,000 in human red blood cell membranes is cleaved by tryptic treatment of the membranes into soluble glycopeptides of about 10,000 molecular weight, while the remaining portions are quite hydrophobic" (p. 199). Trypsin treatment did not cause gross changes in the membranes, which remained intact.

Singer's review also included many more studies in this area. In the end, though, the data available in 1971 did not conclusively prove Model C was correct. As more data have accumulated, this model of membrane structure has been accepted by the scientific community.

Reference

Singer, S.J. (1971) The molecular organization of biological membranes. In *Structure and Function of Biological Membranes* (Rothfield, L.I., ed.), pp. 145–222, Academic Press, Inc., New York.